NORSK POLARINSTITUTT
SKRIFTER NR. 158

A. HJELLE and Y. OHTA

Contribution to the geology of north western Spitsbergen

NORSK POLARINSTITUTT
OSLO 1974

DET KONGELIGE DEPARTEMENT FOR INDUSTRI OG HÅNDVERK

NORSK POLARINSTITUTT

Rolfstangveien 12, Snarøya, 1330 Oslo Lufthavn. *Norway*

SALG AV BØKER

Bøkene selges gjennom bokhandlere, eller bestilles direkte fra:

SALE OF BOOKS

The books are sold through bookshops, or may be ordered directly from:

UNIVERSITETSFORLAGET

Postboks 307	*16 Pall Mall*	*P.O. Box 142*
Blindern, Oslo 3	*London SW 1*	*Boston, Mass. 02113*
Norway	*England*	*USA*

Publikasjonsliste, som også omfatter land- og sjøkart, kan sendes på anmodning.

List of publications, including maps and charts, will be sent on request.

NORSK POLARINSTITUTT
SKRIFTER NR. 158

A. HJELLE and Y. OHTA

Contribution to the geology of north western Spitsbergen

NORSK POLARINSTITUTT
OSLO 1974

Manuscripts received June 1973
Printed May 1974

Aas & Wahl

Contents

Preface

When the observations of the Norsk Polarinstitutt geological reconnaissance expedition to Albert I Land in 1964 were compiled, it was clear that many of the questions which arose concerning the stratigraphic, structural and metamorphic development in north-west Spitsbergen could only be answered by more detailed mapping. This commenced in 1965, when A. HJELLE worked for two weeks on the north-west islands, and continued in 1966, when he and Y. OHTA worked jointly in the Smeerenburgfjorden–Sørgattet–Danskøya–Amsterdamøya area. OHTA planned to continue his work further towards the east, on the east side of Svitjodbreen in 1968; however, unfavourable ice conditions that year prevented this, and instead he continued detailed mapping towards the south, in the Magdalenefjorden area.

Each of the geologists worked with two assistants, and as helicopter transport was not available, small boats were the main means of transportation.

Preliminary maps (scale 1 : 50 000) served as a topographic base for the mapping together with oblique air photographs. These were supplemented in 1968 by vertical air photographs.

The approximate location of the mapped area is north of 79° 30′ N, and west of 11° 30′ E, within the sheets A4 and A5 of the Norsk Polarinstitutt 1 : 100 000 topographical map series. The total area mapped amounts to approximately 375 km^2.

The geology of Danskøya and Amsterdamøya north-west Spitsbergen

By Audun Hjelle

Abstract

The area considered lies within the highly metamorphic part of the Caledonides of north-west Spitsbergen. The rocks comprise various para-gneisses, migmatites, syntectonic granitic rocks, and post-tectonic granitic dyke intrusions. A sillimanite-cordierite-almandine paragenesis in biotite gneiss and diopside-wollastonite in skarn rocks suggest the highest grade of metamorphism to be of upper amphibolite facies and of low to intermediate pressure. An anatectic origin is suggested for at least parts of the migmatites and syntectonic granites. The regional structure and the lithology of the metasediments indicate a stratigraphical correlation with the assumed late Precambrian Signehamna and Generalfjella Formations described from the areas around Krossfjorden approximately 50 km further south.

Three main fold phases are distinguished: F1 – late Precambrian and/or early Caledonian gentle folding with axial trend towards SSE. F2 – main Caledonian folding with tight isoclinal folds mainly trending SSW. F3 – late Caledonian open folding with axial trend towards NW and W developed during the formation of the migmatites.

аннотация

Рассматриваемая в настоящей работе область расположена в пределах высокометаморфизованной части каледонид северо-западного Шпицбергена. В её строении принимают участие различные парагнейсы, мигматиты, синтектонические граниты и посттектонические гранитные дайковые интрузии. Силлиманито-кордиерито-альмандиновый парагенезис в биотитовых гнейсах и диопсидо-волластонитовый - в скарновых породах свидетельствуют о принадлежности наивысшей степени метаморфизма к верхней ступени амфиболитовой фации при низком-среднем давлении. Предполагается анатектическое происхождение по крайней мере для части мигматитов и синтектонических гранитов. Региональная структура и литология затронутых метаморфизмом метаосадков указывают на стратиграфическую корреляцию с предположительно позднедокембрийскими свитами Сигнехамна (Signehamna) и Генералфьелла (Generalfjella), описанными в области вокруг кросс-фьорда (Krossfjorden), расположенной в 50 км южнее.

Выделяются три основные фазы складкообразования: F1 - позднедокембрийская и/или раннекаледонская пологая складчатость с простиранием осей на юго-юго-восток. F2 - основная каледонская складчатость с пережатыми изоклинальными складками, в основном простирающимися на юго-юго-запад. F3 - позднекаледонская открытая складчатость с северо-западным и западным простиранием осей, образовавшаяся во время формирования мигматитов.

Introduction

GEOLOGICAL SETTING

Danskøya and Amsterdamøya are situated in the northern area of highly metamorphic rocks within the Caledonian orogenic zone of western Spitsbergen. Mica schist of supracrustal origin, migmatites and foliated granitic rocks constitute the main part of the area. South of Smeerenburgfjorden a post-tectonic batholithic granite is discordantly intruded into the rocks mentioned above. On the eastern side the metamorphic rocks are in fault contact against Devonian deposits in the east. Towards Kongsfjorden–Krossfjorden the degree of metamorphism decreases gradually and the gneiss and migmatite are transitional to relatively unaltered sedimentary rocks estimated to be about 7000 m thick. Within the gneiss and migmatite area it is difficult to obtain a stratigraphical thickness of the involved supracrustals. However, in western Vasahalvøya the thickness is estimated at about 5000 m. All the supracrustal rocks are thought to belong to the Lower Hecla Hoek (Stubendorffbreen super-group, HARLAND et al. 1966) of late Precambrian age.

PREVIOUS WORK

The earlier contributions to the geology of north-west Spitsbergen, from DUROCHER (GAIMARD 1855) to HARLAND (1961) are summarized in ORVIN (1940), GEE and HJELLE (1966), and HJELLE (1966). A brief account only will be given here.

Before HOEL's and HORNEMAN's investigations during the ISACHSEN expedition of 1906 (SCHETELIG 1912, HOEL 1914) the geological information from this area only comprised the coastal areas.

SCHETELIG, who first described the coarse reddish granitic rock from the inner part of the mainland, considered this to be clearly younger than the surrounding gneisses and grey granites. This view has been confirmed by later investigations. SCHETELIG also mentioned the possibility of the gneisses being metamorphosed Hecla Hoek rocks, a view supported by HOLTEDAHL (1914 and 1926). Due to the gradually rising metamorphism from the Hecla Hoek rocks of the Kongsfjorden–Krossfjorden area northwards into the granite-gneiss area, HOLTEDAHL suggested a regional metamorphism of Caledonian age, thus rejecting the theory of an archean basement in the north-west, on which the Hecla Hoek sediments were deposited. The regional metamorphism was later described by SCHENK (1937) as being characterized by static anatexis of metasediments with a corresponding comprehensive granitisation.

K/Ar isotope dating of granitic rocks and gneisses from Danskøya and the Smeerenburgfjorden area (KRASIL'ŝĉIKOV 1965) gave average values around 400 m.y., confirming the earlier assumptions that the granitic intrusions and the regional metamorphism are of a Caledonian age.

GEE and HJELLE (1966) distinguished three stratigraphical groups in north-west Spitsbergen, all being considered to belong to the Lower Hecla Hoek,

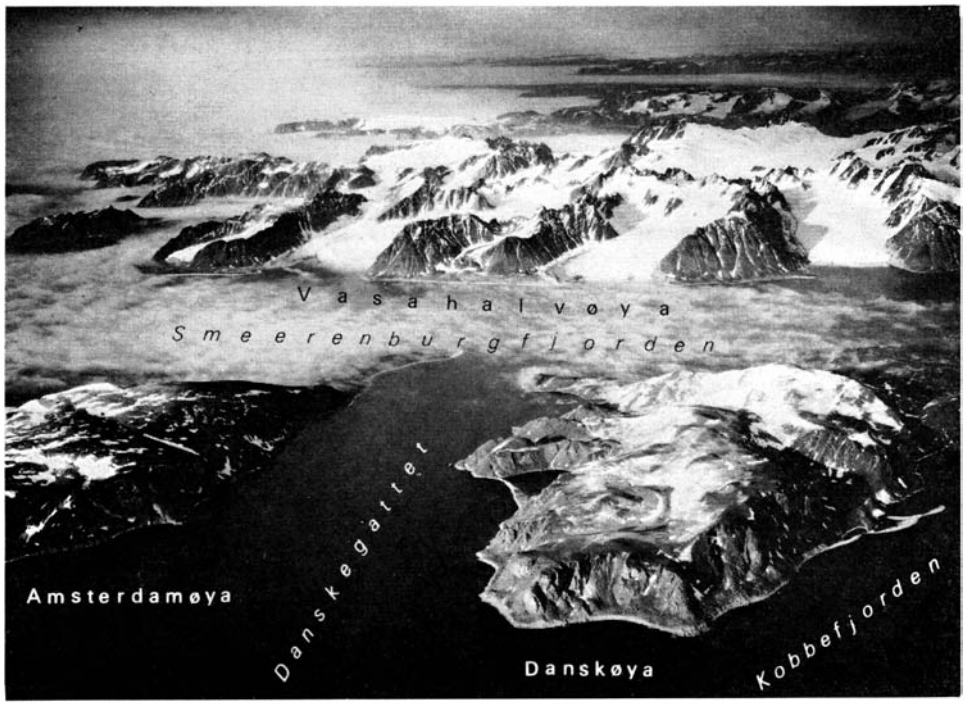

Fig. 1. *Danskegattet, with parts of Amsterdamøya and Danskøya. View towards east-northeast.*

Due to generally south-plunging folds, successively lower horizons were suggested to be exposed northwards, confirming HOLTEDAHL's view of an increasing depth of the orogenic zone in that direction. Marginal to the transition zone between Hecla Hoek sediments and the gneisses/migmatites, sheets of soda granite, aplite and pegmatite were seen to cut the schistosity of the sediments and the folds crenulating these sediments. Three fold generations were recorded: F1: Possible late Precambrian; F2: Caledonian, prior to migmatization; F3: Late Caledonian(?) refolding.

Several exposures of the post tectonic intrusion south of Smeerenburgfjorden were visited. The typical rock is a coarse reddish monzogranite, discordantly intruded into the migmatites. In the northern part of the outcrop the roof zone of the batholith is well exposed.

OHTA (1969), who carried out detailed structural investigations in the western part of Vasahalvøya (east of Smeerenburgfjorden), also distinguished three different kinds of tectonic elements, thus supporting the division of tectonic phases suggested by GEE and HJELLE: F1: Regional folding of metasediments, development of schistose cleavage. F2: Refolding of schistose cleavage, development of layered gneiss with axial plane gneissosity. F3: Flow structures of mobilized granitic rocks, development of migmatite and emplacement of plagioclase-porphyroblastic granite. F1 and F2 have a gentle to moderate dip to the south, while F3 structures have a gentle dip to the southeast.

In addition to the published material mentioned above, the author has also used collections and unpublished observations from north-west Spitsbergen, made by T. GJELSVIK in 1963.

PRESENT WORK

The present work deals with the geology of the two main islands of northwesternmost Spitsbergen (Fig. 1). The main purpose of the investigations was to prepare a provisional map and to give a general account of the petrography and the structure, with special regard to the relationship between the different types of granitic rocks.

The nomenclature for igneous rocks proposed by A. L. STRECKEISEN (1967) is used here when describing the mineral composition of both igneous and metamorphic rocks e.g. "quartz diorite dyke", "gneiss with a quartz dioritic composition".

Maps in the scale of 1:50 000, and oblique air photographs served as a basis for field mapping. All references to degrees in this paper refer to a 400 degree circle.

The main part of the field work was done during six weeks in the summer of 1966.

Geomorphological outline

As shown in Fig. 2 there is a distinct contrast between the two relatively low islands in northwesternmost Spitsbergen and the higher adjacent mainland. The hills and mountains of the islands mostly exhibit rounded forms, whereas sharp ridges and crests occur commonly on the mainland. However, no major lithological differences occur which should favour a selective denudation of the island areas. DUROCHER (GAIMARD 1855, p. 476) suggested the morphological difference to be a result of a relatively pronounced frost denudation of the islands due to humid ocean winds and frequent thawing and freezing. The present observations show that an earlier more extensive glaciation must be responsible for the main difference in geomorphological development. The following traces of an earlier extensive glaciation are: 1) Roche moutonnees east of Kobbefjorden. 2) Glacial fjord troughs in Smeerenburgfjorden and Kobbefjorden. 3) Cirques and cirque valleys along the western and northern coasts of the islands. 4) Submarine terminal moraines north of Smeerenburgfjorden (c. 15 km NNE of Amsterdamøya), in the western part of Danskegattet, in outer Kobbefjorden and along western Danskøya south of Kobbefjorden (LIESTØL 1972). 5) Numerous erratics of Horneman monzogranite, especially south of Kobbefjorden.

The suggested directions of ice flow deduced from the observations are indicated in Fig. 2.

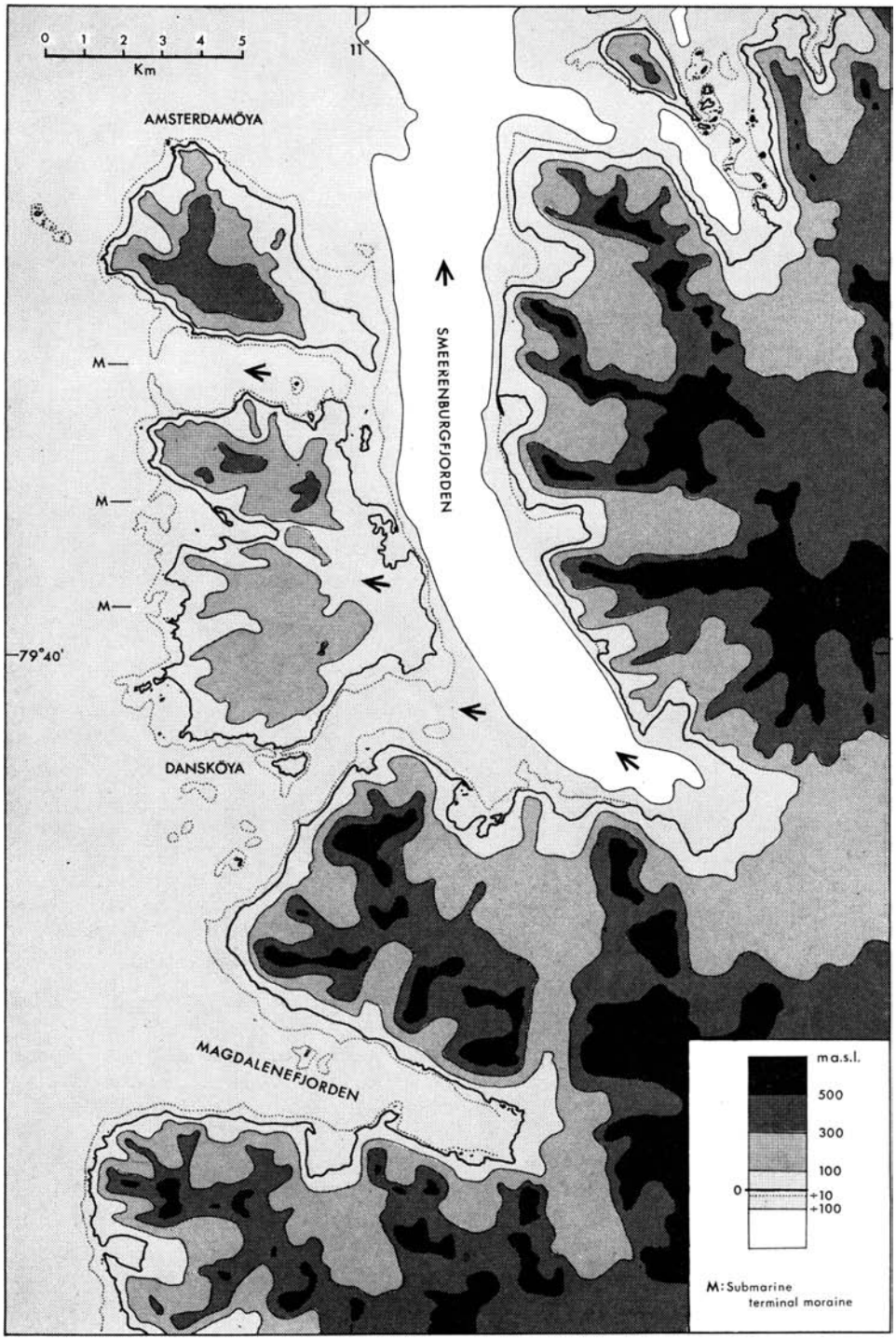

Fig. 2. *Relief map of north-west Spitsbergen. Arrows indicate suggested directions of earlier ice flow.*

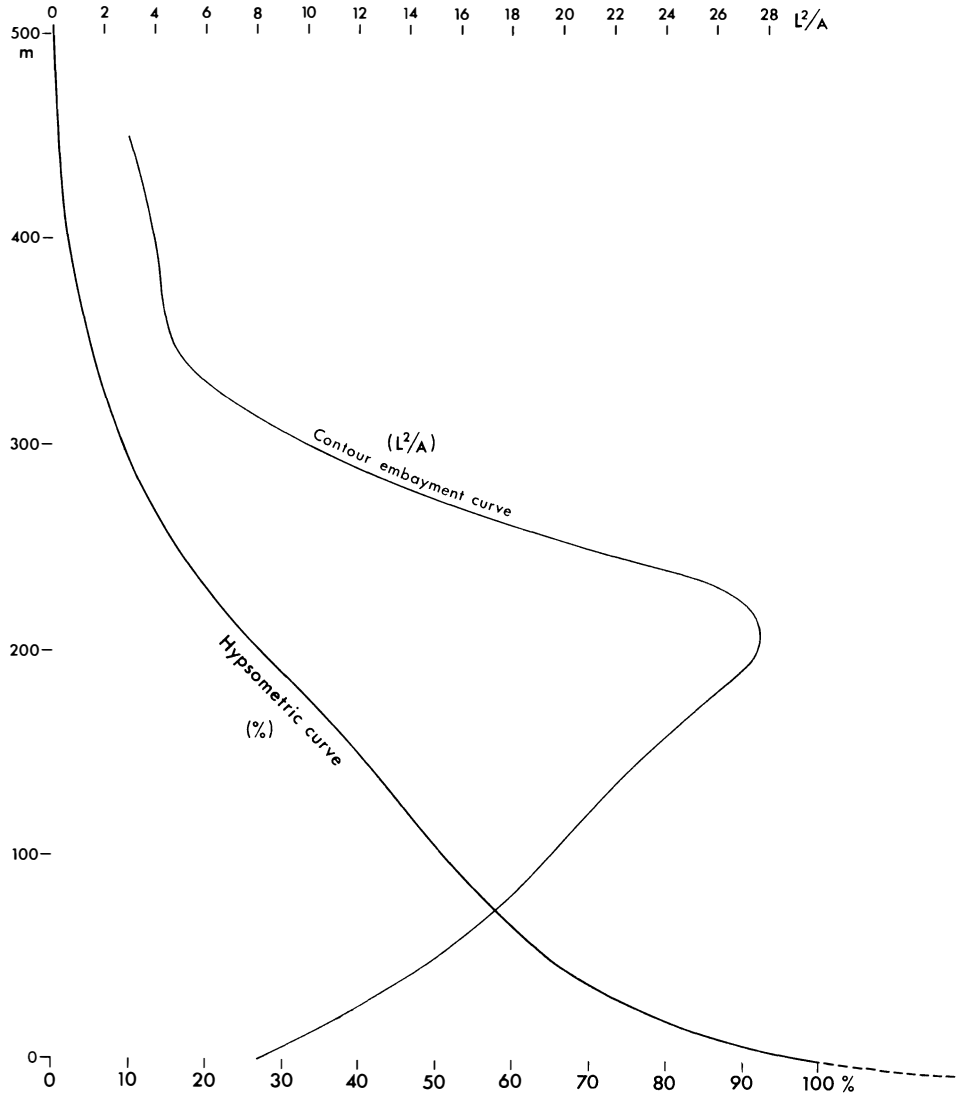

Fig. 3. *Hypsometric and contour embayment curves. Danskøya and Amsterdamøya. L=length of contour lines, A=area enclosed by contour lines. Contour interval 50 m, scale 1 : 25 000.*

The hypsometric curve for Danskøya and Amsterdamøya (Fig. 3) is relatively steep from 50 to 150 m and then shows a more gentle course, suggesting the upper limit of the main glacial erosion to be c. 150 m. This is also suggested by the curve L^2/A (the relative embayment of the contour lines), with maximum at about 200 m. This maximum may indicate a high degree of local excavation in the areas not exposed to the main glaciation, especially just above the upper limit of this. At about 340 m the L^2/A curve flattens out, suggesting an older, mature surface. One such is recognized on Amsterdamøya, where a slightly undulating plain with extensive blockfields occupies the greater part of the

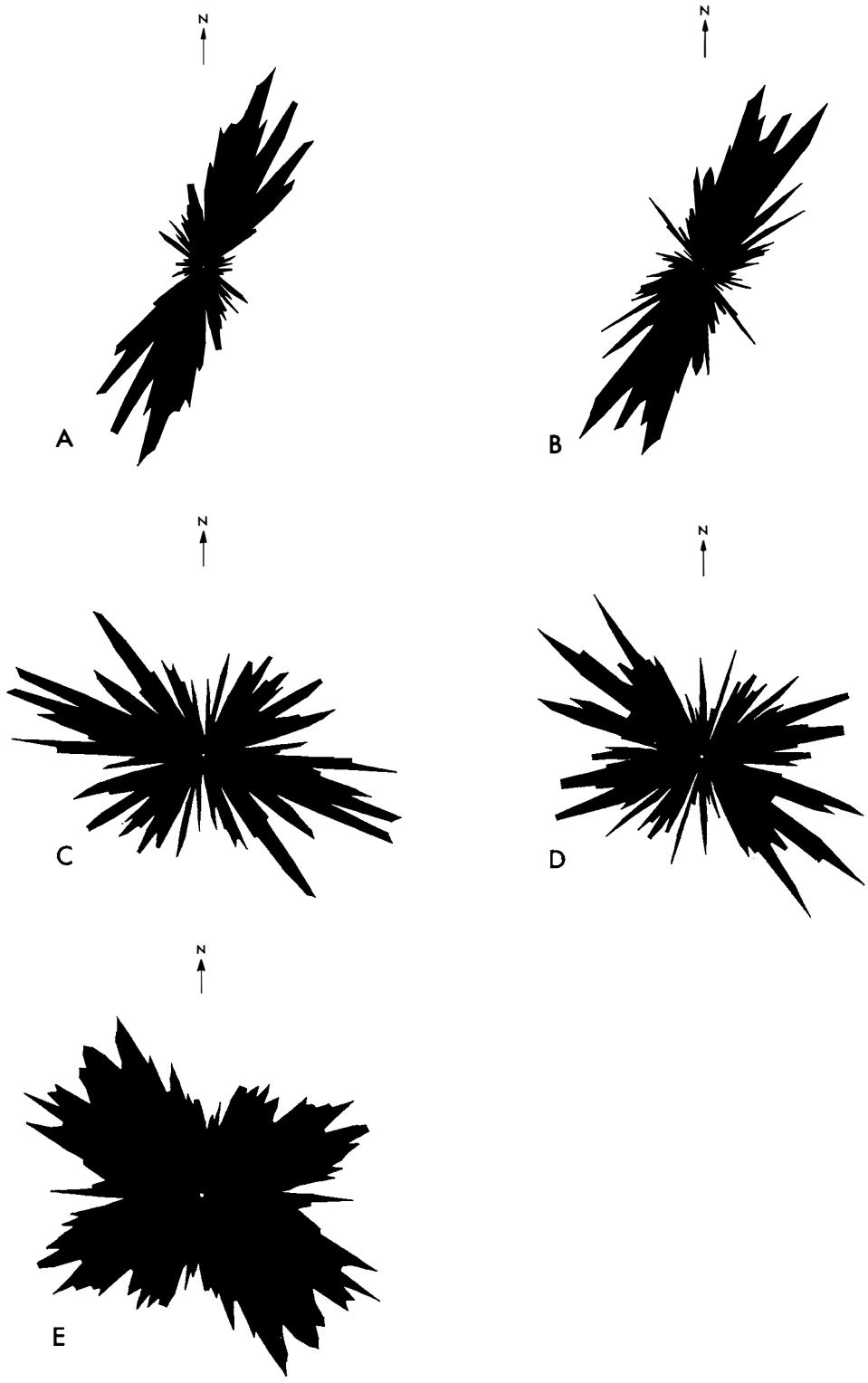

Fig. 4. *Direction of structural elements on Danskøya and Amsterdamøya. A: gneissosity, schistosity, 616 obs. B: axes of mesoscopic folds and associated linear structures, 414 obs. C: vertical or almost vertical joints, 536 obs. D: granitic dykes, 219 obs. E: strike of morphological features, 1006 measured points. Every second degree counted, counting cell 5g. The strike of morphological features was measured using a 1 cm grid net superimposed on a 1 : 25 000 scale map, considering contour lines (except on glaciers), shore lines and rivers.*

island above 250 m (Pl. 1A). In the north and north-west of Amsterdamøya, the margins of this plain are developed as steep cliffs dissected by cirques and cirque valleys.

The directional trend of the morphologic features depends mainly on the structural elements of the rock and the direction of glacial flow. From the strike diagram in Fig. 4E it is evident that the main morphological trends coincide with the directions of jointing and dyke intrusions rather than with the strike of the main folding and gneissosity. On Danskøya, both Kobbefjorden, the cirque valleys, and many of the lakes were developed in fracture zones, the most important being around 290, 330 and 375°.

The stratigraphical position of the metasediments

The transition from sedimentary rocks into gneissic varieties of the sequence is obvious northwards and eastwards from the Krossfjorden area into the adjacent areas. In the north and east the sedimentary characteristics are less obvious owing to intensive migmatization and simultaneous folding, and difficulties arise in stratigraphical correlation. Phyllite, limestone/marble and subordinate quartzite are the rocks most frequently found in the area of sedimentary rocks (the Signehamna and Generalfjella Formations, GEE and HJELLE 1966), while their equivalents within the migmatite/gneiss area are biotite mica schist and to a smaller extent marble, amphibolite and quartzite. As some marble horizons have remained relatively unaffected by the migmatization, they form a significant element of the metamorphosed rocks and may be used as stratigraphical guides. North of the innermost part of Kongsfjorden calcareous beds occur, which are considered to belong to the Generalfjella Formation. The beds are traced northwards into the migmatite/gneiss area where they are disturbed by the migmatization and folding. Though split up the calcareous beds apparently continue northwards, and marble bands and lenses occur as far as to the western side of Raudfjorden (Fig. 5). These eastern marbles at least, may be correlated with the Generalfjella Formation. In the western part of the migmatite/gneiss area, including Danskøya and Amsterdamøya, a number of relatively small marble bodies also occur, however, the stratigraphical connection southwards into the sedimentary region is less distinct than in the east, due to fewer observations and an apparently more complicated structural pattern south of Magdalenefjorden.

In the areas east and west of Smeerenburgfjorden (p. 31) the eastern and western marble belts may possibly belong to the same part of the succession, being repeated by folding. One may then suggest a correlation between the metasediments of Danskøya and Amsterdamøya and the Generalfjella Formation, or, taking the conspicuous biotite mica schist and biotite gneiss into consideration, a correlation may be suggested with the lower part of the Generalfjella Formation and the upper part of the Signehamna Formation. An attempt was made to calculate the approximate average composition of the

Table 1

Estimated average composition of rocks from Danskøya and Amsterdamøya. (Assuming 65% biotite gneiss with 1/5 pelitic schist, 15% granite gneiss, 10% biotite-amphibole gneiss, 5% aplitic metatect, 2% granitic dykes, 1% amphibolite, 1% calcite marble and 1% quartzite.) Calculated mainly from table 2 and 3.

Mode		Chemical composition	
Quartz	29.2%	SiO_2	64.5%
K-feldspar	9.3	TiO_2	0.8
Plagioclase	34.1	Al_2O_3	15.9
Muscovite	4.1	Fe_2O_3	0.4
Biotite	18.7	FeO	5.1
Chlorite	1.0	MgO	2.0
Amphibole	0.7	CaO	2.7
Epid., zois.	0.1	Na_2O	3.1
Apatite	0.1	K_2O	3.3
Sphene	0.1	H_2O^+	1.3
Ore mins.	0.4	P_2O_5	0.1
Garnet	0.6	CO_2	0.4
			99.6%
Sillimanite	0.3		
Cordierite	0.2		
Calcite	1.1		
	100.0%		
% An in plag.	27		
Spec. gravity	2.73		

Danskøya and Amsterdamøya rocks (Table 1). It seems obvious that if these rocks are isochemical metamorphosed equivalents of the original supracrustal rocks, the bulk of the latter most probably was of pelitic and/or greywacke composition, with only subordinate amounts of calcareous rocks. Even if one, tentatively, presumes that one third of the rocks present in the north-west islands represent granitic material introduced from the outside, the amount of calcareous sediments in the succession must have been less than 10%. This then clearly permits the suggestions above that the metasediments in Danskøya and Amsterdamøya are metamorphosed parts of the lower, mainly pelitic sequence described from around Krossfjorden.

The marble zones in north-west Spitsbergen, being consistent for long distances, suggest an almost horizontal regional fold axis. Except for small areas with a deviant trend of the fold axis, the structural observations confirm this suggestion, that only slightly lower stratigraphical levels are exposed to-

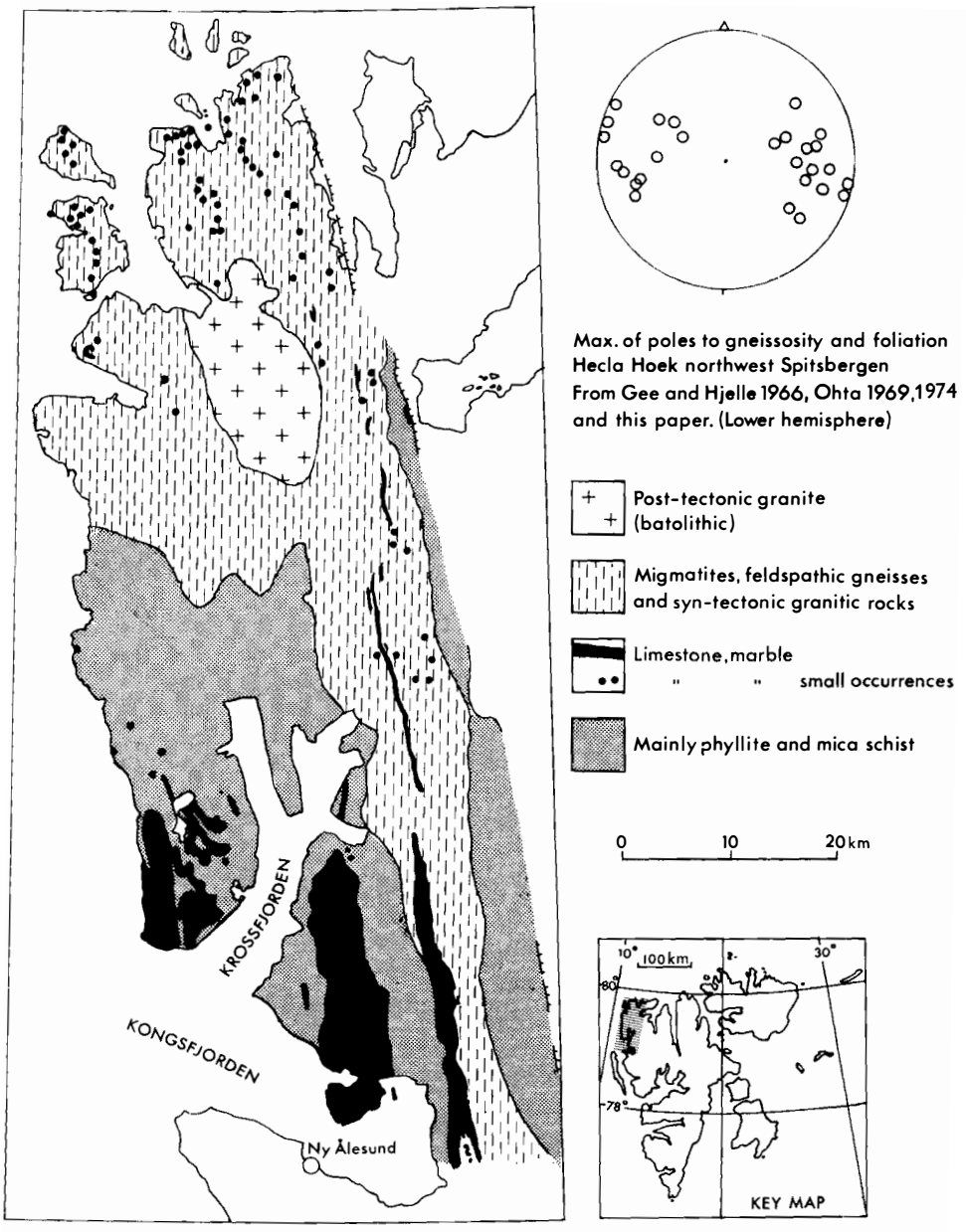

Fig. 5. *Outline lithology and structure of the Hecla Hoek rocks of north-west Spitsbergen.*

wards the north, with metasediments which belong to the Generalfjella and Signehamna Formations.

HARLAND (1960) considered all the Hecla Hoek supracrustals of north-west Spitsbergen to be correlated to the Lower Hecla Hoek Finlandveggen series of Ny Friesland. The later detailed observations of Y. OHTA and the author show a rather homogeneous development of the metasediments of the north-west and support this view.

Petrography

METASEDIMENTS

Pelitic and psammitic rocks

Pelitic schists represent the most common type of sedimentary relics in the gneisses, and cumulatively they make up a considerable fraction of the gneiss complex. The schists occur mainly as ½–10 m wide discontinuous and scattered bands which by increasing feldspatization often grade into biotite gneiss with a series of schist lenses and boudins.

The uniform and often intensely folded schists show primary compositional banding only occasionally and undisputable primary cross-bedding has not been observed. However, tectonic pseudo crossbedding occurs frequently. Where visible banding is observed, it is due to varying contents of biotite and to variations of average grain size which is reflected in different colour shades. At some localities thin layers (2–10 cm) rich in amphibole were also noted in the pelitic schists.

A typical sample of the biotite schist is of fine to medium grain and with pronounced lepidoblastic texture. The approximate mode is: 30 vol% quartz, 35% albite to andesine, 25% dark reddish brown biotite, 5% muscovite, 2% chlorite, 1% potassium feldspar, and 1% garnet. In the southwestern part of Danskøya rocks of this composition occur abundantly.

Inclusions and narrow, nonpersistent zones, less than 5 m wide, of impure quartzitic rocks were seen at several localities. These rocks contain such additional components as biotite, plagioclase, and muscovite and the composition varies from a relatively pure quartzite to a fine-grained quartz-rich biotite schist or biotite gneiss. The metamorphism has obliterated practically all sedimentary structures; the traces which remain, however, mostly coincide with the suggested primary trend of the quartzites, around NNW–SSE.

Psammitic rocks were seen at eastern Moseøya, at Danskøya NNE of Moseøya, at south-west Danskøya, and at the western part of Amsterdamøya.

Marble, skarn mineralization

Numerous small occurrences (<1 m) of boudinaged, granular marble with skarn (Pl. 2 C), and some more extensive outcrops of marble (10 to 100 m length) were seen, both in Danskøya and Amsterdamøya. Intercalations of psammitic horizons within many of the marbles suggest the primary rocks to be calcareous sediments with sandy or silty beds. This component of more or less impure marble normally exceeds the skarn; many of the smallest inclusions are almost totally digested, however, and wedge out in the gneiss, leaving carbonate-free zones of skarn.

Besides calcite and quartz the typical paragenesis of the skarn deposits includes sphene, hematite, vesuvianite and wollastonite. Vesuvianite is a "durchläufer" and gives little information about the condition of crystallization. The presence of diopside and wollastonite, however, suggests the temperature of formation to be respectively >c. 350 and >c. 450°C. Considering a pressure of 2000 bar (depth c. 8 km) these transition temperatures probably

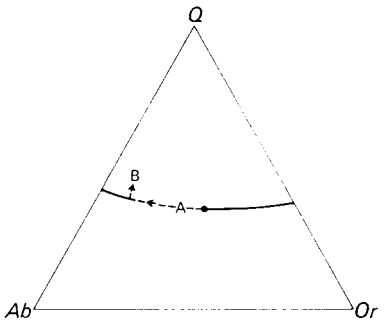

Fig. 6. *The point of "minimum melt" composition (dot), and the approximate position of the cotectic line in the system Q–Ab–An–Or–H_2O with an Ab/An ratio of 2.9, at P_{H_2O}=5000 bars (values from* v. PLATEN *et al. 1966). A represents the composition of the average aplitic mobilisate (Table 2, No. 4), and B the unchanged biotite gneiss.*

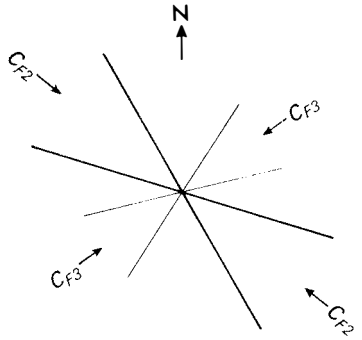

Fig. 7. *Suggested mode of origin for the main conjugate joint systems. C_{F2} and C_{F3}: axes of compression during F2 and F3 fold phases.*

exceed 500 and 700°C (WINKLER 1967), which corresponds to amphibolite facies, also recognized in the surrounding gneisses.

Diopside was found in all of the skarn localities, sphene in 75%, hematite in 60%, wollastonite in 50%, and vesuvianite in 50%. Vesuvianite and hematite seem to develop most frequently near granitic rocks and sphene near biotite gneiss, while wollastonite shows no significant trend of distribution in the 22 skarn localities examined.

GNEISS, MIGMATITES, AND SYNTECTONIC GRANITIC ROCKS

Biotite gneiss

Biotite gneiss which constitutes the bulk (about two thirds) of the islands, comprises rocks ranging in modal composition between pelitic schists and granitic gneiss. The biotite gneiss is distinguished from the pelitic schists by a generally higher content of potassium feldspar and its discontinuous planar schistosity and segregation banding; it is distinguished from granite gneiss by abundant biotite and a lower content potassium feldspar. Generally the rock is rather homogeneous, although some variations occur, e.g. in the content of plagioclase, which may show uneven porphyroblastic development. Characteristic features of the biotite gneiss are the occurrence of sporadic patches and lenses of igneous-textured rock rich in feldspar, and gradual transitions into local "spots" or zones of migmatite, the latter containing agmatitic or lensoid palaeosomes of biotite gneiss composition in an aplitic metatect. There is also

a general increase of grain-size as the biotite gneiss gradually evolves into granitic gneiss, migmatite or massive syntectonic granitic rocks. In these transition zones the biotite gneiss is normally veined, with more or less well-developed bands of quartzo-feldspathic and micaceous composition. The main range of biotite gneiss composition is: 20–30 vol% quartz, 5–10% potassium feldspar, 30–40% plagioclase (An 25–35), 0–10% muscovite, and 20–25% biotite (Table 2 No. 1, and Table 3 No. 11). The muscovite occurs mainly as sericite inclusions in clouded plagioclase. Characteristic minor constituents are almandine, sillimanite and cordierite. The sillimanite is generally in intergrowth with biotite and the cordierite contains poikilitic inclusions of quartz and muscovite as alteration products. Almandine is present in c. 80% of the examined thin sections, sillimanite in c. 60%, and cordierite in c. 25%.

Two types of exposure of biotite gneiss are seen, suggesting two possible modes of origin: 1) continuations of zones of pelitic schists near syntectonic granitic rocks and migmatites which must be considered as "granitized" parts of the pelitic schists; 2) layers in pelitic schists and with no obvious relation to granitic rocks, most probably representing metamorphosed arkosic sediments.

Biotite-amphibole gneiss, amphibolite

Though apparent similarities to the biotite gneiss are frequently met, most biotite-amphibole gneiss is compositionally rather well-defined and is therefore considered as a separate group.

Its most striking difference when compared with the biotite gneiss is the content of green hornblende. Further the biotite-amphibole gneiss differs markedly in the content of biotite and plagioclase, which are respectively lower and higher, than in the biotite gneiss. The modal composition is granodioritic to quartz dioritic. The range is approximately: 25–30 vol.% quartz, 5–15% potassium feldspar, 40–50% plagioclase (An25–30), 7–12% biotite, 1–6% hornblende, 1–3% muscovite, and less than 1% apatite+sphene+ore minerals (Table 2 No. 2 and Table 3 No. 12). The thin sections indicate the succession of crystallisation of the main minerals to be: hornblende-biotite-plagioclase-microcline-quartz. Myrmekite and poikilitic intergrowths of quartz occur frequently.

The texture varies considerably from a medium-grained homogeneous poikiloblastic somewhat schistose type, which is the most common, to a relatively coarse-grained migmatitic hypidioblastic type, which has its main extension in south central Danskøya.

As shown in Fig. 5 the metasupracrustal rocks of Albert I Land have a general NNW-SSE trend. The main outcrops of biotite-amphibole gneiss and marble in Danskøya and Amsterdamøya, though distorted through folding and granitization mainly occur in a zone with approximately the same trend. This may suggest that the content of amphibole in the gneiss to a great extent is due to originally NNW-SSE-striking calcareous metasediments, now almost digested.

Amphibolites are observed in two types of occurrences 1) As boudines,

Table 2

Average modal compositions and calculated chemical compositions of the main rock types on Danskøya and Amsterdamøya.

	1 Biotite gneiss (40)		2 Biotite-amphibole gneiss (38)		3 Granite gneiss (20)		4 Aplitic metatect (6)		5 Granitic dykes (29)	
	M	C	M	C	M	C	M	C	M	C
Quartz	27.4	22	27.2	14	33.4	12	33.0	17	32.2	10
K-feldspar	7.2	89	8.4	78	15.9	40	34.4	16	22.1	35
Plagioclase	33.5	23	46.1	11	34.3	16	26.7	27	32.6	21
Muscovite	5.0	79	2.4	44	2.5	66	1.9	51	4.5	51
Biotite	23.5	23	10.8	30	12.1	44	1.5	79	6.9	41
Chlorite	1.0	101	0.7	92	0.7	91	0.5	91	0.9	77
Amphibole	–	–	3.8	83	–	–	–	–	–	–
Epid. Zois.	x	–	x	–	x	–	x	–	0.3	141
Apatite	0.1	130	0.2	59	0.1	119	x	–	0.1	108
Sphene	0.1	188	0.1	147	0.1	267	x	–	x	–
Ore mins.	0.5	85	0.3	51	0.3	70	0.3	61	0.4	54
Garnet	0.7	154	–	–	0.4	237	1.4	135	x	–
Sillimanite	0.5	205	–	–	–	–	–	–	–	–
Cordierite	0.4	239	–	–	–	–	–	–	–	–
	99.9		100.0		99.8		99.7		100.0	
% An in plag.	28	14	29	14	27	9	16	32	29*	17
Spec. gravity	2.75	1.1	2.71	0.7	2.70	1.1	2.66	0.9	2.68	0.8
	Wt. %		Wt. %		Wt. %		Wt. %		Wt. %	
SiO_2	64.0		67.4		70.5		74.7		70.6	
TiO_2	1.1		0.5		0.5		0.3		0.4	
Al_2O_3	16.1		16.0		14.4		13.8		15.2	
Fe_2O_3	0.8		0.7		0.5		0.4		0.7	
FeO	5.2		3.1		3.0		1.1		2.4	
MgO	2.4		1.6		1.3		0.4		0.6	
CaO	2.3		3.6		2.2		1.0		2.2	
Na_2O	3.1		4.1		3.4		3.5		3.3	
K_2O	3.6		2.3		3.4		4.6		4.0	
H_2O	0.9		0.5		0.5		0.2		0.5	
P_2O_5	x		0.2		x		x		x	
	99.5		100.0		99.7		100.0		99.9	

M = modal %. C = coefficient of variation in %. Wt. % = approximate weight % calculated from mode.
( ) = number of specimens examined.
* = zoned; average value.

Table 3

Chemical analyses of rocks from Danskøya and Amsterdamøya.

	1	2	3	4	5	6	7	8	9	10	11	12
SiO_2	71.9	75.5	70.80	68.45	69.40	69.99	72.17	70.19	69.93	70.20	63.04	64.71
TiO_2	0.24	0.19	0.18	0.35	0.27	0.40	0.28	0.36	0.38	0.48	0.91	0.59
Al_2O_3	14.4	13.0	16.24	16.40	16.37	15.24	14.40	15.46	15.31	14.50	16.63	16.18
Fe_2O_3	0.1	0.2	0.29	1.05	0.81	0.09	0.14	0.08	1.20	0.03	0.18	0.43
FeO	1.6	1.6	1.22	2.73	1.87	2.79	1.82	2.47	1.56	3.38	6.21	3.97
MnO	0.03	0.07	0.02	0.06	0.03	0.05	0.03	0.04	0.01	0.07	0.13	0.09
MgO	0.5	0.4	0.34	0.51	0.31	0.87	0.43	0.89	0.81	1.13	2.33	2.14
CaO	1.4	1.1	1.31	1.80	1.28	2.57	1.40	3.01	2.45	2.06	1.87	4.24
Na_2O	3.0	2.7	3.50	3.74	2.77	3.44	2.86	3.36	3.31	3.58	3.15	4.33
K_2O	5.2	4.6	4.03	4.08	5.57	3.49	5.54	3.10	3.90	3.39	3.46	2.85
H_2O^+	0.8	0.6	n. d.	n. d.	n. d.	0.79	0.61	0.72	0.74	0.77	1.55	0.74
P_2O_5	0.09	0.06	0.06	0.11	0.10	0.08	0.03	0.06	0.05	0.05	0.06	0.07
CO_2	0.02	0.03	n. d.	n. d.	n. d.	0.08	0.04	0.07	0.10	0.04	0.05	0.07
BaO	0.10	0.14	n. d.	n. d.	n. d.	n. d.	n. d.	n. d.	n. d.	n. d.	n. d.	n. d.
	99.38	100.19	97.99	99.28	98.78	99.88	99.75	99.81	99.75	99.68	99.57	100.41

No. in Table	N. P. specimen No.	°N	°E	Location	Type
1	63 Gj. 1	79° 38.5′	11° 0.2′	Bjørnhamna	Granitic dyke, 4 m(?) wide
2	63 Gj. 20	79° 44.4′	10° 54.6′	S Amsterdamøya	,, ,, 1 m wide
3	66 Hj. 26B	79° 45.4′	10° 40.4′	NW Amsterdamøya	Migmatite metatect
4	66 Hj. 26C	,,	,,	,,	Granitic dyke, 10 m wide, cutting the migmatite (No. 3)
5	66 Hj. 64C	79° 46.3′	10° 49.0′	N Amsterdamøya	Granitic dyke, 6 m wide
6	64 Hj. 230A	79° 38.9′	10° 47.7′	SW Danskøya	,, ,, 50 m(?) wide
7	66 Hj. 38	79° 45.8′	10° 47.1′	Centr. Amsterdamøya	,, ,, 50 m(?) wide
8	66 Hj. 84	79° 42.5′	10° 46.4′	NW Danskøya	,, ,, 40 m wide
9	65 G 118	79° 39.2′	11° 39.1′	S Vasahalvøya	Hornemantoppen monzo-granite batholith. Typical
10	64 Hj. 212A	79° 40.1′	11° 6.0′	SE Danskøya	Typical granite gneiss
11	66 Hj. 105	79° 44.5′	10° 53.5′	S Amsterdamøya	Typical biotite gneiss
12	66 Hj. 82A	79° 43.1′	10° 51.5′	N Danskøya	Typical biotite-amphibole gneiss

Nos. 1 and 2 analyst B. ÅKERLUND, Sveriges Geologiska Undersökning
Nos. 3, 4, 5 analyst Y. OHTA.
Nos. 6, 7, 8, 9 analyst P. R. GRAFF, Norges geologiske Undersøkelse.
Nos. 10, 11, 12 analyst J. RØSTE, Norges geologiske Undersøkelse.

lenses and narrow concordant layers in biotite gneiss and biotite schist. This type occasionally occurs in connection with marble relics and might reflect the position of former beds of calcareous metasediments in a mainly pelitic sequence. 2) As zones of severely deformed or broken up amphibolite that cuts across the main gneissosity and thus probably represent relics of basic dykes.

Both types may occur in migmatites and they have essentially the same composition; a typical sample contains 0–15% quartz, 30–45% plagioclase (An 50–70), 30–60% hornblende, and 5–15% biotite + chlorite + ore minerals.

Granite gneiss, migmatite, syntectonic granite

The migmatites are mostly related to biotite gneisses and other paragneisses, which by introduction of granitic material may grade into heterogeneous migmatites. Variable amounts of granitic material are associated with lensoid or agmatitic inclusions of biotite gneiss, schists and amphibolite. The inclusions are in different stages of assimilation, some rotated and some in parallel orientation with the country rock (Pl. 2, AB).

The general impression is that compared with the surrounding gneisses, the metasters are enriched in biotite and plagioclase, and they are suggested to be mafic restites produced by in situ anatexis of the paragneisses with partial melting and subsequent differentiation. However, some migmatites contain metasters which could not be megascopically distinguished from the gneisses. This might imply that at least some of the migmatites were formed by injection of leucocratic mobilisates into the country rock without affecting the latter significantly. If the bulk of the migmatites was formed through anatexis in situ of supracrustal rocks and isochemical metamorphism is presumed for the other gneisses, the CaO content of the calculated average analysis suggests that the amount of calcareous supracrustal rocks involved has not exceeded 10%, even if the amount of calcareous restites in the present gneisses is estimated as high as 5%, instead of 1% (Table 1).

Adjacent to some migmatites the metasupracrustal gneisses are characterized by pronounced potash feldspar blastesis, and a migration of potassium has obviously taken place. The metatect of the migmatite occasionally penetrates discordantly into these partly granitized gneisses, apparently without affecting them chemically, resulting in agmatitic migmatites containing granitized metasters, which contrast pronouncedly with the mafic restite metasters of the common migmatites.

At some localities two generations of migmatite could be traced. The older migmatite occurs in banded gneiss and is closely connected to the F2 isoclinal folding. This migmatization took place before the folding ceased and the metatect possesses a slight but consistent gneissosity in the F2 direction. The younger, more extensive agmatitic migmatite was developed by introduction of aplitic and pegmatitic material along fissures and cracks in the older migmatite, which at that time was in a brittle condition. The occurrences of agmatitic migmatite coincide with the syn- to late tectonic granitic doming

associated with NW-SE-trending open F3 folds. This is also the case with most of the other migmatites observed.

Several observations of transitions from agmatitic to nebulitic migmatite suggest a progressive assimilation process, beginning with formation of agmatitic migmatite by injection and ending with nebulitic migmatites and ghost granites.

The contacts between biotite gneisses and migmatitic domes are often marked by 5–50 m wide transition zones in which granite gneiss predominates. There seems to be a direct connection between the size of the migmatite bodies and the width of the transition zones. The shape of the domes is vaguely defined and the contact with the surrounding gneisses is always concordant.

Towards the central parts of the domes, the palaeosomes gradually become smaller and less abundant, and the migmatites grade into massive or weakly foliated granitic rocks. Within these syntectonic granites only a few small inclusions are to be found, more or less parallel to the structures around the granitic dome.

The granites might thus be considered as "mature" migmatites with a high metatect/metaster ratio, and being a complex product of assimilation, remelting, and possibly addition of outside material.

When migmatites occur in areas of biotite-amphibole gneiss or with calcareous restites, the metatect frequently contains amphibole instead of biotite. By increasing assimilation these migmatites may grade into hornblende-bearing granites (slightly foliated "feldspathic biotite amphibole gneiss").

In the transition zone between migmatite and granite, the contacts with the most persistent rocks such as quartzite, marble, and amphibolite are still rather sharp, and these rocks are frequently found as boudins and fragments. Biotite schist and biotite gneiss, however, are often altered beyond recognition, with diffuse boundaries, and nebulitic metasters occur which tend towards the composition of the granite.

The composition of the granitic rocks often varies progressively from quartz diorite gneiss in the outer zone to weakly foliated or massive granodiorite and granite in the core. Local variations in petrography also occur, due to the difference in composition of assimilated inclusions. Thus considerable variations in mineral composition are apparent, and different specimens are often representative of only small areas. In general there is no significant difference in mineral mode between the granite gneiss and the syntectonic granitic rocks. Compared to biotite gneiss the content of potassium feldspar is considerably higher and biotite lower. The granite gneiss and the syntectonic granite have medium to coarse grain, and the granites often have a plagioclase porphyroblastic texture with porphyroblasts up to 4 cm across. The main range of mode is: 30–40% quartz, 10–20% potassium feldspar, 30–40% plagioclase (An 25–30), 1–5% muscovite, 10–20% biotite (Table 2 No. 3 and Table 3 No. 10).

In the migmatites containing mafic restites, the metatect often exhibits a pronounced felsic composition showing an aplitic to pegmatitic texture. A high content of potassium feldspar and the presence of comparatively large amounts

of light red almandine garnet are characteristic (Table 2 No. 4). A typical restite metaster of biotite gneiss origin contains about 30% biotite, 30% quartz, and 35% plagioclase (An ~ 40). To obtain a bulk composition of the whole migmatite which would approximate the common biotite gneiss, the metaster/metatect ratio would be about 3 : 1, a condition frequently met with. Another feature which points towards an anatectic differentiation origin of the migmatite, is the composition of the metatect, which closely approximates the cotectic ratio of the main minerals involved. The Ab/An ratio of the unchanged biotite gneiss is normally 2.5–3.0. Using the cotectic line in the Ab–Or–Q diagram for Ab/An=2.9 and P_{H_2O}=5000 bar (V. PLATEN et al. 1966), the point representing the composition of the average mobilisate (Table 2 No. 4) falls near this line and the initial anatexis takes place at a temperature of around 665° (Fig. 6).

The observations suggest that at least some of the migmatites are developed by in situ anatexis. One may estimate the PT-conditions of this anatexis to be 650–700° and c. 5 kb.

POST-TECTONIC DYKE ROCKS

Granitic dykes

Throughout the highly metamorphic area of north-west Spitsbergen, a large number of granitic dykes and veins are known, both fine- to medium-grained and pegmatitic. They cut discordantly through the para-gneiss as well as the synorogenic granitic rocks, displaying well defined borders and narrow contact zones. They represent the youngest intrusive event (Pl. 2B). These types of dykes are scarce in the adjacent areas of less metamorphic rocks and are obviously related to the regional migmatitization.

The composition of the medium-grained dyke rocks recorded from the north-west islands is rather homogeneous and seems to be rather independent of the composition of the invaded rocks. The dykes show texturally sharp contrasts to the syntectonic, relatively coarse and mainly gneissic granites. However, compositionally they show resemblances, being mainly of a monzogranitic and granodioritic composition (Fig. 8, Table 2 No. 5, Table 3 Nos. 1, 2 and 4–8).

Important characteristics are the rather high potassium feldspar content, mostly around 25%, and a clearly perceptible regular zoning of the larger plagioclase grains, in which the rims are between 10 and 20 mol% more sodic than the core.

The medium grained, common granitic dykes show both compositional and structural similarities with the adjacent Horneman granite on the mainland, and a genetical connection at depth is suggested (Fig. 8 and Table 3).

Small lenses of pegmatite and aplite are occasionally developed in the schists and gneisses adjacent to the more massive granitic or migmatitic bodies. The lenses are usually conformable with the foliation of gneiss, but occasionally there are discordant veins and patches. It is, therefore, highly probable that

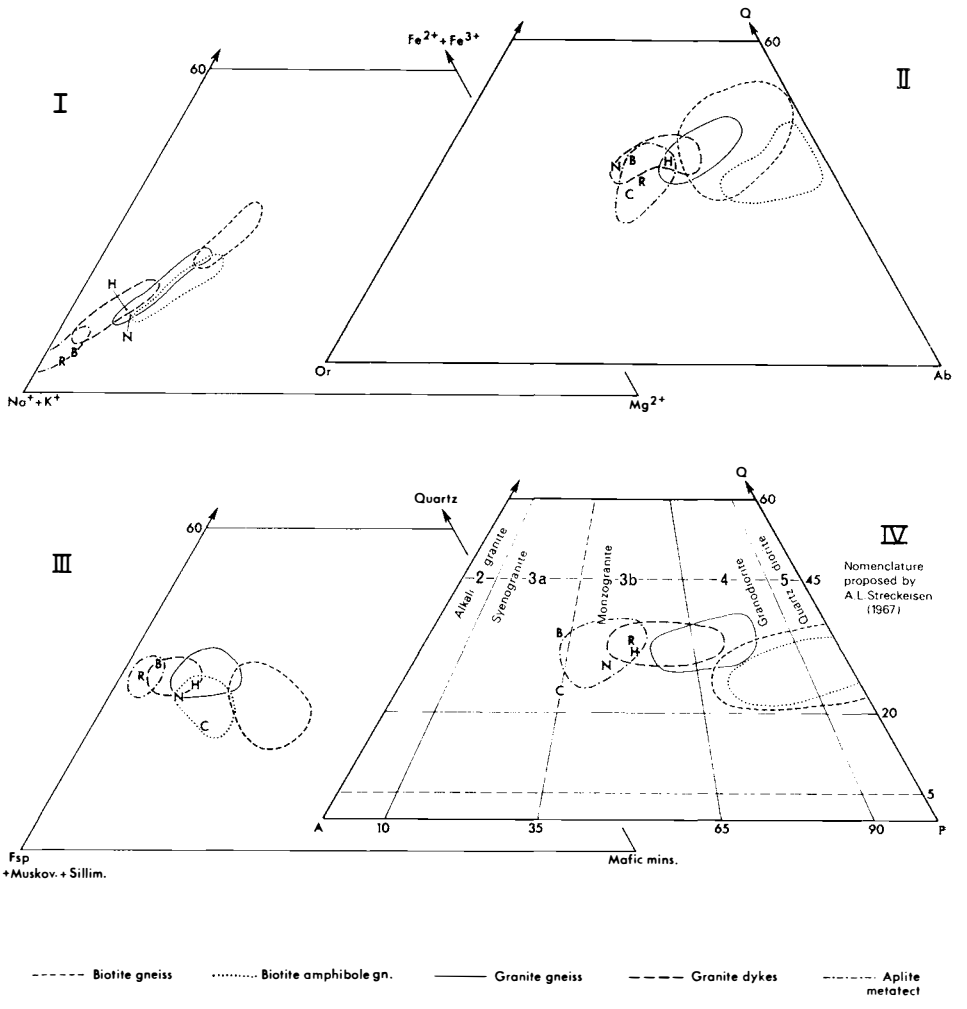

Fig. 8. *Compositional ranges of rocks from Danskøya and Amsterdamøya. The letters H, C, B, N, and R indicate the average compositions of the Hornemann Granite (H) northwest Spitsbergen: the Chydenius Granite (C) north central Spitsbergen, and the Brennevinsfjorden (B), Nordkapp (N) and Rijpfjorden (R) granites of Nordaustlandet.*

some of the aplitic and pegmatitic dykes observed in the vicinity of granites and migmatites are migmatite mobilisate extensions, and thus not really post-tectonic. Some are also actually cross-cut by younger medium-grained granitic dykes.

The pegmatite veins and dykes are normally more felsic than the fine- to medium-grained dykes, and both in composition and general appearance they approach some of the migmatite metatect.

Of the post-tectonic pegmatite veins and dykes recorded, only c. 10% exceeded ½ m in width, compared with c. 65% of the medium-grained granite dykes. At almost all localities where age relations between the two types were seen, pegmatite veins represented the youngest intrusions.

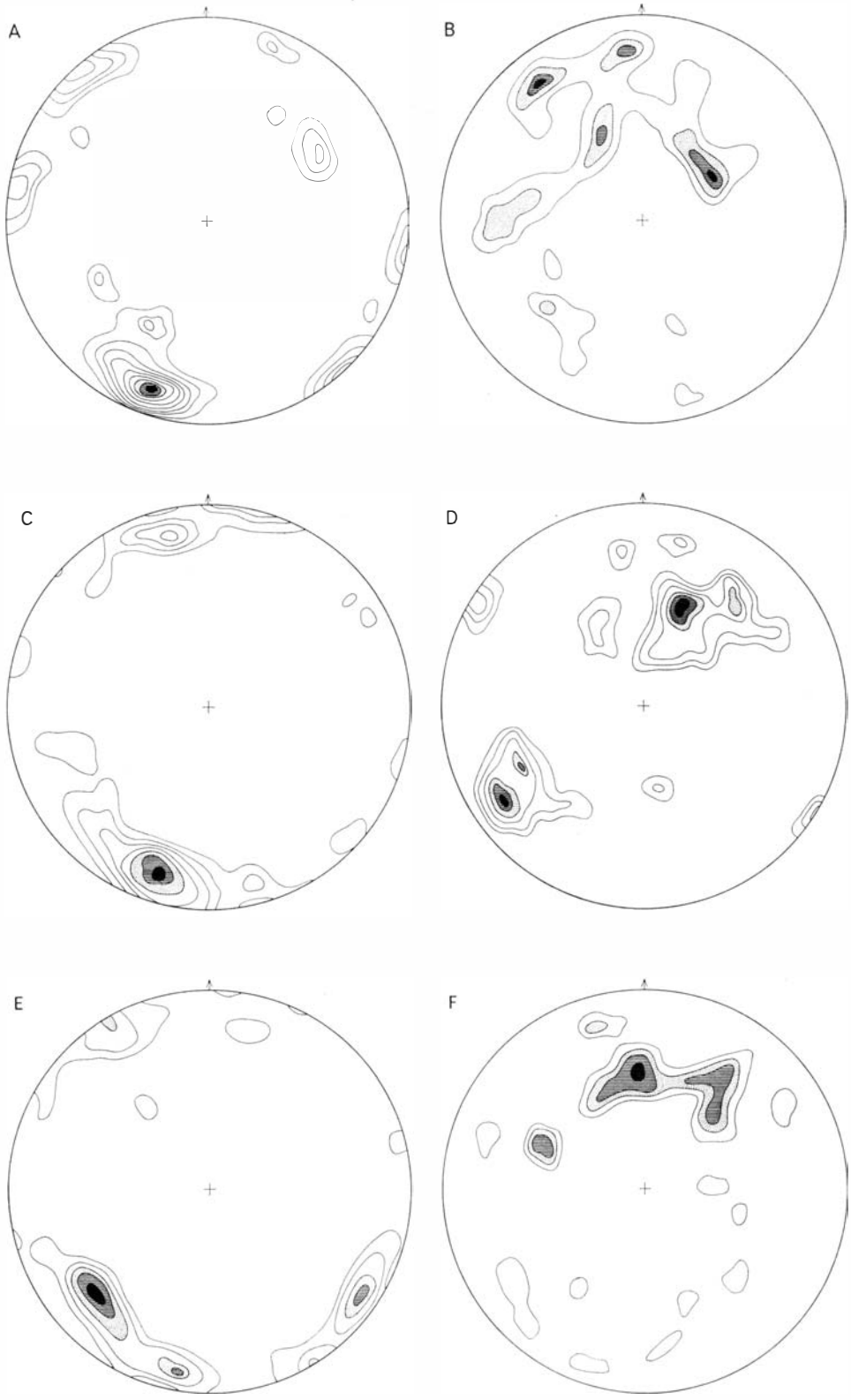

Fig. 9. *Structural elements on Danskøya and Amsterdamøya. Poles to joint planes: A=Amsterdamøya, 121 obs. C=northern Danskøya, 141 obs. E=southern Danskøya, 274 obs. Poles to granitic dykes: B=Amsterdamøya, 84 obs. D=northern Danskøya, 62 obs. F=southern Danskøya, 73 obs. Northern and southern Danskøya refer to the areas north and south of Kobbefjorden respectively. Stereographic projection, lower hemisphere equal area plot. Contours 2, 3, 4, 5, 6, 7, 8, 9, 10% per 1% area.*

The synoptic strike pattern of the dykes suggests that the two conjugated joint systems of the main fold phases F2 and F3 are important in controlling the intrusion tectonics of the granitic dykes (Figs. 4 D and 7).

Mafic dykes

At five localities dioritic to gabbroic dykes of c. ½ m width have been observed. The dykes cross-cut the gneiss with a general SW-NE strike, and display a variation in texture from fine-grained ophitic to medium-grained granoblastic. The specimens examined all contain less than 10% quartz, and hornblende is the main dark mineral. When relations to the post-tectonic granitic dykes were seen, the mafic dykes were always the older. At two localities granitic dykes have "reopened" mafic ones, producing multiple dykes.

The scarcity of mafic dykes and the observed local variation in texture and composition suggest they are products of local magmatic differentiation and of late to post-tectonic age.

Structure

MAIN EVENTS

In the areas of non-gneissic supracrustal Hecla Hoek rocks in north-west Spitsbergen north of Kongsfjorden, the fold style is relatively simple, characterized by open isoclinal folds with gently plunging N-S axes and with limbs parallelling the compositional banding (Fig. 11). Traces of this early (F1) folding may still be seen in the highly metamorphic area of the north-west islands in the regional N-S trend of the marble zones. Superimposed on this early structure is a tight isoclinal folding (F2), with axial trend around NNE-SSW. This fold phase is closely related to the regional metamorphism which produced the NNE-SSW trending biotite gneisses and other paragneisses. The regional gneissosity, which in the north-west islands has a steep dip towards WNW, is parallel to the axial plane of these folds.

The F2 structures were in turn partly refolded by late tectonic (F3) folding. The F3 phase is represented by open folds with a relatively steep axial dip, mainly towards W to NW. F3 anticlines often coincide with migmatitic doming and are evidently related to the development of the more extensive migmatites of the area.

The F1 phase

In the less metamorphic metasediments around and just north of Krossfjorden, the F1 axes have a N-S to NNW-SSE strike. They are horizontal or have gentle plunges towards the south (Fig. 11). In this area the Caledonian metamorphism has made a limited impression on the suprastructure, and subhorizontal undulating beds may in some areas be followed for several kilometers. Towards the north the F1 structure gradually becomes overprinted

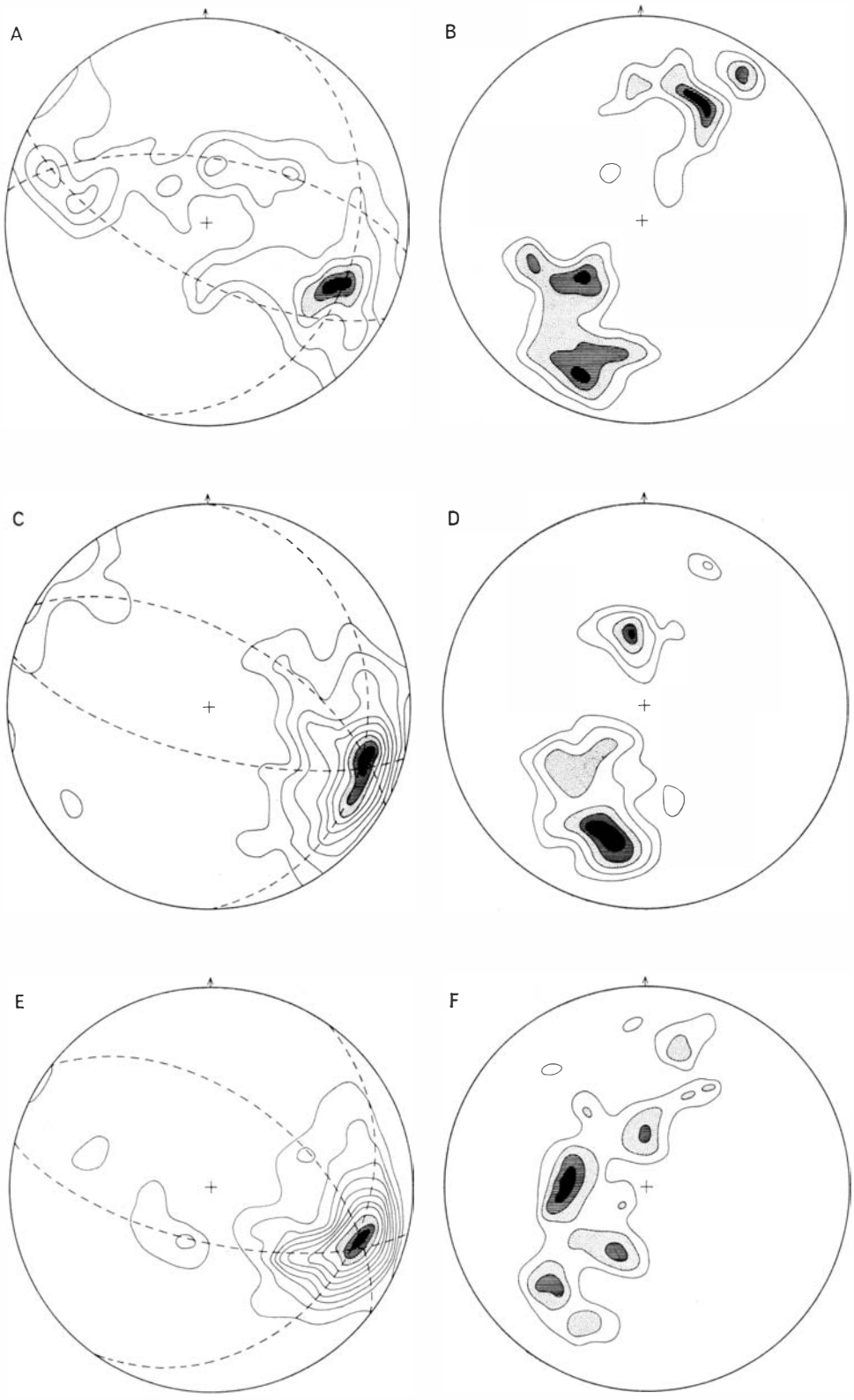

Fig. 10. *Structural elements on Danskøya and Amsterdamøya. Poles to gneissosity and schistosity: A=Amsterdamøya, 188 obs. C=northern Danskøya, 216 obs. E=southern Danskøya, 212 obs. Fold axes and associated linear structures: B=Amsterdamøya, 109 obs. D=northern Danskøya, 127 obs. F=southern Danskøya, 163 obs. – Northern and southern Danskøya refer to the areas north and south of Kobbefjorden respectively. Stereographic projection, lower hemisphere equal area plot. Contours 2, 3, 4, 5, 6, 7, 8, 9, 10% per 1% area.*

by younger structures, and the small-scale F1 patterns gradually become less distinct. Of mesoscopic traceable F1 structures only the regional trend of calcareous restites with associated skarn deposits and biotite-amphibole gneisses remains.

In the strike patterns of gneissosity and of axes of mesoscopic folds (Fig. 4 A, B), the F1 direction is represented by minor maxima around NNW-SSE. A sub-maximum in the same direction which occurs in the topographical strike diagram suggests that the F1 structure only influenced the sculpturing of the north-west islands moderately.

The F2 phase

In an area extending southwards from the north-west coast of Spitsbergen, c. 50 km along the west coast and c. 100 km between Raudfjorden and the innermost part of Kongsfjorden, the structural patterns differ considerably from those in the area around Krossfjorden. The differing patterns are mainly due to a regional development of tight NNE to NE striking isoclinal folds.

It is evident from the observations in the field that, due to difference in competency, this F2 folding is more distinctly developed in gneisses of pelitic origin than in e.g. the marble outcrops. Associated with this folding high-grade metamorphism occurs, resulting in a variety of gneisses and schists. As a result of local mobilization of quartz-feldspathic material, pegmatite and aplite often occur as schlieren parallelling the gneissosity and as fillings in the cores of small folds (Pl. 2 D).

The fold axes are distinctly oblique to the regional compositional banding (F1) and the folding is evidently younger than the latter.

In the north-west islands there is a definite predominance of this super-imposed F2 pattern, which are the most prominent structures of mesoscopic scale in this area (Figs. 4 A, B, and 10). However, despite the pronounced F2 structures, the geographical distribution of the gneiss areas of north-west

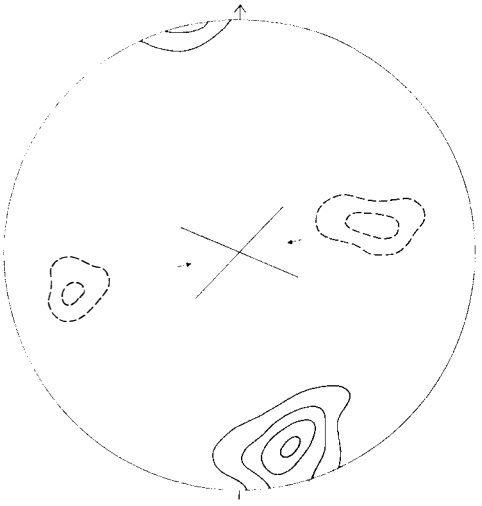

Fig. 11. *Structural elements in the area south and west of Sjettebreen–Lilliehöökbreen–Krossfjorden, observations by* GEE *and* HJELLE *1964. Lines: fold axes and associated linear structures, 221 obs. Broken lines: poles to bedding, schistosity and gneissosity, 242 obs. The main joint system is indicated at the centre of diagram. Stereographic projection, lower hemisphere equal area plot. Contour lines 5, 10, 15 and 20%.*

Spitsbergen as a whole and also of the Horneman granite batholith seems to be largely controlled by the regional NNW-trending F1 structure (Fig. 5).

The wave lengths of the F2 folds range from less than 1 m to more than 1 km, with horizontal or gently plunging axes (Fig. 10). The strike diagrams of the gneissosity and fold axes (Fig. 4 A, B) also display maxima around NNE to NE. These maxima seem to be split into three submaxima, a feature which might be owing to post-F2 refolding of F2-structures and/or to late block movements.

Comparing the gneissosity diagrams of the three subareas, the most pronounced isoclinal development occurs in southern Danskøya, the least in Amsterdamøya. The small fold axes diagram of southern Danskøya show a marked maximum distinctly oblique to F2, i.e. with a steep dip towards the west. The pronounced isoclinal pattern in this area may be due to the combined maxima of the F2 gneissosity and the superimposed gneissosity caused by the younger steep folds.

The F3 phase

In all the pole diagrams of gneissosity, the NNE-striking F2 structure is represented by two girdles (Fig. 10 A, C, E). The trend of the girdles is c. SE-NW, suggesting a later refolding with the main axis in this direction. This coincides well with the other fold axis deduced from the gneissosity diagram. The orientation of the latter, i.e. steeply inclined towards north-west, is remarkably constant in all three subareas, and this confirms the suggested relatively young age of this phase. As the NW-SE folds seem mainly to appear in or near areas of migmatite and synorogenic granitic rocks, a connection between the formation of migmatite and the F3 fold phase is assumed.

The sketch in Fig. 12 shows a tentative explanation of the relationship

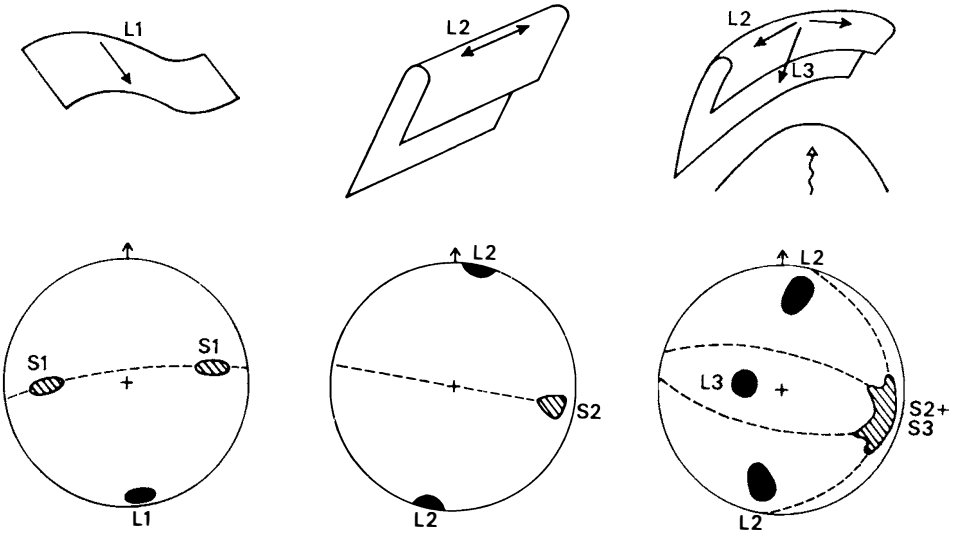

Fig. 12. *Suggested relationship between the different fold phases. Simplified sketch.*

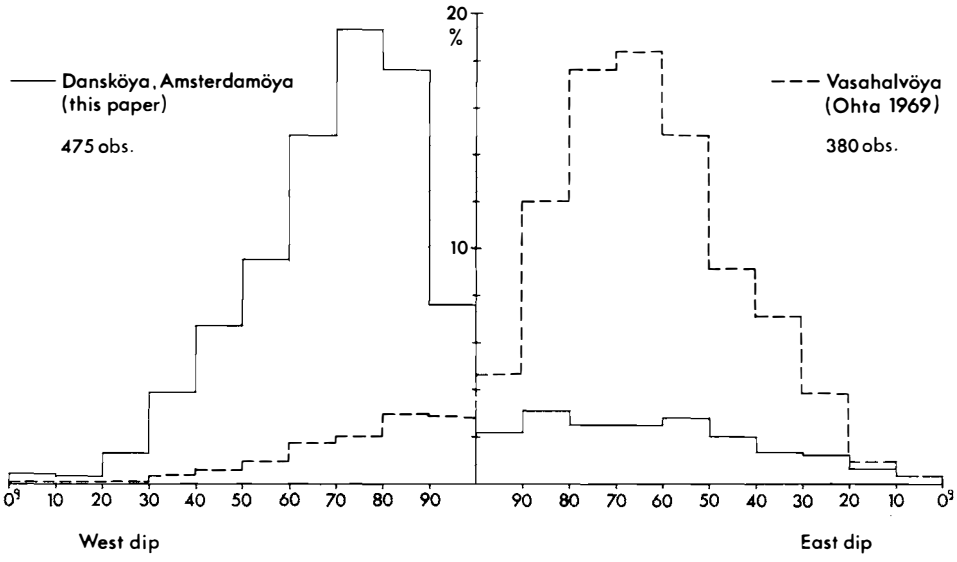

Fig. 13. *Dip of gneissosity planes east and west of Smeerenburgfjorden, considering strikes between 190g (390g) and 260g (60g).*

between the different fold phases. The F1 phase, which plays only a subordinate role in the highly metamorphic areas, is omitted in the two last sketch diagrams. The pronounced F2 gneissosity controls to a great extent the effect of emplacement during the F3 phase, and the fold axes of the latter are on the whole located in the main S2 plane, which dips c. 75g towards WNW. The angle between the two F2 girdles, which vary between 50 and 65g, might to some extent reflect the shape of the migmatitic domes.

The difference in fold style between the F2 and F3 indicates that we are dealing with the superimposition of two different deformations rather than with an interference pattern of two simultaneous deformations.

An identification of some of the main F2 antiforms and synforms was tried, based on comparisons of the dips of the F2 gneissosity planes. The result is presented in Fig. 14. On the same map deduced F3 antiforms and synforms are shown, based on observations of the dip of the distorted F2 fold axes. Although the deduced F2 and F3 synforms and antiforms often lack confirmation by direct observations, their trends correspond well to those deduced from the synoptic gneissosity diagrams in Fig. 4 A and also show similarities to the trend of the small-fold axes (Fig. 4 B).

In contrast to the pronounced west dip of the gneisses in Danskøya and Amsterdamøya, the dip east of Smeerenburgfjorden (OHTA 1969) mainly is to the east (Fig. 13). Mylonitic rocks along parts of the east side of the fjord support the existence of a tectonic discontinuity here (GEE and HJELLE 1966), and an east-dipping thrust plane is suggested. The general structure east and west of Smeerenburgfjorden, and a tentative interpretation of the tectonic development is summarized in Fig. 15.

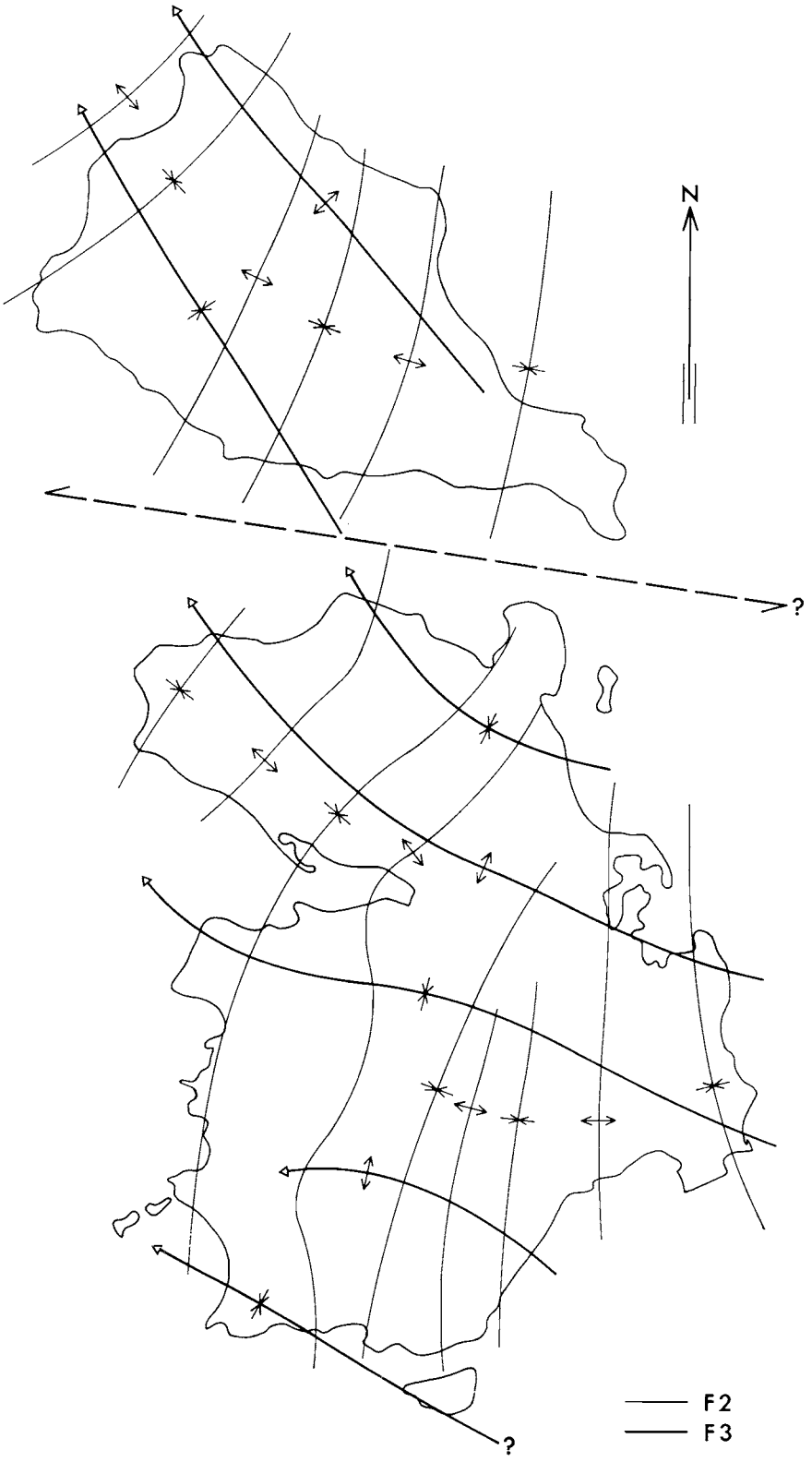

Fig. 14. *Axes of main synforms and antiforms. F2 axes are compiled from F2 schistosity and gneissosity, F3 axes from the distortion of the F2 axes.*

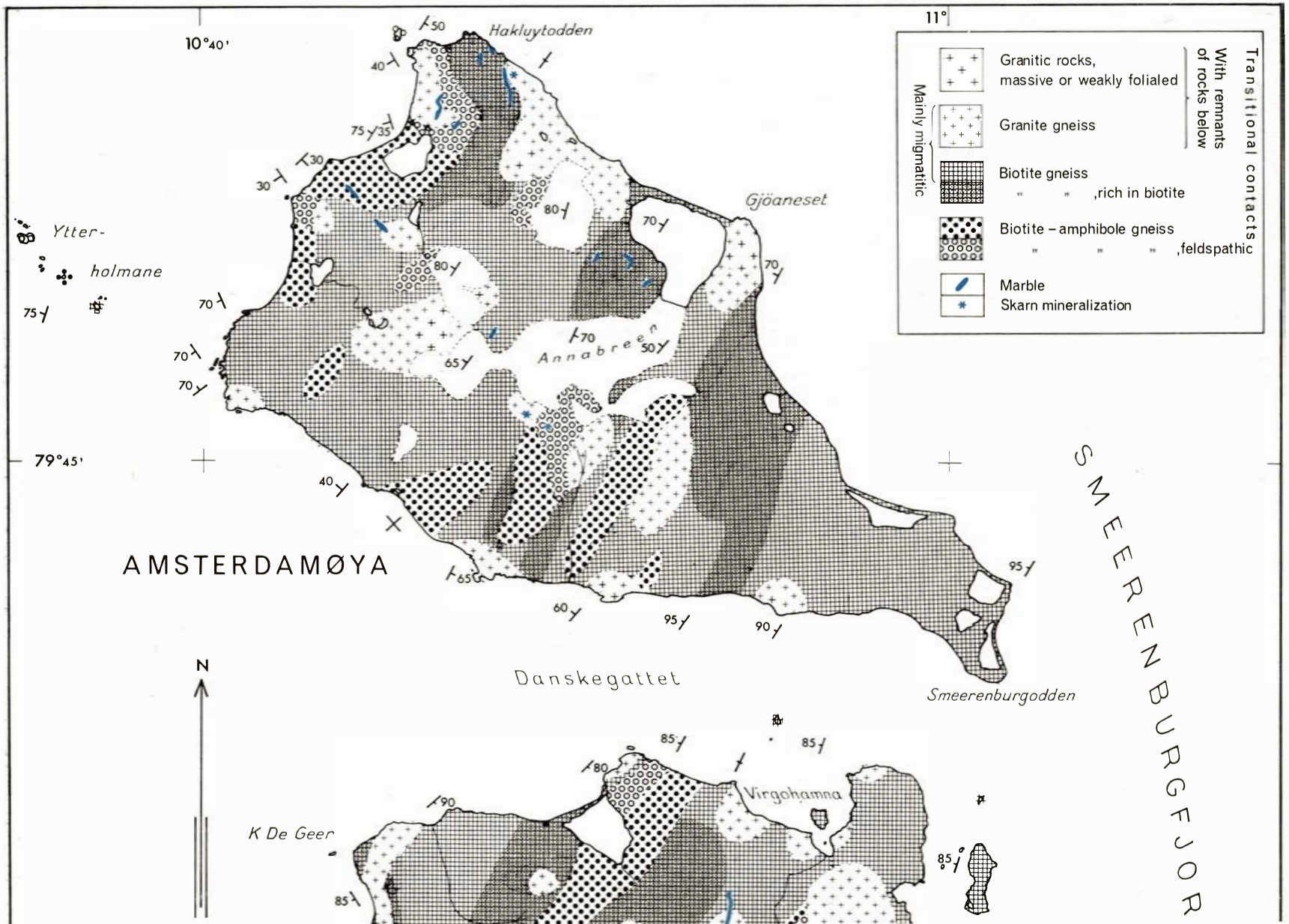
10°40'
11°
79°45'
Hakluytodden
Gjöaneset
Ytter-
holmane
Annabreen
AMSTERDAMØYA
Danskegattet
Smeerenburgodden
SMEERENBURGFJORD
K De Geer
Virgohamna
N
Transitional contacts
With remnants of rocks below
Mainly migmatitic
Granitic rocks, massive or weakly folialed
Granite gneiss
Biotite gneiss
" " ,rich in biotite
Biotite – amphibole gneiss
" " " ,feldspathic
Marble
Skarn mineralization

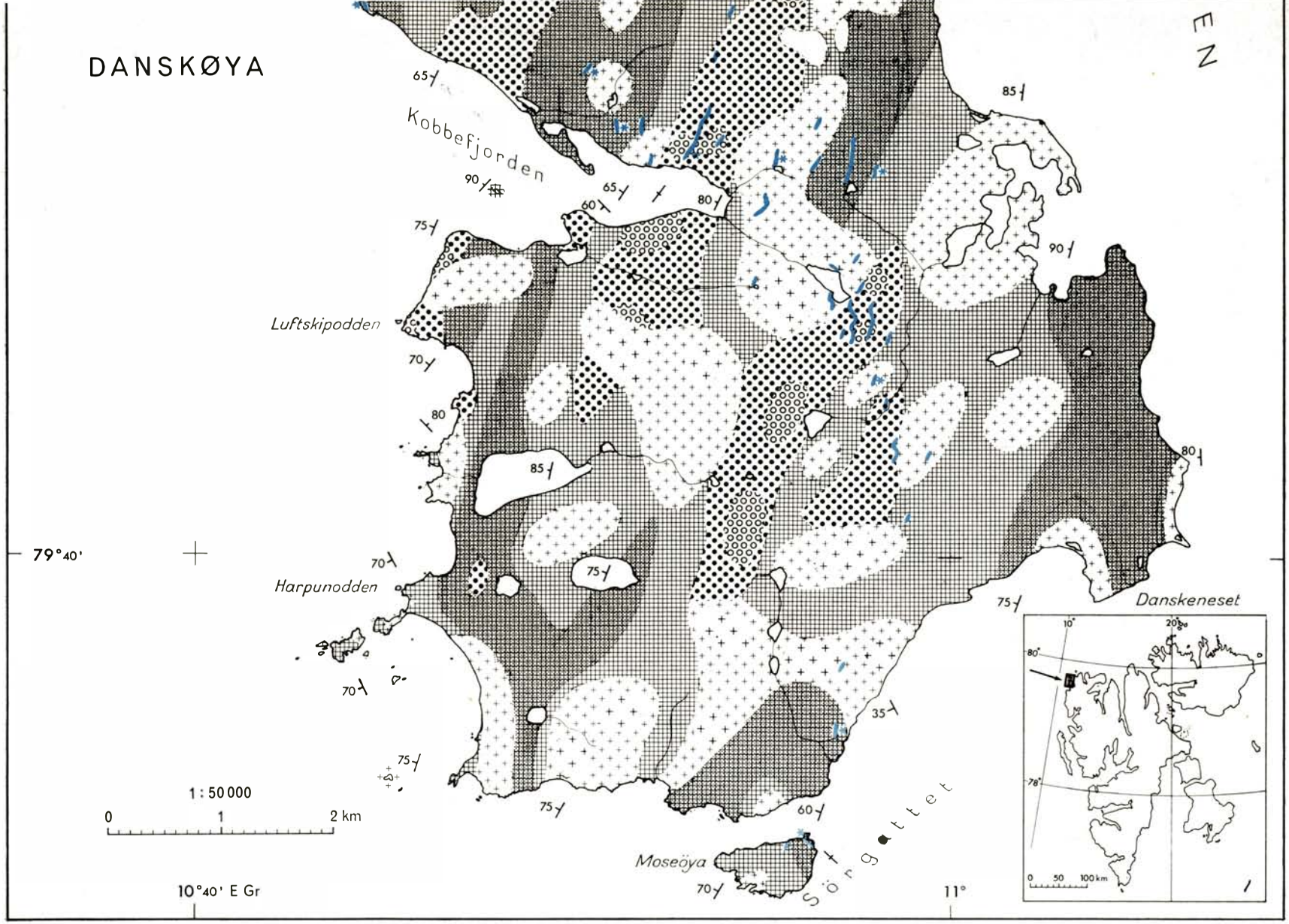

Fig. 16. *Preliminary geological map of Danskøya and Amsterdamøya.*

Joints

The strike diagram of joints in Fig. 4 C shows that the most pronounced maxima have directions around NW-SE, i.e. perpendicular to the strike of the F2 gneissosity and folding. Another, less marked set of joints trends NE-SW, which is approximately perpendicular to the F3 fold axis. This relationship between the main structures and the joint maxima suggests that these represent two conjugate sets of compressive joints around the F2 and F3 stress axes (Fig. 7).

The maxima mentioned above also appear in the stereographic joint diagrams of the three subareas (Fig. 9 A, C, and E), however, these diagrams display in addition marked asymmetrical features, with prominent joint planes dipping steeply to NNE or NE, corresponding to a WNW or NW strike. About two thirds of the small thrusts and faults which are observed along these joints, show a relative movement of the SW-sides towards NW. The WNW-NW direction may also be traced in the topography of north-west Spitsbergen, as in Danskegattet, Kobbefjorden, Bjørnefjorden, and Magdalenefjorden.

Comparing the strike diagrams of jointing and morphologic features (Figs. 4 C and E), the mutual relationship is evident. This suggests the jointing to be one of the main factors affecting the relief of the north-west islands.

Plausible explanations of the pronounced joint maximum are: 1) the maximum represents superimposed maxima of joints developed during both the F2 and F3 fold phases, and 2) the maximum is related to late or post-Caledonian dislocations. Actually, younger dislocation lines trending NNW to NW are rather common along the coast of Spitsbergen, e.g. in the Kongsfjorden area, and the direction also coincides rather well with observed and suggested trends of submarine relief at the mid-oceanic ridges north and west of Spitsbergen.

Metamorphism

In Table 4 the common mineral paragenesis in the metamorphic rocks of Danskøya and Amsterdamøya is listed. The occurrence of sillimanite and cordierite obviously depends largely on the Al content available. However, the paragenesis in general is distinctive of the high temperature range of the amphibolite facies. The occurrence of principal metamorphic minerals also depends on the amount of calcareous material in the original supracrustals. A high content of original Ca would produce relatively more plagioclase, and leave less Al for sillimanite and cordierite formation. With less cordierite formed, more Fe^{2+} and Mg is available for biotite formation. The observations seem to confirm this. The average content of plagioclase is about 40% in the gneisses with no observed sillimanite or cordierite and about 30% in gneisses containing (av. 2% of) these minerals. The average biotite content is c. 20% in cordierite-bearing gneisses and c. 25% in those without. In about $^1/_3$ of the examined thin sections sillimanite and cordierite occur together, indicating a low to medium pressure metamorphism of the Abakuma type

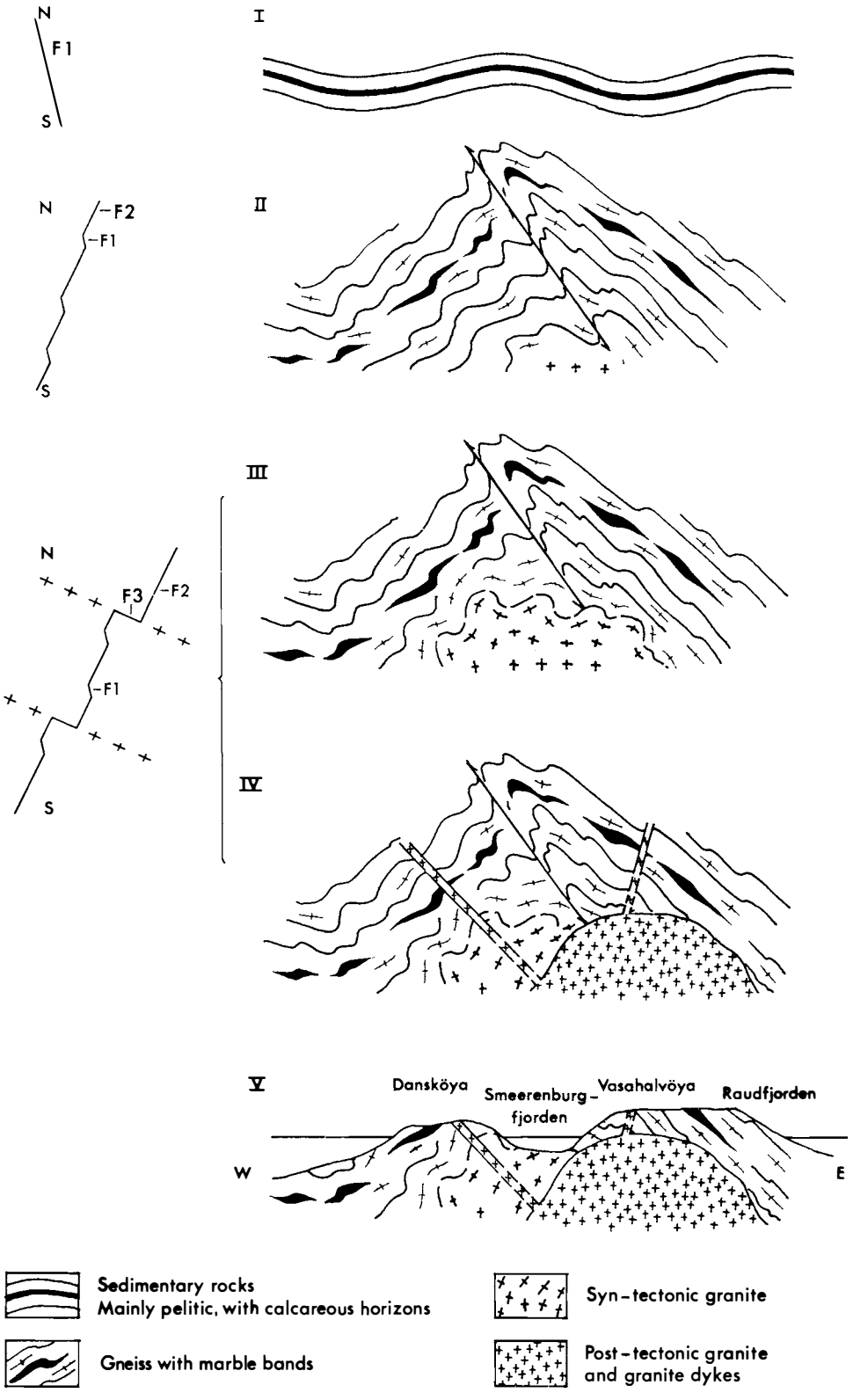

Fig. 15. *Tentative interpretation of the tectonic development in the area around Smeerenburgfjorden.*

(3–3.5 kb, WINKLER 1968). The occurrence of wollastonite in gneisses carrying calcareous restites (p. 17) indicates that the metamorphism took place in the high temperature range of the sillimanite-cordierite-orthoclase-almandine subfacies. This is a condition where at least partial melting of sedimentary rocks of pelitic and psammitic composition would take place and where formation of migmatitic rocks is expected.

Thus, the suggestion that at least some of the migmatites were developed by in situ anatexis with initial PT-conditions about 650–700 °C and 5 kb (p. 24), is in rather good agreement with what is deduced from the mineral paragenesis of the gneisses.

Table 4

Common mineral parageneses of the metamorphic rocks on Danskøya and Amsterdamøya.

Biotite gneiss: Quartz-(microcline)-oligoclase-biotite-almandine-sillimanite-cordierite.
Biotite-amphibole gneiss: Quartz-(microcline)-oligoclase-biotite-hornblende.
Granite gneiss: Quartz-microcline-oligoclase-almandine.
Migmatite metatect: Quartz-microcline-oligoclase-almandine.
Calcareous rocks: Calcite-quartz-diopside-wollastonite-vesuvianite-(sphene-hematite).

Comparison with other metamorphic areas in Svalbard

The metamorphic rocks of Danskøya and Amsterdamøya show the same general structural trend as those of the adjacent areas to the south and east (GEE and HJELLE 1966, OHTA 1969 and 1974. Several fold phases are distinguished, of which the most prominent are: 1) north-south trending folds related to the main Caledonian regional metamorphism of upper amphibolite facies, and 2) south-east – north-west to east-west trending folds related to the later Caledonian feldspathization and migmatitic upwelling of lower amphibolite facies. In the Vasahalvøya, east of Smeerenburgfjorden, a corundum-spinel-(sapphirine?) paragenesis occurs rather commonly in the pelitic rocks, suggesting that the metamorphic grade is somewhat higher than in the two other areas.

Thus it is evident that these three areas of north-west Spitsbergen show essential similarities. Stratigraphically related supracrustals of assumed late Precambrian age were metamorphosed and mobilized in Caledonian time, and now show a rather uniform mineral paragenesis of low to intermediate pressure amphibolite facies.

In the Biskayerhuken area east of Raudfjorden (GEE 1966), and in the south-western part of Ny Friesland (BAYLY 1957), the metamorphic rocks show little evidence of mobilization and migmatization, and only small outcrops of granitic rocks occur within the gneiss areas. The fold pattern shows a pronounced north-southerly trend, and folds with axial directions around east-west, which are frequently developed in the north-west migmatite area, are

absent or poorely developed. The occurrence of kyanite-bearing rocks suggests that these areas have suffered greater overburden pressures than the north-west gneiss region.

South of Biskayerhuken, along Monacobreen, the development seems to be similar to that in the north-west, with granites and gneissic rocks of amphibolite facies in the northern part, near Liefdefjorden, and with a transition into greenschist facies rocks to the south (PRESTON 1959).

Although detailed information from the gneiss areas of Nordaustlandet is still limited, the similarities with the gneiss areas of north-west Spitsbergen are striking (FLOOD et al. 1969). Amphibolite facies paragneisses and migmatites with remnants of meta-supracrustals from the lower part of the Hecla Hoek succession prevail; the gneisses are frequently intruded by granitic rocks. An occurrence of staurolite-andalusite south of Duvefjorden, indicates that the amphibolite facies, at least locally, is of the low to intermediate pressure type. Preliminary structural observations within the gneiss areas suggest that some folds which have a relatively steep plunge towards the south-east may be related to the migmatization.

Acknowledgements

The author wishes to express his thanks to Dr. T. GJELSVIK and Dr. Y. OHTA for criticism and interesting discussions, and to Prof. P. REITAN for critically reviewing the manuscript of this paper.

Acknowledgement is also due to my companions in the field, to the technical staff of Norsk Polarinstitutt, and to Dr. D. WORSLEY who corrected the English language.

References

BAYLY, M. B., 1957: The Lower Hecla Hoek Rocks of Ny Friesland, Spitsbergen. *Geol. Mag.* **94** (5), 377–392.

FLOOD, B., D. G. GEE, A. HJELLE, T. SIGGERUD, T. S. WINSNES, 1969: The geology of Nordaustlandet northern and central parts. *Norsk Polarinstitutt Skr.* nr. 146.

GAIMARD, P., 1855 : *Voyages en Scandinavie, en Lapponie, au Spitzberg et aux Feröe, pendant les années 1838, 1839, et 1840 sur la corvette La Recherche.* Observations géologiques sur la Scandinavie et le Spitzberg, par M. J. DUROCHER. Livraison 29c., 469–478.

GEE, D. G., 1965: A note on the occurrence of eclogite in Spitsbergen. *Norsk Polarinstitutt Årbok* 1964.

— 1966: *The structural geology of the Biskayerhuken peninsula, north Spitsbergen.* Unpubl. Ph. D. thesis, University of Cambridge.

GEE, D. G. and A. HJELLE, 1966: On the crystalline rocks of northwest Spitsbergen. *Norsk Polarinstitutt Årbok* 1964. 31–45.

HARLAND, W. B., 1960: The development of Hecla Hoek rocks in Spitsbergen. *Report of the 21st International geological congress*, part 19. 7–16.

— 1961: An outline structural history of Spitsbergen. *Geol. of the Arctic.* **1**. 68–132. Univ. of Toronto Press.

HARLAND, W. B., R. H. WALLIS, R. A. GAYER, 1966: A revision of the Lower Hecla Hoek succession in central north Spitsbergen and correlation elsewhere. *Geol. Mag.* **168** (1). 70–97.

HJELLE, A., 1966: The composition of some granitic rocks from Svalbard. *Norsk Polarinstitutt Årbok* 1965. 7–30.

HOEL, A., 1914: Exploration du Nord-ouest du Spitsberg (Mission Isachsen). *Res. des campagnes scient. du Prince de Monaco.* **XLII** (III). Géologie.

HOLTEDAHL, O., 1914: New Features in the Geology of Northwestern Spitsbergen. *Am. J. Sci.* Ser. 4, **37** 415–24.

— 1926: Notes on the Geology of Northwestern Spitsbergen. *Result. av Statsunderst. Spitsbergeneksp.* **1** (8). 1–28.

KRASIL'ŠČIKOV, A. A., 1965: Nektorye osobennosti geologičeskogo razvitija severnoj časti arhkipelaga Špicbergen. *Materialy po geologii Špicbergena.* Naučno-issledovatel'skij institut geologii Arktiki. Leningrad. (In Russian.) [Some aspects of the geology of the northern part of Spitsbergen.]

LIESTØL, O., 1972: Submarine moraines off the west coast of Spitsbergen. *Norsk Polarinstitutt Årbok* 1970. 165–168.

OHTA, Y., 1969: The geology and structure of metamorphic rocks in the Smeerenburgfjorden area, north-west Vestspitsbergen. *Norsk Polarinstitutt Årbok* 1967. 52–72.

— 1974: Tectonic development and bulk chemistry of rocks from the Smeerenburgfjorden area, Spitsbergen. *Norsk Polarinstitutt Skr.* nr. 158 (this volume).

— 1974: Geology and structure of the Magdalenefjorden area, Spitsbergen. *Norsk Polarinstitutt Skr.* nr. 158 (this volume).

PLATEN, H. v. and H. HÖLLER, 1966: Experimentelle Anatexis des Stainzer Plattengneises von der Koralpe, Steiermark, bei 2, 4, 7 und 10 kb H_2O-Druck. *N. Jb. Miner. Abh.* **106**. 106–130.

PRESTON, J., 1959: The geology of the Snøfjella and Dovrefjella in Vestspitsbergen. *Geol. Mag.* **96**. 45–57.

SCHENK, E., 1937: Kristallin und Devon im nordlichen Spitzbergen. *Geol. Rdsch.* **28**. 112–24.

SCHETELIG, J., 1912: Exploration du Nord-Ouest du Spitsberg (Mission Isachsen). *Res. des campagnes scient. du Prince de Monaco.* **XLIII** (IV). Les Formations Primitives.

STRECKEISEN, A. L., 1967: Classification and Nomenclature of Igneous Rocks (Final Report of an Inquiry). *N. Jb. Miner. Abh.* **107** (2, 3). 144–240.

TVETEN, E., 1973: The geology of Mitrahalvøya, north-west Spitsbergen (in prep.).

WINKLER, H. G. F., 1967: *Petrogenesis of metamorphic rocks.* Revised second edition. (Springer Verlag).

Geology and structure of the Magdalenefjorden area, Spitsbergen

By

YOSHIHIDE OHTA

Abstract

Lithology and geologic structure of the metamorphosed Hecla Hoek rocks in the Magdalenefjorden area, NW Spitsbergen, are described based on the field survey of 1968. The rocks were highly metamorphosed under conditions of the upper amphibolite facies, and a large amount of syntectonic grey granite and associated migmatites occur very widely in the central part of the mapped area. Several deformation phases with different metamorphic conditions are distinguished and are synthesized into the tectonic development of Caledonian orogeny in NW Spitsbergen.

Аннотация

На основе полевой съемки 1968-го года описаны литология и геологические структуры метаморфизованных пород комплекса Гекла-Хук района Magdalenefjorden на северо-западе Шпицбергена. В условиях верхней амфиболитовой фации породы подверглись высокой степени метаморфизма и в большом количестве распространены очень широко в центральной части картированного раиона синтектонический серый гранит и ассоциированные с ним мигматиты. Выделено несколько деформационных фаз с разными метаморфическими условиями, синтезированных в тектоническое развитие каледонского орогенеза северо-запада Шпицбергена.

Introduction

One of the most beautiful fjords on the western coast of Spitsbergen, Magdalenefjorden, and its adjacent areas were mapped during the 1968 expedition of Norsk Polarinstitutt.

The outline of geology of this area is presented by GEE and HJELLE (1966) in their geological map of northwest Spitsbergen. This knowledge is limited to the western coast, including pelitic crystalline schists around Hamburgbukta, and a migmatite region which also includes a marble layer on Knatten and some amphibolites east of Bjørnhamna.

During the summer of 1968, the present author mapped Reuschhalvøya, the northern half of Hoelhalvøya and Losvikfjella around Magdalenefjorden. This report, based totally on field observations, presents a geological map with estimated lithologic successions of the metasediments and some information on the Caledonian tectonic events in this area evaluated from the structural studies.

I. Geological setting

The mapped area is situated in the northern part of the Northwest Anticlinorium of the Caledonian poly-orogeny (HARLAND 1961); the axis of the Anticlinorium plunges south from the northwestern end of Spitsbergen to Kongsfjorden (Fig. 1, Location map). Thus, while the upper stratigraphic and tectonic successions are exposed in the south, the rocks of the present area are regarded as metamorphosed lower Hecla Hoek.

The reconnaissance work of GEE and HJELLE (1966) elucidated a general stratigraphic succession for the Northwest Anticlinorium. They introduced the Nissenfjella formation to include the rocks of the present region and correlated this unit with the Finnlandveggen series of Ny Friesland.

The grade of metamorphism increases from the south to the north and the rocks of the present area are mostly of amphibolite facies associated with a large amount of migmatites and Caledonian granites. There is no detailed work on the adjacent area to the south. In the north some detailed mapping has been done in Danskøya and Amsterdamøya (HJELLE, 1974) and on the eastern side of Smeerenburgfjorden (OHTA, 1969). The present study is a link in the regional work on the highly metamorphosed region of the Northwest Anticlinorium to establish the tectonic history of Caledonian orogeny of this region.

II. Lithological descriptions

A. CLASSIFICATION

The meta-sediments of the present area are so intensely metamorphosed that the grouping of rocks is largely based on the mesoscopic texture, with the aid of metamorphic index minerals.

1. Fine-grained gneisses
   a. Pelitic biotite schist
   b. Fine-grained biotite gneiss
   c. Felsic gneiss and quartzite.
2. Layered gneisses, amphibolites, marbles and skarns
3. Plagioclase porphyroblastic gneiss and nebulitic gneiss
4. Migmatites
5. Grey granite
6. Pink coloured aplite and pink nebulitic gneiss

Descriptions of these rocks will be presented below based only on the field observations.

1a. Pelitic biotite schist

This is an almost black rock, rich in biotite, having a strong schistose cleavage; it alternates locally with thin layers of fine-grained biotite gneiss with a relatively felsic composition (Pl. 1–1). Weak graded bedding structure is sometimes observed in this alternation. Schistose cleavages are parallel to the axial surface of drag-type tight folds which are well seen in the felsic biotite gneiss. Biotite flakes are strongly oriented parallel to the cleavage. Garnet grains occur showing spotted structure on the cleavage plane. A few amphibolite blocks of round or boudinage shape follow the schistosity. Many irregular layers and dykes of grey granite cut roughly along the cleavage and joints of the pelitic schist; their pinch and swell structures cause gentle undulations of the cleavages.

1b. Felsic biotite gneiss and quartzite

These rocks often occur together in alternating and gradational layers. They are fine-grained dense rocks. They dominate no region and are not distinguished on the map, but have a tendency to occur more frequently in the upper structural succession than in the lower one (see next chapter). Most of these rocks are rich in quartz and have subordinate amounts of feldspars and biotite; garnet is occasionally found. Cleavages are weak, while the compositional layering is distinct. Sometimes structures that appear to be graded bedding and cross laminae are seen. Very tight asymmetrical and isoclinal small folds are observed in these rocks and weak axial surface cleavages occur only in the fold crests. Pure quartzite is rare, but impure quartzite with less than 20% feldspars and biotite occurs very often. These quartzitic rocks are frequently met with in the layered gneisses and migmatites as thin layers.

2. Layered gneisses

These are the most common rocks in the mapped area, having a wide range of mineral composition from micaceous to quartzitic varieties. A distinct compositional layering is characteristic in these rocks and their grain size is several times coarser than the fine-grained gneisses although there are gradational transitions.

Micaceous layered gneiss is the most dominant rock with well developed thin alternation of mica-rich and quartzo-feldspathic layers. Cleavages are also distinct parallel to the layering. Biotite is the predominant mafic constituent and garnet, cordierite, and sillimanite are often observed. Sillimanite is especially abundant where the rock shows strong chevron folds (Pl. 1—2). Prisms of corundum (a few cm long) were found in the eastern side of Waggonwaybreen.

The fine-grained gneisses, often observed in the centre of relatively thick micaceous layered gneiss layers, sometimes show rootless isoclinal folds. The

quartzo-feldspathic layers have similar grain size of constituent minerals as those in the micaceous layers and show gradational transition to the latter. Lensoid or irregular pools of quartzo-feldspathic material often have cordierite aggregates and rarely radial clusters of tourmaline. Red garnet grains are also scattered in the quartzitic layers.

There are many sub-parallel discontinuous layers of quartz-dioritic composition, which have sharp contacts with the surrounding layered gneisses, sometimes slightly oblique to the layered structure (Pls. 1—3 and 1—4). These leucocratic layers have a coarse-grained granitoid texture and have more plagioclase and less biotite than the quartzo-feldspathic part of the layered gneisses. The foliation is very weak. They are folded together with the layered gneisses in tight isoclinal style. Plagioclase porphyroblasts occur very often in the micaceous layered gneiss near granitoid layers.

This evidence suggests that the layered structure developed along the axial surfaces of isoclinally folded fine-grained gneisses, succeeded by post-deformational grain coarsening under the metamorphic conditions of the upper amphibolite facies. The small folds of layered gneisses were formed after the format tion of layered structure and the granitoid layers were intruded in the incipien- stage of the development of small folds.

3. Amphibolites and marbles

The amphibolites occur as lensoid and irregular shaped blocks of less than a few metres maximum dimension, but they are mostly thin layers concordant with the layered structure of micaceous gneisses, while they are sub-angular blocks in siliceous migmatitic rocks. They consist of medium- to coarse-grained granoblastic gneissose rock with various amounts of biotite and quartz, besides the main constituents of hornblende and plagioclase.

Hornblende-bearing biotite gneiss with inclusions of thin amphibolite layers often occurs in the micaceous layered gneiss.

The amphibolite at about 1.5 km N of Hamburgbukta is not gneissose and shows local ophitic texture. This seems to be a later intrusion than all the other amphibolites which were metamorphosed together with surrounding layered gneisses, but is definitely earlier than the intrusion of grey granite which sent small veins into the ophitic amphibolite.

Marbles occur as thin layers, up to 4–6 metres thick, and are often discontinuous in the layered gneisses. This rock is mostly banded with medium- to coarse-grained calcite layers and quartz-rich siliceous layers. The latter are always thin (3–10 cm) and accompany thin discontinuous dark bands of diopside and garnet. Vesuvianite and wollastonite are observed in some realtively thick parts of the skarn layers. Some skarn layers have thin amphibolites around them, showing gradual composition change, and some amphibolites having a skarn core are also found in the layered gneisses and migmatites. An anthophyllite-fels was found in the E side of Evatindane around a thin marble.

The skarn lenses occurring along both sides of Miethebreen are hedenbergite-grossuralite-epidote skarn. Pyrite, chalcopyrite, magnetite and their

secondary products of acicular heamatite and malachite have been identified from the skarns. These skarns occur along a shear zone and are very closely associated with the pink aplite.

4. The plagioclase porphyroblastic gneiss and nebulitic gneiss

Plagioclase porphyroblastic gneiss has characteristic sub-angular and ovoidal white plagioclase grains of up to a few cm long in a matrix of normal micaceous layered gneiss (Pl. 2–2). These plagioclase porphyroblasts occur in the layered gneiss around the granitoidal layers and in the gneissic paleozomes of various migmatites. They also occur in the granitoid layers, in some parts of the migmatitic metatect, and in the grey granite. It is evident that one of the porphyroblastesis of plagioclase was associated with the granitoidal layer which was formed in the earlier stage of folding of the layered gneisses.

The nebulitic gneiss occurs in the transitional zone between the layered gneisses and grey granite. This rock shows faint shadow structures of small folds and compositional layering, and quartz and feldspar are more abundant than in the layered gneisses (Pl. 2–3); thus, the structures of this rock are always faint. The gneissic rocks in the grey granite are mostly this kind. A shadowy agmatitic texture is also seen in the nebulitic gneiss (Pl. 2–4). The distribution and relict structures of the nebulitic gneiss suggest that this rock is a product of quartz-feldspar enrichment derived from the grey granite, uniformly infiltrating the whole rock after the formation of layered gneisses and agmatitic migmatites. The gneissic paleozomes of nebulitic migmatite have an appearance similar to the nebulitic gneiss. Biotite is the only visible mafic constituent in this rock.

5. The migmatites

Two types of occurrence of migmatite are distinguishable: (a) in concordant alternations with layered gneisses and (b) as transitional rocks between the layered gneisses and grey granite.

The migmatites of type (a) occurrence mostly have an agmatitic structure with a heterogeneous, weakly gneissose, quartz-dioritic metatect and gneissic paleozomes of micaceous layered gneiss and amphibolite. The paleozomes are ovoidal to sub-angular in shape, up to several metres long, and are rotated in the metatect (Pls. 4–3, 4–4). Plagioclase grains are distributed heterogeneously in the metatect and round quartz pools of 20 to 40 cm in diameter occur locally. Impure quartzite layers often occur concordantly with the metatect gneissosity.

From these observations, it is thought that the migmatites of type (a) occurrence were derived from arenaceous sediments that alternated with the argillaceous layers.

The migmatites of type (b) occurrence show more variety than those of the type (a) occurrence. A gradational change from diktyonite (Pl. 2–1), through agmatite, to nebulite (Pl. 4–1) is often observed around the grey granite masses. The fine-grained gneisses of quartzitic composition show

agmatitic structure at the contact with the grey granite (Pl. 4–2). A distinct small folded polyvenite occurs around the NW corner of Hoelhalvøya. All these varieties of migmatites of type (b) occurrence suggest that the grey granite was essentially intrusive into the surrounding gneisses. Biotite is the dominant mafic constituent and cordierite clusters are sometimes seen in all migmatites.

6. The grey granite

This is a homogeneous, white to grey rock with a well developed systematic joint system. The composition is a biotite quartz-diorite. Very faint foliation is observed everywhere and is represented by thin layers of quartz-rich and biotite-rich layers. Marginal parts of the grey granite masses are often characterized by the occurrence of scattered sub-angular plagioclase grains. Small lensoid and streaky masses of micaceous gneiss are rarely included in the granite. A few white aplite veins some tens of cm thick occur elsewhere, but no pegmatite has been found in the grey granite.

7. Pink aplite and pink nebulitic gneiss

Both of these rocks are characterized by pink coloured potash feldspar and are fine- to medium-grained rocks of restricted occurrence. The pink aplite occurs as narrow veins up to 3 m thick and is mainly composed of quartz and pink potash feldspar, with small amounts of white plagioclase and biotite. These veins occur along a shear zone roughly parallel to the gneissosity of surrounding rocks in the eastern side of Alkebreen and are associated with the skarn masses (see pp. 42-43).

The pink nebulitic gneiss is a hornblende-bearing biotite gneiss showing only faint compositional layering because of even distribution of pink potash feldspar in the whole rock. The leucocratic layers of this rock are very similar to the pink aplite.

Pink potash feldspar is never found in the gneisses, migmatites or grey granite of the present area, and occurs only in the Hornemantoppen granite, which is widely distributed outside and to the east of the mapped area.

C. SUMMARY OF PETROGRAPHY

The fine-grained gneisses are the oldest rocks distinguishable in the mapped area. They vary from extremely pelitic to more or less quartzitic rocks and are associated with small amounts of marble and amphibolite. All these rocks are relics from successive grain coarsening and migmatization. The isoclinal rootless folds of these rocks suggest that the deformation that accompanied the formation of these rocks was very strong. Characteristic metamorphic minerals of these rocks are biotite, garnet, hornblende, and diopside, indicating a metamorphic grade of lower amphibolite facies.

The layered gneisses are characterized by coarse grain size and distinct compositional layering parallel to the axial surface of isoclinal rootless folds of the fine-grained gneisses. The occurrence of biotite, garnet, cordierite, sillimanite, and corundum indicate the upper amphibolite facies. Basic rocks were transformed into gneissose amphibolite and the marbles gave rise to skarns with diopside-grossuralite-wollastonite paragenesis through reaction with the surrounding rocks under these metamorphic conditions.

Small tight folds were formed later than the formation of layered gneisses, and the granitoid layers intruded in the early stage of this deformation, accompanying plagioclase porphyroblastesis.

The arenaceous layers were converted into quartz-dioritic migmatite during the period of layered gneiss formation and were mobilized to form agmatite.

Various kinds of migmatites were formed during the emplacement of grey granite masses in the central zone of the mapped area and the introduction of quartz and feldspars from the granite resulted in the nebulitic gneiss. The metamorphic conditions were not higher than the lower amphibolite facies during this period.

The last plutonic event in this area was the injection of the pink aplite veins along shear zones associated with a special type of skarn deposit and pink nebulitic gneiss. This event seems to be closely connected to the emplacement of the Hornemantoppen granite in the eastern part of the mapped area.

III. Distribution of rocks and litho-stratigraphy

A. DISTRIBUTION OF ROCKS

The metamorphic rocks and migmatites occur dominantly as two zones in both eastern and western parts, and the grey granite occupies the central part of the mapped area, all the zones following a NNE-SSW trend (Fig. 3). This zonal distribution of rocks matches well across opposite sides of Magdalenefjorden. The western gneiss-migmatite zone is the southern continuation of similar rocks on Danskøya (HJELLE 1974), and the eastern gneiss-migmatite zone is the southern extension of the rocks of the Smeerenburgfjorden area (OHTA 1969).

1. The fine-grained gneisses

The pelitic biotite schist occurs in a narrow area along the west coast of the Hoelhalvøya (main place-names in Fig. 4), separated from other rocks by a narrow intrusion of grey granite and amphibolite. This rock is situated in the uppermost structural position in the profile along the southern side of Magdalenefjorden (Fig. 3).

Fine-grained biotite gneiss, felsic gneiss, and quartzite occur together as thin, alternating layers throughout the micaceous layered gneisses. They occur very frequently in the layered gneisses of the eastern gneiss-migmatite zone. They are observed as relatively thick layers in three areas: both sides of the northern part of Alkebreen, Knatten in the SW corner of Reuschhalvøya, and

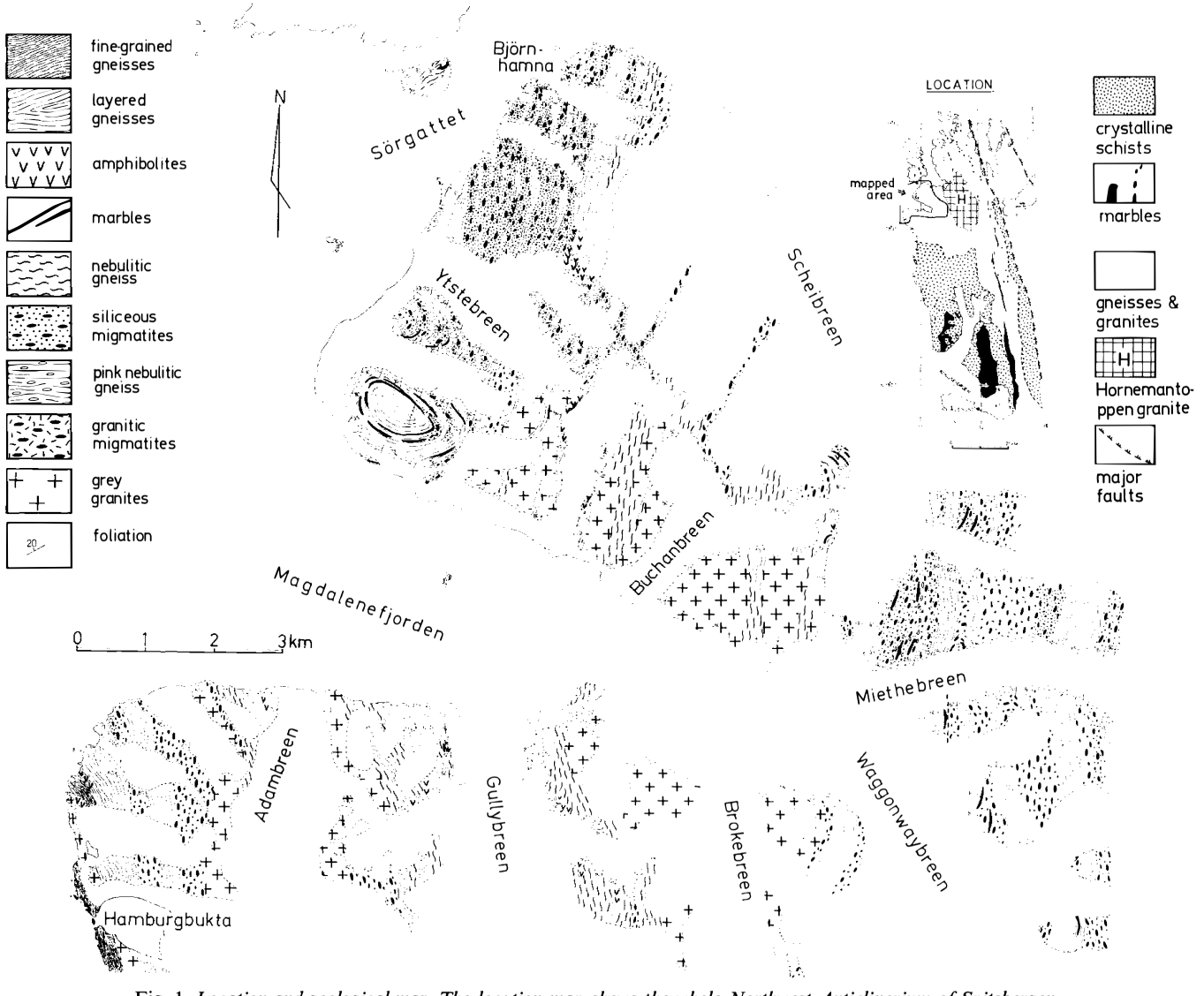

Fig. 1. *Location and geological map. The location map shows the whole Northwest Anticlinorium of Spitsbergen.*

the northern sides of Evatindane and Adamsteinen on the southern side of Magdalenefjorden; the latter two localities may be continuous. These rocks generally dominate the upper structural position, although the lithostratigraphic position of the rocks on the southern side of Magdalenefjorden is unknown because of the intrusions of grey granite. Marble, skarn, and some amphibolites occur together with these rocks.

2. The layered gneisses, amphibolites and marbles

These rocks occur as the main constituents of both the eastern and western gneiss-migmatite zones. They alternate with migmatites a few to several hundred metres thick and follow the general structural trend; the thickest lithologic succession was observed in the northern half of Reuschhalvøya (Fig. 2, a and b). The alternation of layered gneisses and migmatite is considered to reflect the original lithologic succession of sediments.

Amphibolite and hornblende-bearing micaceous gneiss occur very often in the layered gneisses in the middle part of lithologic successions from Reuschhalvøya and the Gullybreen area in Hoelhalvøya. A few amphibolites occur in the eastern gneiss-migmatite zone. The trend of the amphibolites (N-S) is slightly oblique to the general structural trend (NNE-SSW) followed by the alternating layered gneisses and migmatites (Fig. 1). The amphibolites are always fragmented into large or small blocks both in the layered gneisses and migmatites.

This evidence suggests that the amphibolites are evidently of pre-metamorphic origin and not effusive rocks but intrusive sills at different stratigraphic positions almost parallel to the original sedimentary rocks. It is less possible that the large scale alternation of layered gneisses and migmatites is totally of a metamorphic differentiation origin and that the trend of amphibolites shows the primary stratification of the original sediments (Fig 2).

The correlation of lithologic successions between the eastern and western gneiss-migmatite zones is difficult because the eastern zone lacks any distinct amphibolite, and the occurrence of many shear zones on the eastern side of Alkebreen indicates that a structural gap may pass along the western side of Alkebreen and Waggonwaybreen following the eastern border of the central grey granite zone.

The most distinct layers of marble occur in Knatten, at the SW corner of Reuschhalvøya where the following succession was observed (Pl. 2-1):

Upper layered gneisses:	100 m
3 marble layers with intercalated layered gneisses and fine-grained biotite gneiss:	10 m
siliceous layered gneiss:	80 m
small-folded micaceous layered gneiss:	100 m
siliceous migmatite:	50 m
(several dm unexposed)	
Lower layered gneisses with a marble layer:	several metres thick

The northern extension of these marbles is observed in the western part of Ytstekollen. These marbles occur in the synclinal depression along the western shore of Reuschhalvøya, and belong to the upper part of the lithologic succession (Fig. 2, c and d). A small discontinuous marble occurs in the eastern part of Moseøya in Sørgattet and is certainly the northern extension of those in Knatten. This trend of marble extends to Danskøya to the north of the present area with N-S strike parallel to the general large scale trend of folded original sediments as seen in the eastern half of the Northwest Anticlinorium (Fig. 1, Location map).

A few thin layers of marble occur on the western side of Alkebreen, where they alternate with the fine-grained gneisses and layered gneisses. Lithologically, this succession may be correlated with the upper lithologic succession (Fig. 2, f).

The calcareous rocks of the eastern gneiss-migmatite zone marked on the geological map are not regarded as a significant lithologic member because of their later origin (see pp. 42-43).

3. The migmatites, plagioclase porphyroblastic gneiss and nebulitic gneiss

The migmatites of the type (a) occurrence outcrop as distinct wide zones in both the eastern and western gneiss-migmatite zones and are shown on the geological map (Fig. 1), while those of the type (b) occurrence are mostly too small to be shown on the map. The plagioclase porphyroblastic gneiss also occurs in very small scattered bodies in the layered gneisses. The nebulitic gneiss mostly occurs in the grey granite. The migmatites of type (a) occurrence are reasonably well fixed in the lithologic succession, but the others are not as they are closely related to the emplacement of grey granite.

4. The grey granite

This rock occurs widely in the middle of the mapped area and has a wider distribution to the north than to the south of Magdalenefjorden. The grey granite mass is a large wedge-shaped layer concordant with the surrounding rocks, but is split into several narrow zones in the western gneiss-migmatite zone. The eastern boundary of the grey granite, i.e., the structurally lower contact, is relatively sharp.

5. The pink aplite and pink nebulitic gneiss

The pink aplite veins and pink nebulitic gneiss occur along a shear zone in the western part of the eastern gneiss-migmatite zone. Another locality of the pink nebulitic gneiss is along the western border of the largest grey granite mass. Since they are the rocks of the latest origin in this area, their distribution has no litho-stratigraphic significance but is indicative of a structural gap.

B. LITHOSTRATIGRAPHY

The lithologic succession determined is shown in Fig. 2. From this and the distribution of rocks, the general lithostratigraphic succession is as follows:

Upper group:	areno-argillaceous gneisses, relatively rich in fine-grained gneisses, and characterized by the intercalation of marble layers	> 500 m
Lower group I:	thick alternations of micaceous layered gneiss and siliceous migmatite Pelitic biotite schist is tentatively grouped in the upper part of this group.	>1000 m
Lower group II:	layered gneisses and migmatites characterized by intercalations of amphibolite layers	> 800 m
Lower group III:	thick alternations of layered gneisses and migmatite	> 500 m

The thickness is mostly obtained from the succession in the western gneiss-migmatite zone and is difficult to estimate in the area where the grey granite occurs. The succession of the eastern gneiss-migmatite zone is not comparable to that given above.

In regional correlation with the succession given by GEE and HJELLE (1966), the intercalation of marble suggests that the upper group is equivalent to the Generalfjella formation; the lower group II is correlated with the Nissenfjella formation because of frequent intercalations of amphibolite, and the lower

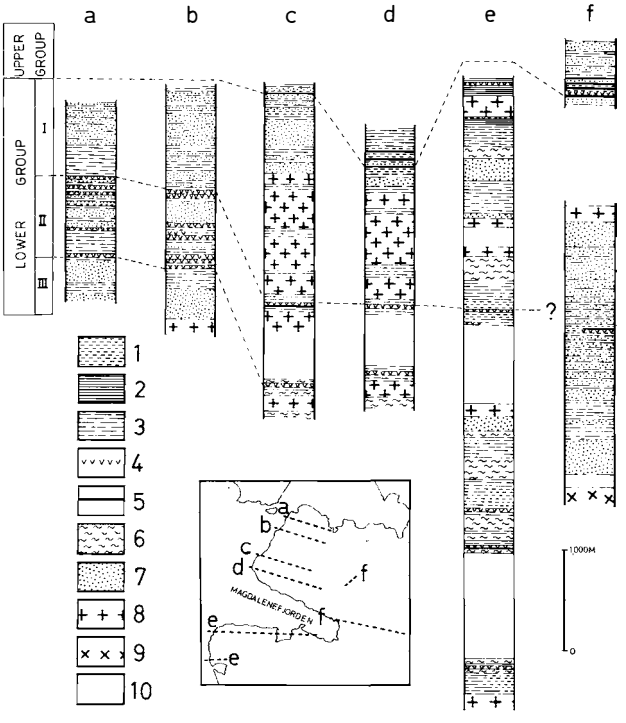

Fig. 2. *Lithological successions of the metamorphic rocks. 1. fine-grained gneisses, 2. pelitic schists, 3. micaceous layered gneisses, 4. amphibolites, 5. marble, 6. nebulitic gneisses, 7. siliceous migmatites, 8. grey granite, 9. Hornemantoppengranite, 10. unexposed.*

group I may be equivalent to the Signehamna formation. The lower group III, which is dominantly migmatite, is believed to be modified Nissenfjella formation.

The marble-bearing upper group may be correlative with the marble-bearing rocks of Vasahalvøya (Fig. 1, Location map), which are discontinuously traceable to the SSE on the eastern side of Kongsfjorden. If the marble-bearing successions on the northern side of Kongsfjorden are equivalent to the upper group of the present area, the metamorphism is discordant to the regional folding in the Northwest Anticlinorium.

IV. Geological structure

A NNE-SSW striking structure dominates the area including the grey granites. Dips are very steep, 50^g - 80^g to the west, and vertical foliations are common in the granites. Several shear zones in the eastern gneiss-migmatite zone are slightly oblique to the strike of the foliation, but no large displacement is estimated to have occurred.

Presented below is an account of local fold structures, followed by structural analyses based on the observed foliations and lineations.

A. DESCRIPTION OF FOLD STRUCTURES

The dominant structure of this area is a large NNE-SSW striking monocline dipping steeply to the west (Figs. 3 and 4). Several subordinate scale folds were found in the western and eastern gneiss-migmatite zones.

(*a*) *Open gentle folds*

1. – One of the most pronounced folds occurs at the SW corner of Reuschhalvøya, the Knatten synform (Fig. 3, A–1), and sections normal to the fold axis are exposed on both the northern and southern walls of Knatten. This fold is a slightly asymmetric, non-concentric fold with a steeper western limb. The axial plane dips steeply to the west and the axis strikes N10^g - 20^g E with 0^g–10^g N plunge. This fold is beautifully brought out by the marble layers of the upper litho-stratigraphic group, which themselves show small scale recumbent isoclinal folds (Pl. 3–1). These isoclinal folds are gently refolded in the open synform, and are certainly older than the latter. Several thrust planes having a slightly steeper dip than the foliation are developed locally along the western limb of this fold.

2. – A similar type of open antiform is observed on both the northern and southern sides of Miethebreen in the eastern gneiss-migmatite zone (Fig. 3, A–2). This fold is of gentle non-concentric style in the northern outcrop, while it becomes an open monocline with gentle undulations in dip in the south. The crest of the antiform in the southern side of Miethebreen is cut by three

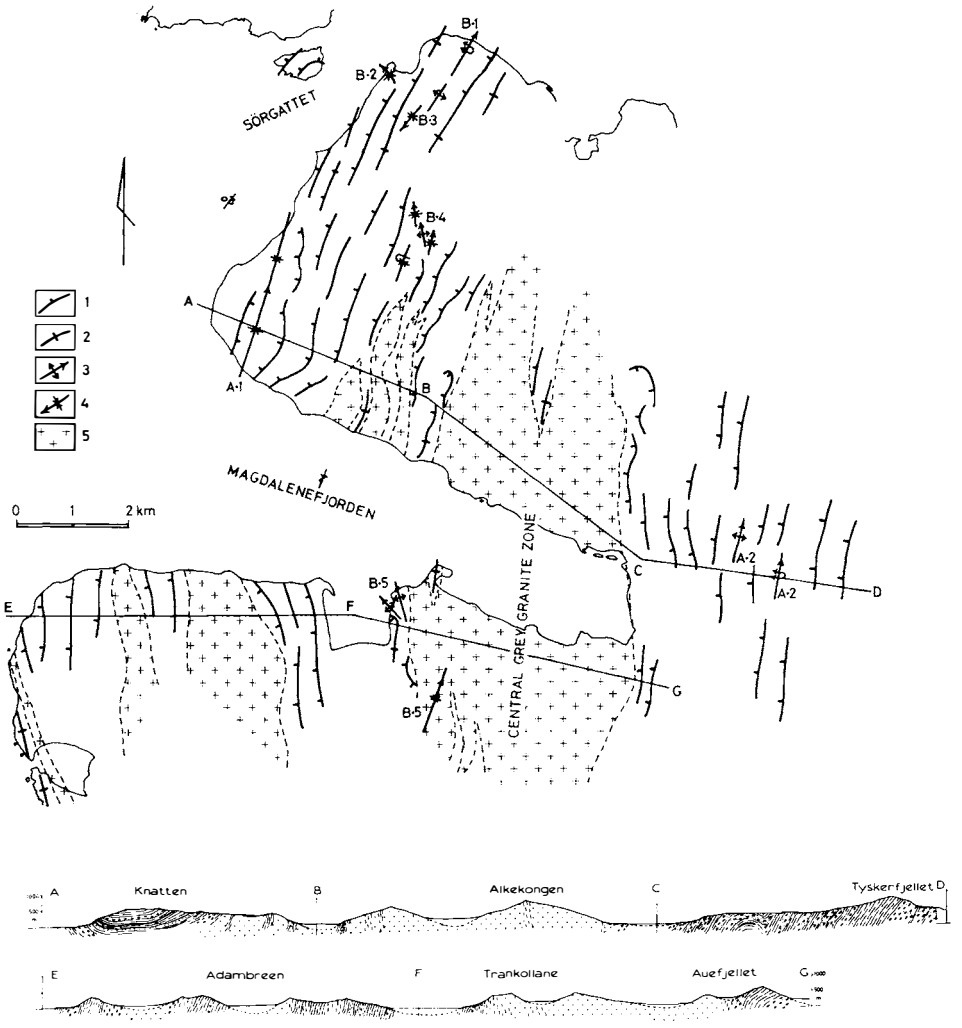

Fig. 3. *Structural map and profiles. Legend for structural map: 1. strike and dip, 2. strike with vertical dip, 3. antiform with axial plunge, 4. synform with axial plunge, 5. grey granite. A–B–C–D and E–F–G show the profiled position. The symbols for profiles are the same as for the geological map (Fig. 1).*

high angle reverse faults and shows an imbricated structure. Small scale isoclinal folds of several dm wavelength are well exposed, folded by later open antiform. The axis of this antiform strikes N20^g E with 0^g - 10^g N plunge, and the axis of the folded isoclinal folds strikes NW-SE with 20^g - 60^g NW plunge.

From the observations of these two open folds, two phases of deformation can be evaluated:

F_1 – earlier phase: small scale isoclinal folds with the axis striking NW-SE and variable plunge.

F_2 – later phase: large scale open folds striking NNE-SSW with gently plunging axis. These structures have the same strike as the general monoclinal structure.

(*b*) *Tight folds*

Several crests of tight isoclinal folds were observed in the western gneiss-migmatite zone.

1. – Along the shore about 2 km ENE of Bjørnhamna an incomplete antiformal crest is exposed for a distance of 100 m (Fig. 3, B–1). This is an overturned concentric isoclinal fold but its eastern limb is obliterated by migmatites. The axis strikes N20^g E with a 20^g - 30^g N plunge. The axial plane dips steeply to the west and is roughly parallel to the local regional foliation trend.

2. – An open synform crest is observed 200 - 300 m west of Bjørnhamna (Fig. 3, B–2), the axis striking NW-SE with a 70^g - 80^g N plunge. The axial trend changes to NNE-SSW in a short distance parallel to the local gneissosity.

3. – On the western side of Tvistegbreen, an acute antiform with steeply west dipping axial plane was estimated from the change of foliation dip (Fig. 3, B–3). This may be the southern extension of (b) 1. This axial trend is also seen on the west side of Bluffbreen, but there the fold is an acute synform whose axis strikes NE-SW with a 70^g S plunge.

4. – A synform-antiform-synform set is found from Veslekrona to Kvasspiggen in the upper reaches of Ytstebreen (Fig. 3, B–4). The axial planes of these folds dip steeply to the west and the wavelength is a few hundred metres. The axis orientations are: western synform; NNW-SSE strike, plunge 40^g N, antiform; NW-SE strike, 40^g N plunge in the north and 70^g S plunge in the south, and eastern synform; NE-SW strike, 10^g to 60^g N plunge.

5. – Local folds of about 100 m wavelength are also found in the Trankollane (Fig. 3, B–5), viz. two antiform crests in the NW corner and an open synform extending from the southern side of Trankollane to the northern side of Kubben. The antiforms have strikes N20^g W and N40^g W with 15^g and 40^g N plunges, and the synform has a N20^g E strike and 10^g - 15^g N plunge. The axial planes of the three are parallel to the gneissosity of the surrounding rocks.

All these tight, isoclinal folds strike NNE-SSW to NW-SE but the plunges vary considerably. Those with a gentle axial plunge may be local drag-folds within the general monoclinal structure of the gneiss-migmatite zones, and may have formed simultaneously with the open gentle folds (F_2: see p. 50). However, those with steep axial plunge are certainly older than the general NNE-SSW striking monoclinal structure and may be correlated with the small isoclinal folds (F_1) folded by the open folds. The original axial trend of these older folds is suggested to have been NW-SE strike as represented by folds described in 2 and 4 above.

(*c*) *Structure of grey granite*

The grey granite, both in the middle of Magdalenefjorden and around the Adambreen area occurs in intrusions which are sub-concordant with the surrounding layered gneisses and migmatites, except for some small cross-cutting dykes along joints. The internal structures of these granites strike N-S with very steep to vertical dip to the west, and are almost concordant with the structures outside. No independent structure could be distinguished in these granites.

The pink aplite dykes which might be derived from the Hornemantoppen granite to the east, occur often in the western part of the eastern gneiss-migmatite zone and they follow both a randomly orientated linear joint system and a shear zone which is slightly oblique to the general monoclinal structure.

B. STRUCTURAL ANALYSES

(*a*) *Mesoscopic structural elements*

Several types of foliation are distinguished:

1. Compositional banding of the fine-grained gneisses. Thin alternations of quartzite and biotite schist indicate in part primary sedimentary layering, but most compositional banding is parallel to a secondary penetrative cleavage, and is formed by regional recrystallization.
2. Axial plane schistosity developed especially in the pelitic schists of the Hamburgbukta area (Pl. 1–1).
3. Compositional layering typical of the layered gneisses. Leucocratic layers are quartz-dioritic and follow the axial surface of isoclinal rootless folds of the fine-grained gneisses (F_1).
4. Flowage foliation observed in the metatects of various migmatites. Gneiss-paleozomes are evidently rotated in these rocks. The faint foliation of the grey granites is also of this type.

All of these foliations were plotted on the Schmidt net without discrimination of different kinds, because all occur in the same general NNE-SSW striking monoclinal structure.

Three types of linear structure are distinguished:

1. Mineral arrangements (Fig. 7) on the foliation planes of any type: L_1.
2. Small fold axes of folds with less than 0.5 m wavelength: L_2, mostly isoclinal and drag type folds observed in the layered gneisses (F_2) (Pl. 3–2).
3. Large, open undulation axes: L_3, occurring where the migmatitic metatect is dominant, (Pl. 3–3).

The difference between L_2 and L_3 is merely the size and style of the folds, and this grouping is somewhat arbitrary but their successive relation is evident at some localities (Fig. 7). F_3 is represented by the open undulation folds (L_3) in the migmatites.

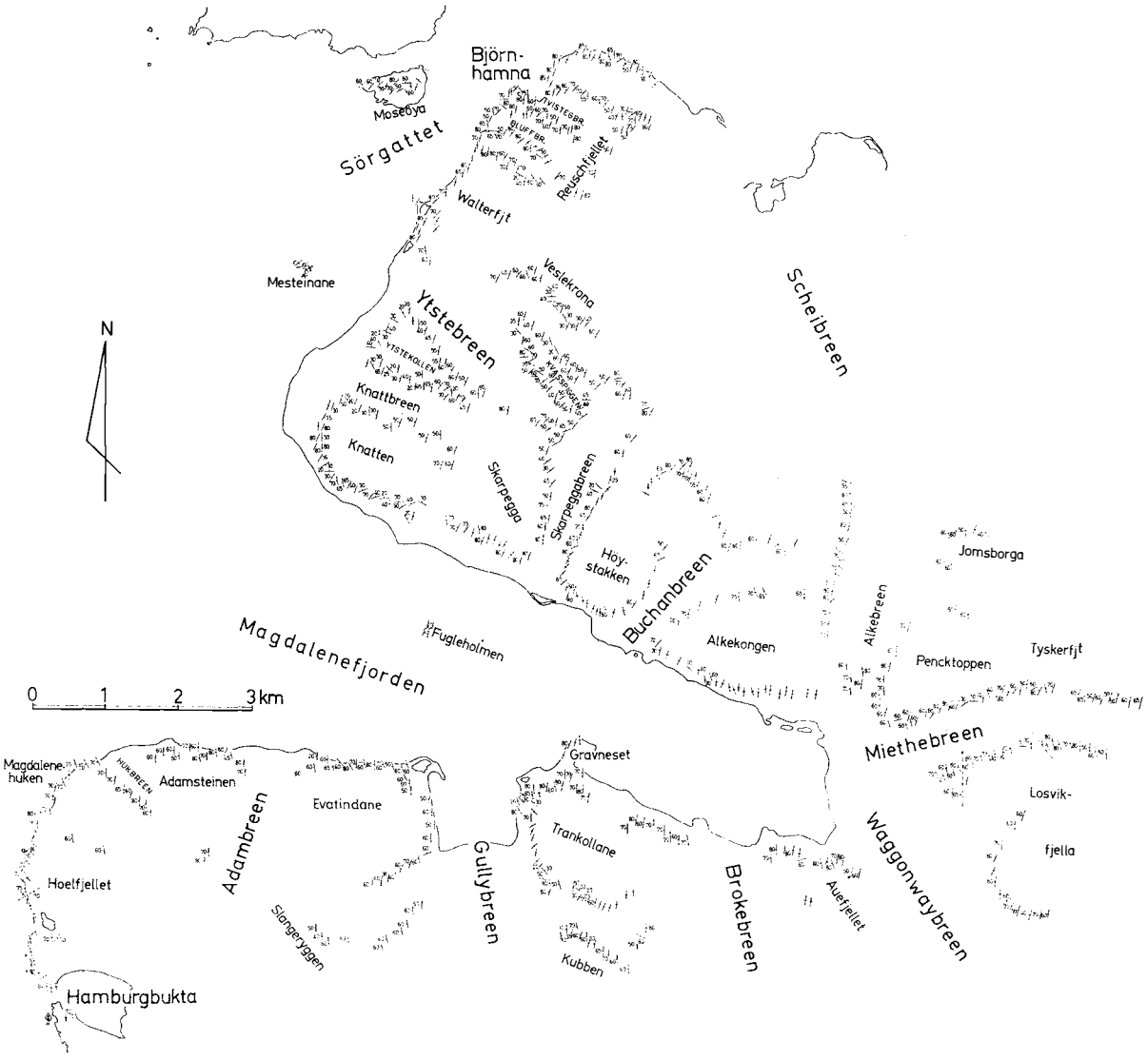

Fig. 4. *Foliation map, including all place names in the text.*

Mutual relations of these foliations and linear structures were examined in a 10×10 m outcrop on the southern shore of Bjørnhamna. The rock is agmatitic migmatite with micaceous layered gneiss paleozomes and quartz-dioritic metatect, partly having pegmatitic pools with cordierite clusters. The foliations of both paleozome and metatect are twisted smoothly from a NE-SW to E-W strike, with a 50^g - 60^g dip to the west (Fig. 8). The β estimated from the foliation diagram coincides well with the observed undulation axes: L_3, however, the small-fold axes (L_2) make a large girdle on the plane of foliation maximum (Fig. 9). This indicates that the small-folds are earlier than the undulation axes which developed due to the fluidal movement of

Fig. 5. *Lineation map: mineral lineations* (L_1).

migmatitic metatect. Actually these small-folds are observed within the rotated gneissic paleozomes and are certainly genetically related to the formation of the layered gneisses. Mineral lineations (L_1) show a pattern (Fig. 9–b) similar to that of the small-fold axes but most of them are evidently folded by the small-folds (L_2) at each observation point. Therefore, it could be concluded that there was one phase of recrystallization earlier than the formation of small-folds.

Mutual relations between these mesoscopic structural elements and observed local fold structures is not always seen in such a small outcrop, but regional mapping indicates that the small-folds (L_2) are closely related to the local tight,

Fig. 6. *Lineation map: small-fold axes (L_2 and L_3).*

isoclinal folds and that the majority of the mineral lineations (L_1) has the same direction as the general monoclinal structure (F_2) of this area.

(*b*) *Structural division and presentation of data*

The three major lithological zones, the western and eastern gneiss-migmatite zones and the central grey granite zone, are sub-divided into 7, 2 and 2 sub-units, respectively (Fig. 10). The measured mesoscopic structural elements are summarized on the Schmidt net for each sub-unit as shown in Fig. 11.

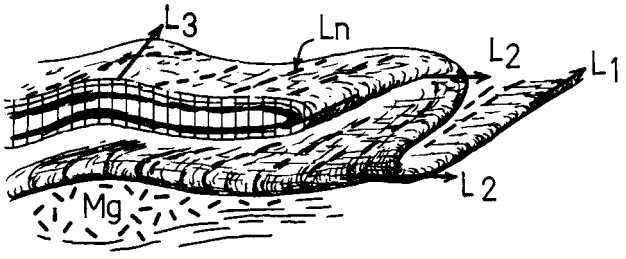

Fig. 7. *Successive relation of different kinds of lineations (West coast of Walterfjellet, Pl. 3–2). Ln: Mineral arrangement, Mg: Migmatite pool.*

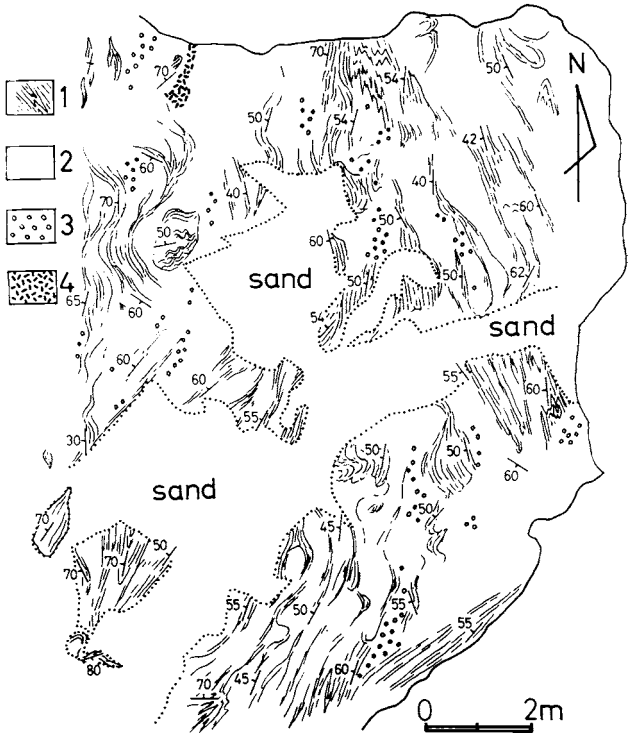

Fig. 8. *A sketch map of Bjørnhamna. 1. layered gneiss, 2. siliceous migmatite, 3. cordierite pegmatite, 4. amphibolite.*

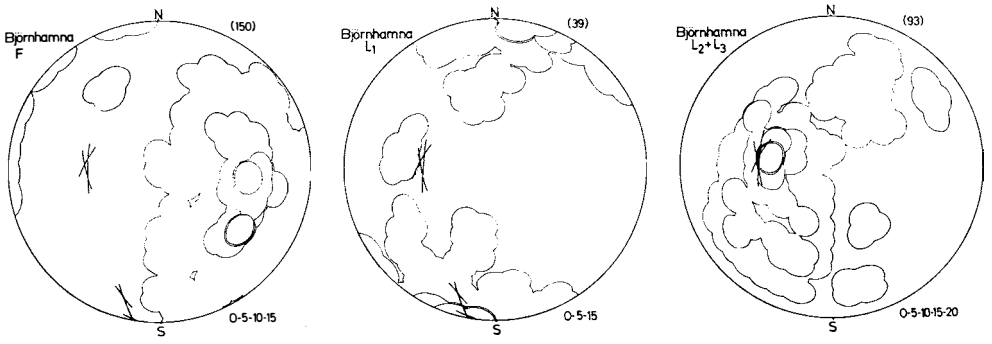

Fig. 9. *Fabric diagrams from Bjørnhamna. F: Foliation diagram.*

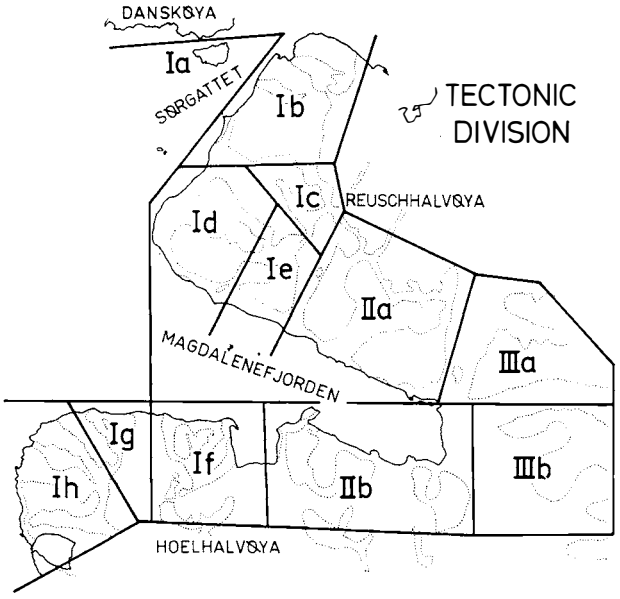

Fig. 10. *Tectonic division of the present area.*

(*c*) *Comments on the diagrams*

Foliation diagrams

1. Comparing the foliation maxima of Ia–Ie to those of If–Ih in Fig. 11, the strike changes slightly from NNE-SSW in Reuschhalvøya to N-S in Hoelhalvøya. Therefore, no displacement has occurred along Magdalene-fjorden.

   The foliation patterns are more complex in Ib and Ic than in the other sub-units (Fig. 11); the gneisses and migmatites are complicated in the former two sub-units. Sub-units in the Hoelhalvøya, viz. If, Ig, Ih, show a simple foliation pattern because the gneisses there occur in narrow zones separated by the grey granites. The rather complex patterns of IIa and IIb are caused by the gneisses of the western zone being included in these sub-units.

   Two different trends of girdles are distinguished in the foliation diagrams; large girdles around axes plunging steeply to the west and girdles around axes striking NNE-SSW to N-S.
2. Large girdles around the steep western plunging axes (Fig. 12–2); this trend of the girdle is seen in all sub-units and is related to a strike fluctuation caused by brecciation and subsequent rotation of agmatitic paleozomes in the metatect (F_3).
3. Girdles around NNE-SSW to N-S striking axes (Fig. 12–3); these are also seen in all sub-units and have the same trend as the general NNE-SSW striking monoclinal structure (F_2) which is the major structure of this area. It is noteworthy that the local open folds of A–1 (Fig. 3) (Id sub-unit) and A–2 (Fig. 3) (IIIa sub-unit) have a non-concentric symmetry.
4. Among local tight and isoclinal folds, those which have gentle NNE-SSW trending axes could be regarded as simultaneous with the formation of the

general monoclinal structure (solid-lined girdles of Fig. 12–3). However, those with steeply plunging axes (broken-lined girdles of Fig. 12–3) are older than the predominant structures with the NNE-SSW striking axes. These older folds (F_1) are observed in Ib and Ic sub-units. The large girdles in the grey granite sub-units, IIa and IIb, are found not within the granite but in the gneisses included along the western edge of these sub-units.

Lineation diagrams

L_1 diagrams

1. The L_1 maxima strike NNE-SSW to N-S with very gentle plunge in both I and III zones, corresponding to the change of foliation strike (Fig. 12–4). This means that the main recrystallization of the rocks was in the stage of NNE-SSW striking F_2 deformation. The maxima of If and Ih have a steep plunge to SW. This indicates that recrystallization was strong in the later migmatization stage (F_3) in these sub-units because the gneisses there are narrow zones sandwiched between grey granite.
2. All L_1 diagrams (Fig. 11) have girdles with the same strike as the foliation maxima, showing multiple girdles and wide-girdle patterns, except for Ia where the measurements are too few in number. Most of these girdles are situated nearly on the large girdle of foliation maximum in each sub-unit. These girdles indicate that pre-existing lineated gneisses were brecciated into agmatitic paleozomes and were moved and rotated with their gneissosity plane roughly parallel to the flowage of the metatect.
3. Multiple-girdles or wide-girdles of L_1 as shown in many sub-units (Fig. 11), except for Ia, Ie and Ih, represent the variation in foliation dip of the general monoclinal structure according to the NNE-SSW striking F_2 deformation (solid-lined girdles of Fig. 12–5).
4. Some weak, but distinct partial girdles deviating from the NNE-SSW striking L_1 girdles can be distinguished in Ic, Id, Ih and IIa. They show a NW-SE striking girdle (broken-lined girdles of Fig. 12–5). These indicate an older recrystallization associated with the tight steeply plunging folds and isoclinal small folds (F_1) folded by the F_2 deformation as seen in Id and IIa sub-units.

L_2 diagrams

1. Most L_2 patterns show girdles with the same strike and similar degree of complexity as those of L_1. The maxima have the same strike as the large girdles of foliation maxima and have very low or flat plunge (Fig. 12–6). The maxima of If and Ih plunge steeply SW, the same as L_1, reflecting a strong recrystallization by the surrounding migmatites and granite. Steep plunging maxima of Ia, Ib have resulted for the same reason. The complexity of the diagram is greater in the Ib, Ic and Id than in the other sub-units (Fig. 11), because the gneisses and migmatites are complicated.

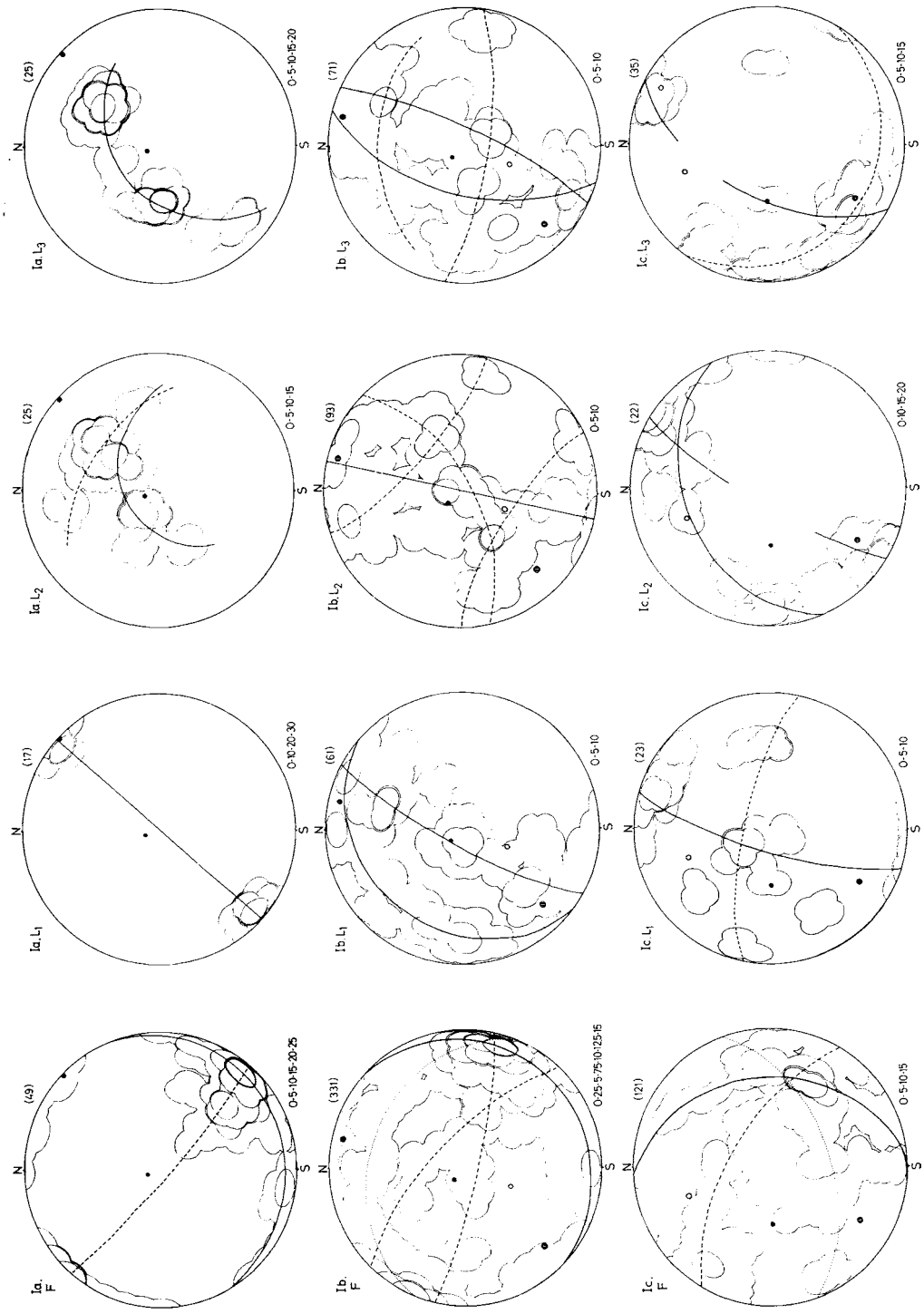

Fig. 11. *Fabric diagrams of foliation and lineations. Foliation diagrams* (*F*) – solid girdle and solid circle (pole): *fluctuation of foliation caused by the development of migmatites* (F_3); broken-lined girdle and lined open circle pole: *folding related to major NNE-SSW deformations* (F_2); dotted girdle and

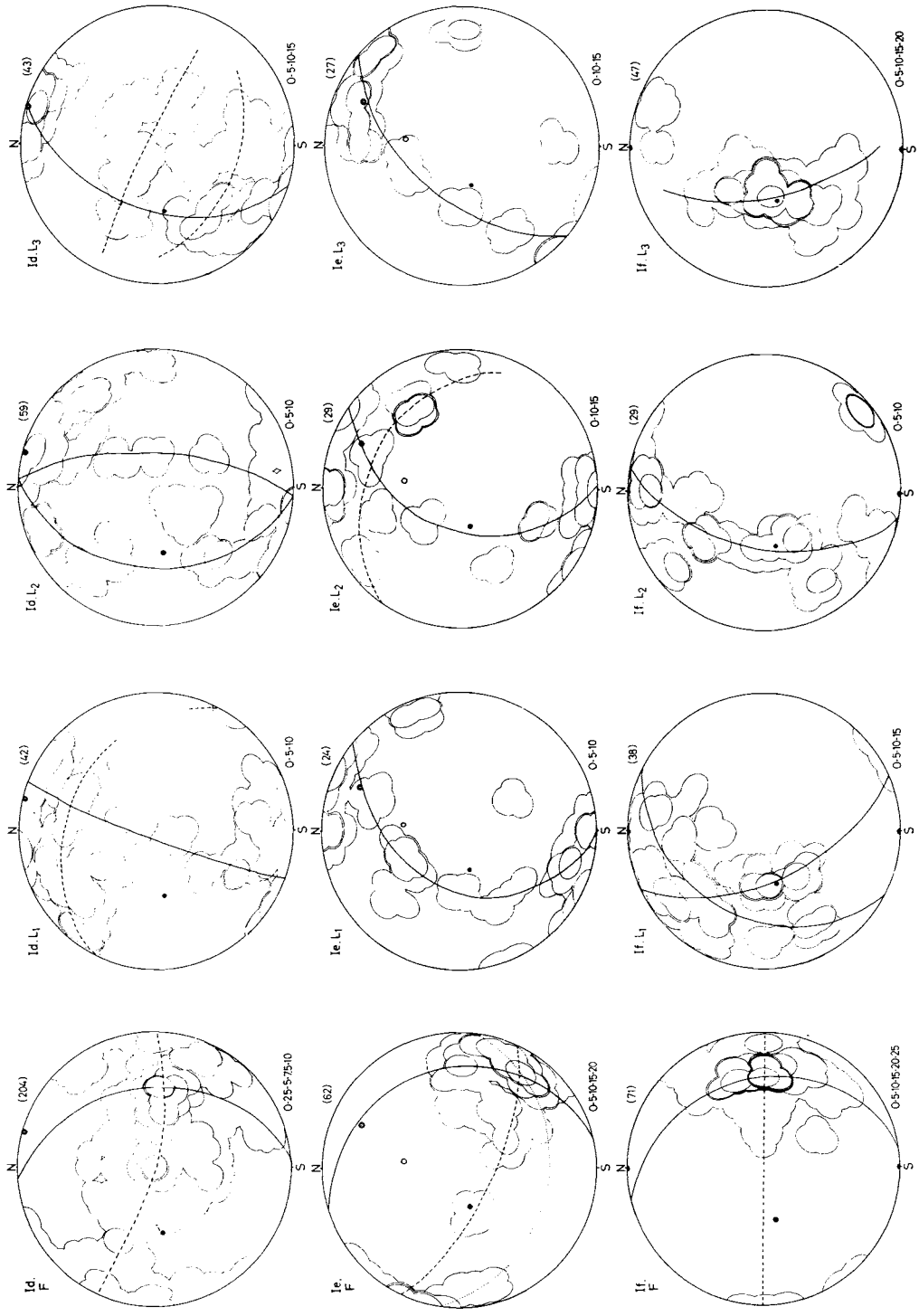

open circle (pole): *older deformation* (F_1). – *Lineation* (L_1, L_2 *and* L_3) *diagrams* – solid girdle: *deviation of linear structures by the rotational movement* (F_3) *of migmatite;* broken-lined girdle: *older lineations. The poles marked are those of the foliation girdles.*

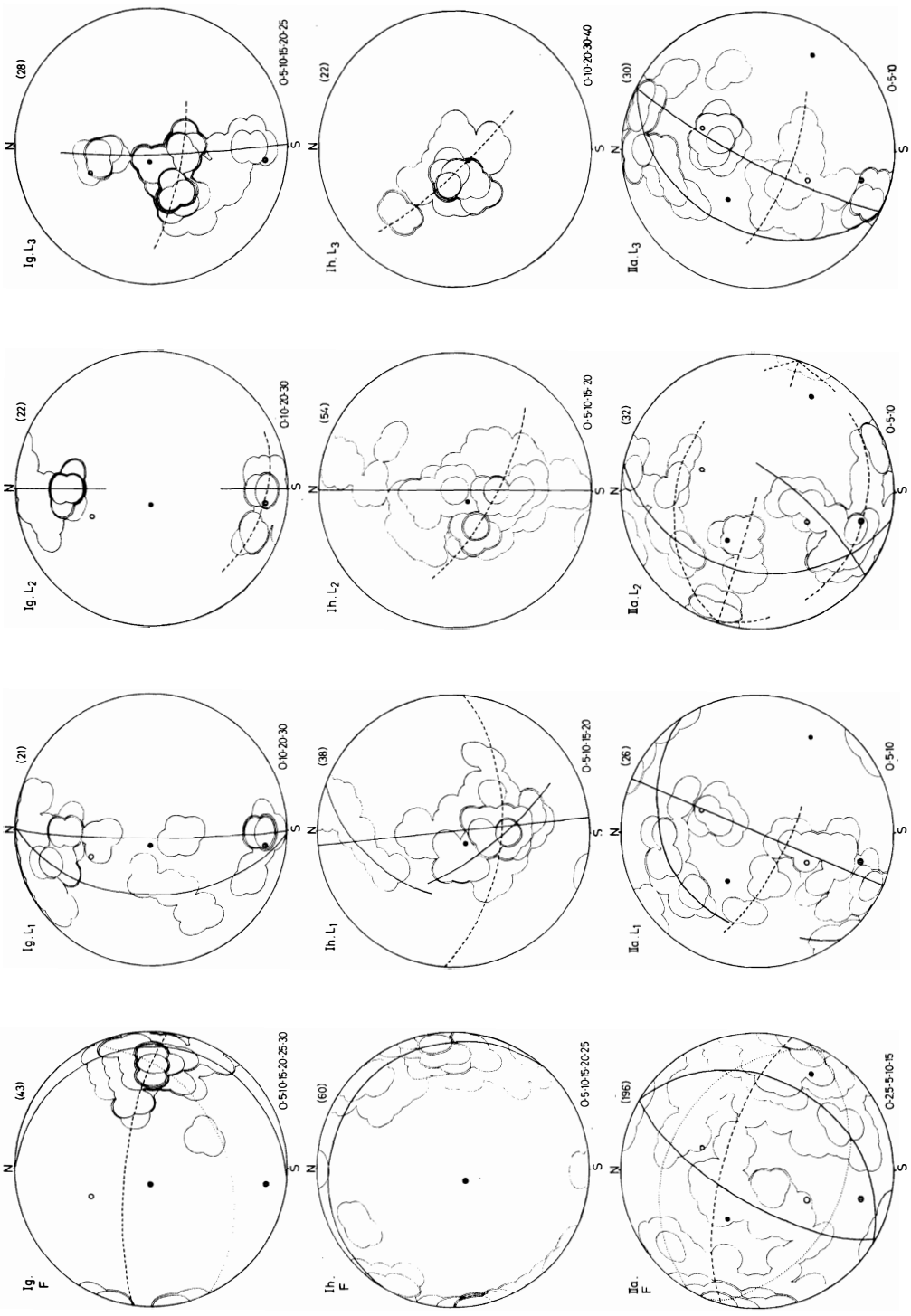
Ig. L3
(28)
0-5-10-15-20-25
Ih. L3
(22)
0-10-20-30-40
IIa. L3
(30)
0-5-10
Ig. L2
(22)
0-10-20-30
Ih. L2
(54)
0-5-10-15-20
IIa. L2
(32)
0-5-10
Ig. L1
(21)
0-10-20-30
Ih. L1
(38)
0-5-10-15-20
IIa. L1
(26)
0-5-10
Ig
F
(43)
0-5-10-15-20-25-30
Ih.
F
(60)
0-5-10-15-20-25
IIa.
F
(196)
0-2,5-5-10-15
N
S

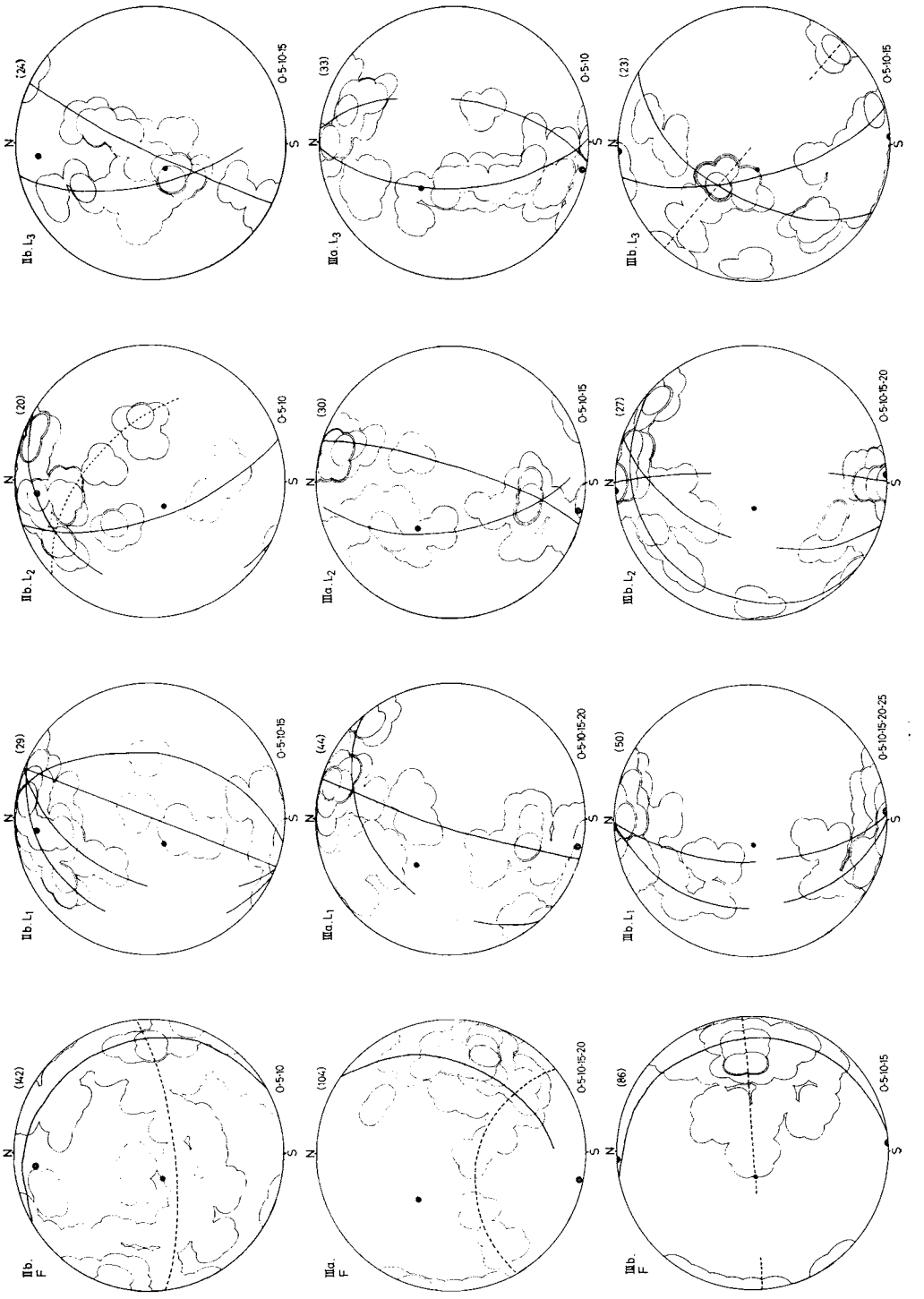
IIb. F
(42)
0-5-10
IIb. L1
(29)
0-5-10-15
IIb. L2
(20)
0-5-10
IIb. L3
(24)
0-5-10-15
IIIa. F
(104)
0-5-10-15-20
IIIa. L1
(44)
0-5-10-15-20
IIIa. L2
(30)
0-5-10-15
IIIa. L3
(33)
0-5-10
IIIb. F
(86)
0-5-10-15
IIIb. L1
(50)
0-5-10-15-20-25
IIIb. L2
(27)
0-5-10-15-20
IIIb. L3
(23)
0-5-10-15
N
S

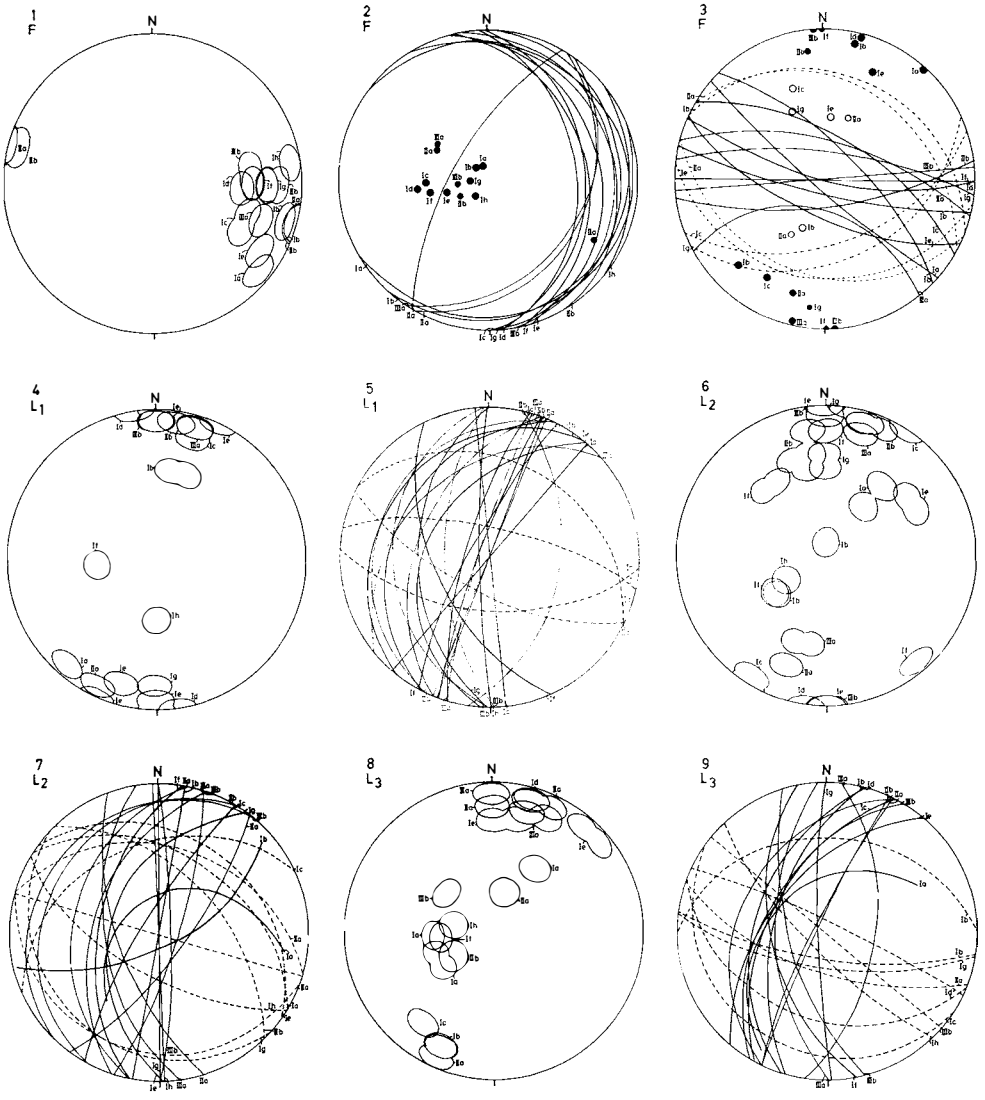

Fig. 12. *Composite fabric diagrams.*

1. *Foliation maxima from all sub-units.*
2. *Foliation girdles and their poles caused by the development of migmatites (F_3).*
3. *Foliation girdles and their poles related to the F_2 NNE-SSW trending deformation (solid girdle and solid pole) and those suggesting the older F_1 deformation (broken-lined girdles and open circle pole).*
4. *L_1 maxima from all sub-units.*
5. *L_1 girdles caused by the F_3 deformation of migmatites (solid girdle) and those of the older F_1 deformation (broken-lined girdle).*
6. *L_2 maxima from all sub-units.*
7. *L_2 girdles caused by the F_3 deformation of migmatites (solid girdle) and those of the older F_1 deformation (broken-lined girdle).*
8. *L_3 maxima from all sub-units.*
9. *L_3 girdles caused by the F_3 deformation of migmatites (solid girdle) and those of the older F_1 deformation (broken-lined girdle).*

2. Most L_2 diagrams show a girdle pattern which roughly coincides with that of the foliation maximum of each sub-unit (solid-lined girdles of Fig. 12–7). This is due to the rotation of gneiss paleozomes by the F_3 deformation.
3. These girdles are mostly wide or show two or more weak girdles (If, IIIb of Fig. 11). These patterns correspond to the change of foliation dips within the F_2 monoclinal structure.
4. Deviating from the NNE-SSW girdles, weak, partial large girdles striking NW-SE are shown in Ia, Ib, Id, Ie, Ih, IIa, IIb and IIIa sub-units (broken-lined girdles of Fig. 12–7). These isoclinal fold axes are older than the deformation as actually seen in the core of open folds A–(a)–1 and A–(a)–2 (see p. 50). These older girdles together with the older ones of L_1, indicate that the F_1 deformation had roughly NW-SE striking axes.

L_3 diagrams

1. L_3 diagrams of most sub-units are simpler than those of L_1 and L_2 (Fig. 11). The maxima are roughly in the same direction as L_1 and L_2 in Reuschhalvøya, but plunge steeply SW in Hoelhalvøya because of the strong influence of migmatites and granite (Fig. 12–8).
2. L_3 plots also project onto a large girdle which roughly coincides with that of the foliation maximum in most sub-units (solid-lined girdles of Fig. 12–9). The L_3 axes are observed as gentle undulations of foliation around migmatitic paleozomes (Pl. 3–3) and the girdle deviation suggests that they were formed as pinch and swell structures before agmatitic brecciation and then rotated by mobilized metatect.
3. The L_3 girdles having a wide deviation of dips (Fig. 11) as seen in Reuschhalvøya, zones II and III, correspond to the change of foliation dips within the F_2 monoclinal structure. The girdle is relatively narrow in the sub-units of Hoelhalvøya, because most of the L_3 measurements were recorded from gneisses which occur in narrow layers among migmatites and grey granite.
4. The weak NW-SE striking partial girdles (broken-lined girdles of Fig. 12–9) are also shown in some sub-units and they indicate that the L_3 type gentle undulations were also formed in the deformation phase older than the F_2 structure. The L_3 measurements of Hoelhalvøya (If, Ig and Ih) and the granite zone (IIa and IIb) were obtained from the fine-grained gneisses in these sub-units.

C. SUMMARY OF GEOLOGICAL STRUCTURE

Three successive phases of deformation are evaluated from the composite diagrams of maxima and girdles (Fig. 12).

They are summarized as follows:

F_1, older phase: NW-SE striking small folds.
F_2, major phase: NNE-SSW striking small folds and mineral lineations.

F_3, younger phase: rotational movement of paleozomes by mobilized migmatitic metatect. The direction of migmatite movement is indicated by the steeply SW plunging maxima of L_1, L_2, L_3 of the If, Ig, Ih, IIb sub-units.

The occurrence of different fold types of successive phases of deformation is evident in a preliminary examination on the southern shore of Bjørnhamna (Figs. 8 and 9), and elsewhere (Fig. 7). However, as seen in the fabric diagrams of L_1, L_2, and L_3, each of these different types of linear elements developed in all three phases of deformation to different degrees. Therefore, it is important to realize that a certain style of small-fold does not always define any definite regional phase of deformation.

These phases distinguished by the geometric analyses of fabric diagrams are correlated with the local fold structures:

F_1, Tight and isoclinal folds with steeply plunging axis, folded in the major monoclinal structure.

F_2, Open folds, tight folds with gently plunging axis, and major monoclinal structure.

F_3, Local undulation of foliation strike associated with migmatization.

Another important structural observation is that the trend of amphibolite is slightly oblique to the general trend of lithologies represented by the alternation of micaceous layered gneisses and siliceous migmatite in Reuschhalvøya. The

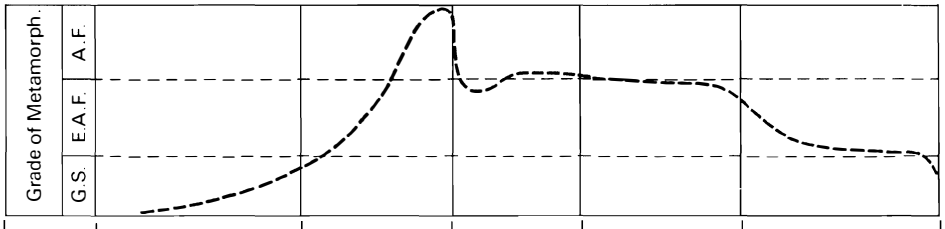

Deform. phase	F_0	F_1	F_2	F_3	F_4
Fold trend, metamorphism & intrusives.	Sinking and upheaval of geosyncline. Regional N-S distribution of limestones and amphibolites.	Regional metamorphism and folding: NW-SE gentle plunge axes, formation of cleavages.	Major monocline; NNE-SSW flat axis. Main recrystallization and development of gneisses.	Gentle undulation: E-W steeply W plunge axis. Migmatization and enplacement of granites.	Block movement: intrusion of Hornemantoppen granite & aplite along shear zones.
Tectonic division	Geosynclinal.	Syn-orogenic.			Post-orogenic.
	Folding.	Regional metamorphism.		Migmatization syn-kinematic granites.	Post-kinematic granites.

Fig. 13. *Tectonic development of Caledonian rocks in the Magdalenefjorden area.*

latter trend strikes NNE-SSW and is conformable to the major monoclinal structure of this area, while the trend of the amphibolites does not fit any structural trend mentioned above. In the large-scale reconnaissance map (Fig. 1, Location map) of GEE and HJELLE (1966), the trend of amphibolite coincides with that of marbles in the Northwest Anticlinorium. Thus, this trend, roughly in the N-S strike, is a regional trend of a Hecla Hoek basin of northwestern Spitsbergen and is older than the F_1 deformation. This oldest trend is defined as F_0 (Fig. 13).

The grey granites show a gradational change from migmatites, though there are some cross-cutting injection contacts, and the granites have many shadowy remnants of nebulitic gneisses and siliceous quartzitic layers. On a regional scale, their occurrences are concordant to the surrounding gneisses. This evidence shows that the grey granites are syntectonic intrusions accompanying migmatitization.

The pink aplitic dykes, often observed in the eastern gneiss-migmatite zone, mostly follow along later shear zones and joints. They must have a close genetic relation to the Hornemantoppen granite to the east, which is evidently one of the post-tectonic granites of the Caledonian orogeny, associated with what is called the F_4 phase (Fig. 13).

The tectonic history of the present area during the Caledonian orogeny is summarized in Fig. 13.

Acknowledgements

The writer wishes to express his thanks to the director of Norsk Polarinstitutt, Dr. T. GJELSVIK, and the expedition leader, Mr. T. SIGGERUD, for again giving him the opportunity to study in Spitsbergen. He is also very much indebted to his two field assistants, Mr. C. HEFFERMEHL and Mr. S. MØLLER jr., who helped him during the whole expedition period, and to Mr. A. HJELLE, Dr. M. B. EDWARDS, and Prof. P. REITAN for their kind discussions and improvement of English.

References

GEE, D. G. and A. HJELLE, 1966: On the crystalline rocks of north-west Spitsbergen. *Norsk Polarinstitutt Årbok* 1964, 31–45. Oslo.

HARLAND, W. B., 1961: An outline structural history of Spitsbergen. *Geol. of the Arctic*, **1**, 68—132. Toronto.

HARLAND, W. B., R. H. WALLIS and R. A. GAYER, 1966: A revision of the lower Hecla Hoek succession in central north Spitsbergen and correlation elsewhere. *Geol. Mag.*, **168**, (1), 70—97. London.

HJELLE, A., 1966: The composition of some granitic rocks from Svalbard. *Norsk Polarinstitutt Årbok* 1965, 7—30. Oslo.

— 1974: The geology of Danskøya and Amsterdamøya. *Norsk Polarinstitutt Skr.* Nr. 158 (this volume).

KLITIN, K., 1964: The Caledonides of Spitsbergen. *Tectonique de l'Europe*, 72—74. Moscow.

OHTA, Y., 1969: The geology and structure of metamorphic rocks in the Smeerenburgfjorden area, north-west Vest-Spitsbergen. *Norsk Polarinstitutt Årbok* 1967, 52—72. Oslo.

— 1974: Tectonic development and bulk chemistry of rocks from the Smeerenburgfjorden area, Spitsbergen. *Norsk Polarinstitutt Skr.* Nr. 158 (this volume).

WINSNES, T., 1965: The Precambrian of Spitsbergen and Bjørnøya. In: K. RANKAMA (ed.): *The Precambrian.* **2**, 1—24. London.

Tectonic development and bulk chemistry of rocks from the Smeerenburgfjorden area, Spitsbergen

By
YOSHIHIDE OHTA

Abstract

Succeeding a paper (OHTA 1969) describing lithology and geological structures, the deformation phases, metamorphism and the composition of rocks are the subject of this paper. Rock textures and metamorphic minerals reveal four phases of deformation each with characteristic metamorphic grades. The culmination of metamorphism and the conditions under which grey granite formed are estimated to be of upper amphibolite facies. Thirty-seven chemical analyses with their modal compositions are presented, and the geochemical characteristics of metamorphic and granitic rocks are considered in comparison with the Scottish Caledonian rocks.

Аннотация

Деформационные фазы, метаморфизм и состав пород предетавляет собои тему настоящей работы, являющей продолжением предыдущей работы (ОНТА 1967), в которой были описаны литология и геологические структуры. Текстуры пород и метаморфические минералы проявляют четыре фазы деформации, имеющие свои характерные метаморфические степени. Кульминация метаморфизма и условия формирования серого гранита, по оценке автора, соответствуют верхней амфиболитовой фации. Приведены результаты 37 химических анализов с их модальными составами и геохимические характеристики метаморфических и гранитных пород рассматриваются по сравнению с шотландскими каледонскими породами.

Introduction

This report is based on mapping and samples collected during the 1966 summer expedition of Norsk Polarinstitutt.

In the report of 1969 by the present author, the megascopic nature of the metamorphic rocks was summarized, and the tectonic development of the area was discussed on the basis of mesoscopic structural elements (Fig. 1). In the present report the deformation phases based on the textural development of the rocks, metamorphic mineral parageneses, modal analyses and bulk chemistry will be discussed.

A rough outline of the geology has been given by GEE and HJELLE (1966), who suggested that these metamorphic rocks may be correlated with the Lower Hecla Hoek Succession of Precambrian age. The age of metamorphism, according to the radiometric methods by GAYER et al. (1966), is late Ordovician to Devonian (318–450 m.y. by biotite or whole rock, rocks from the Smeerenburgfjorden and Danskøya area) which is the main and late Caledonian orogenic event.

The modal and calculated chemical compositions of granitic rocks from the vicinity of the present area were studied by HJELLE (1966).

Based on the series of modal and chemical data of bulk rocks, presented below, the author considers the development of granitization during Caledonian metamorphism.

I. Deformation episodes and metamorphism

A. DEFORMATION EPISODES

As the northwestern part of Spitsbergen is strongly "soaked" by syntectonic grey granite, the paragneisses and metasediments occur as more or less resistant paleozomes of various size in the migmatitic rocks. However, the nature of regional metamorphism and deformation is still well preserved especially in the rocks occurring in a few km wide zone along the eastern side of the Smeerenburgfjorden.

The metamorphic rocks of this area were divided into three groups (OHTA 1969): fine-grained gneisses, layered gneisses, and feldspar porphyroblastic gneisses. There are also many varieties of granitic gneisses which are more closely related to the formation of migmatitic granites. The nature of cleavages and layered structures of these gneisses differ distinctly, making the establishment of successive deformation phases possible.

Four deformation phases distinguished in this part of the area will be described below.

1. *The F_1 deformation, S_1 and S_2*

The fine-grained gneisses occur along the eastern side of the Smeerenburgfjorden and have thin compositional layering showing small tight to isoclinal fold closures of a few cm to dm wavelength, whose axial trends do not always coincide with the regionally distributed small folds of the layered gneisses. Refolding of these layers in the latter folds are rarely observed, but most of the old isoclinal folds show rootless closures within a band of the layered gneisses.

The folded isoclinal rootless folds represent the oldest deformation observed in this area, which is called the F_1 deformation. The compositional layering showing these folds is defined as S_1 and the regionally developed, banded structures of the layered gneisses are called S_2.

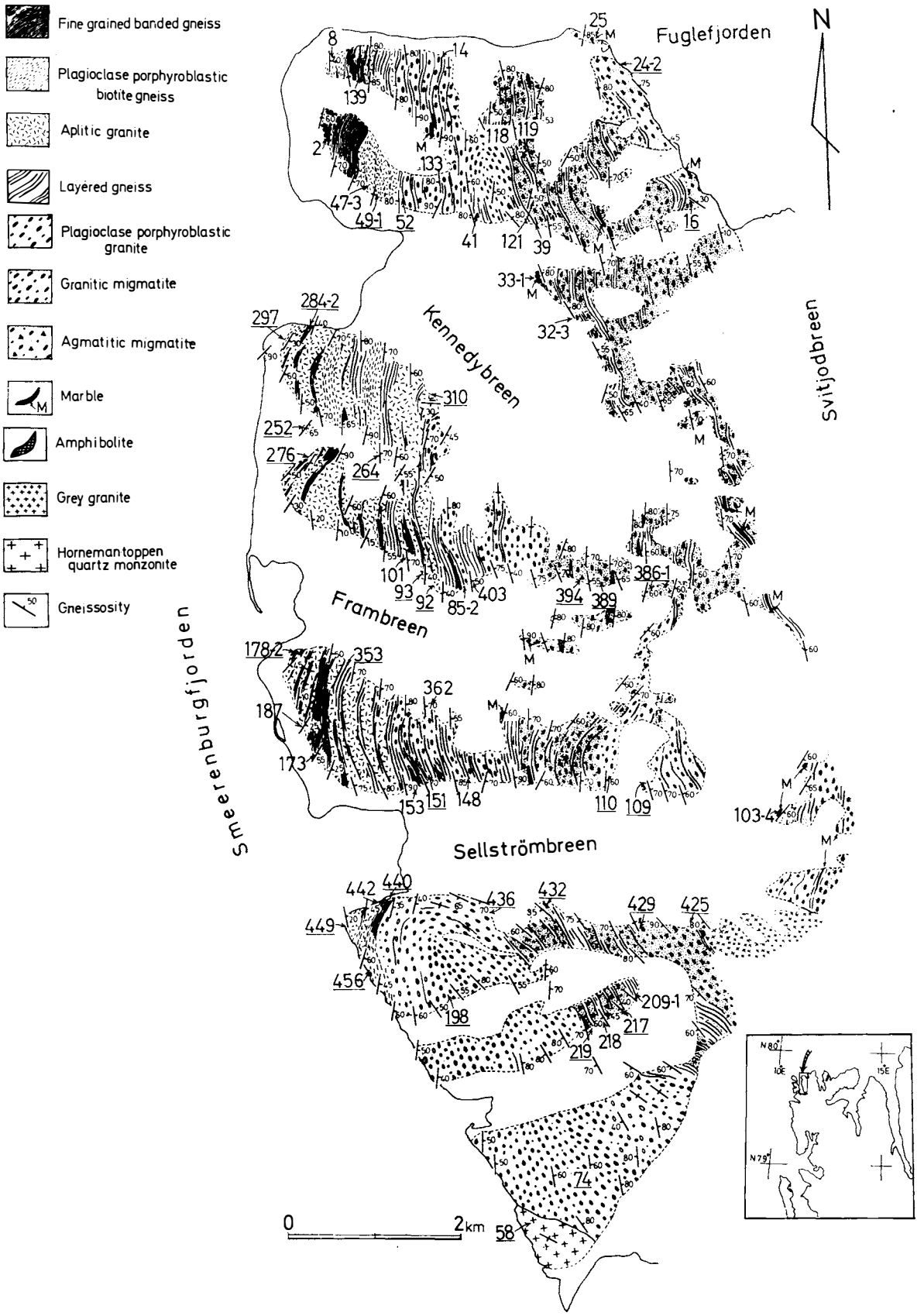

Fig. 1. *Geological map of the Smeerenburgfjorden area, with the locality of the samples mentioned in the tables, figures, and plates. Underlined numbers: both chemically and modally analysed samples. Numbers not underlined: samples examined under the microscope.*

S_1 is seen as gradational alternations of biotite-rich and quartz-rich layers. The latter sometimes contain pure quartzite. Possible relict graded bedding is suggested by biotite and feldspar concentrations in the quartzitic rock (OHTA 1969, Pls. I–a and I–f).

The F_1 folds are observed only in small scale, since they are cut off by S_2 everywhere. They are tight to isoclinal, symmetric or asymmetric similar folds, showing good penetrative strain slip axial cleavage in the biotite-rich layer. Sometimes the cleavage planes show weak fanning and refraction around the quartz-rich layers, indicating in part an intermediate nature between concentric and similar folds. The axial trends of F_1 folds are very much scattered and therefore their general trend is unknown.

S_2 is distinct and universally occurs as banded structure in the layered gneisses. The bands are several cm to several dm thick (OHTA 1969, Pl. II–a) and have medium to coarse grained granoblastic texture in the quartzo-feldspathic layer and lepidoblastic texture in the biotite-rich layer. These bands are parallel to the axial surface of the F_1 folds. Under the microscope, the S_2 cleavages in the fine-grained gneisses are seen as a pair of conjugate glide planes composed of fine biotite flakes in the F_1 fold limbs, the distinct arrangement of relatively large biotite flakes along the axial surface in the fold crests (Pl. I–1), and the dimensional preferred orientation of quartz in the quartzitic layer (Pl. I–2, right half of the picture). The biotite-rich layers are often slipped out in the fold limbs. The axial surface cleavage is very strong when the fold is tight and of an acute style.

The descriptions above suggest that S_1 represents the recrystallized primary sedimentary structure and S_2 is the axial surface foliation of the F_1 folds. S_2 is very well developed in the eastern part of the area and most of the gneissosities measurable in the layered gneisses are caused by F_1. Thus the F_1 folding is responsible for universal layered structure and cleavages in this area.

2. *The F_2 deformation and S_3*

The most distinct and pronounced tight similar folds of up to several metres wavelength fold the S_2 cleavages and layered structures (OHTA 1969, Pl. I–d). These are defined as the F_2 folds. Actual folding of the F_1 folds has not often been observed, however, small rootless isoclinal fold closures are seen within the F_2 fold limbs. The F_2 folds always contain compressed drag-type parasitic folds which cause the siliceous and quartzo-feldspathic layers to assume an en echelon arrangement of boudins showing a tectonic psephite-like structure (Pl. 2–1). Plagioclase porphyroblastic veins and layers occur subconcordantly to the folded S_2 layering and often show intense tight and ptygmatic folds (OHTA 1969, Pl. II–a). Some of them show gentler folding than tightly folded S_2 layering. The plagioclase porphyroblasts themselves do not show any linear arrangement on the gneissosity surface (OHTA 1969, Pl. I–e). Mineral lineations of biotite aggregations, bundles of sillimanite fibers and spinel-corundum-bearing clots are parallel to the F_2 fold axes. The F_2 fold axes (most of measured minor fold axes belong to them) have constant N–S trend (OHTA 1969, Figs.

29 and 32), which coincides with the regional fold trend of this area. The plunges of fold axes vary very much on a large girdle of a fabric diagram because of later disturbance (OHTA, 1969).

Development of a new cleavage with the F_2 folds is very weak. Thin and discontinuous penetrative cleavage planes, shown by the arrangement of coarse biotite flakes, are rarely observed in the biotite-rich layers and the margins of quartzo-feldspathic layers. No distinct compositional layering associated with the F_2 axial surfaces has been observed.

Thus, the most distinct fold structures observed in this area were formed during the F_2 deformation. The grade of metamorphism was the highest from this episode to the succeeding static period. The formation and intrusion of quartzo-feldspathic metatects took place in an early period of the F_2 deformation episode, and not at the time of maximum deformation because they do not follow the very weak axial surface cleavage developed during this episode.

3. *The F_3 disturbance and S_4*

Widely spaced conjugate diaphtolitic shear planes with an acute angle are observed superimposed on the structures earlier than the F_2 folds. They are defined as S_4. These planes, as seen under the microscope, cut through the coarse-grained lepidoblastic texture of the folded S_2 layers and are typically mylonitic with elongated quartz seams and ovoidal porphyroclastic plagioclase (Pl. 2–2). Biotite is also disrupted in these planes without decomposition.

These observations suggest that the F_3 episode did not involve folding but a mechanical mylonitization under conditions of biotite stability, associated with quartz introduction. These diaphtolitic planes occur most frequently around the periphery of the grey granite masses. Their direction is roughly concordant with the elongation trend of the granite masses, following a NNW-SSE strike. Thus, the S_4 diaphtolitic cleavage was formed in close connection with the emplacement of grey granite.

A wide agmatitic and nebulitic migmatite zone occurs around the granite (OHTA 1969, Pls. II–b, and II–c). The granitic metatects of these migmatites follow most frequently along S_4, and also cut randomly across all structures earlier than S_4. The orientation of F_2 fold axes differs from one gneissic paleozome to the next and the gneissosities show local drag folds of various axial trend around the margins of paleozomes.

The disrupted fine biotite flakes in S_4 are superimposed by unoriented medium-grained flakes and the mylonitic quartz occurs as a fine-grained interstitial matrix among large feldspars in the migmatized rocks. Weak flow structures of the grey granite show synform structure, generally concordant to that of the surrounding gneisses. This evidence indicates that the migmatitization succeeded the F_3 diaphtolitic disturbance, introducing a large amount of granitic metatect, and the layered gneisses were fragmented into paleozomes which were moved mainly along the S_4 cleavages producing the girdle distribution of F_2 fold axes (OHTA 1969, Fig. 29). A period of static recrystallization coincident with the consolidation of grey granite followed these disturbances.

4. *The F_4 episode*

This is the episode of post-tectonic granite intrusion during which the Hornemantoppen granite to the south of Smeerenburgfjorden was emplaced. This granite is grano-syenitic in composition. It is intrusive into and has sharp contacts with both grey granite and metamorphic rocks. A small number of thin pink aplite dykes branch out around the periphery. Associated with them is retrogressive metamorphism producing chlorite, sericite and epidote in the surrounding rocks.

B. METAMORPHISM

This area and the surrounding region of the NW part of Spitsbergen are characterized by the occurrence of cordierite-bearing rocks; no kyanite or staurolite, which are common in Ny Friesland, have been found. The highest grade of metamorphism is achieved during or post F_2 deformation, reaching the sillimanite zone. Development of constituent metamorphic minerals and quartzo-feldspathic metatects will be summarized in Fig. 5 based on the textural studies in relation to the deformation phases. The mineral parageneses of metamorphic rocks are listed in Table 1.

Table 1

Mineral parageneses of the metamorphic rocks (Sample locations in Fig. 1)

Sample No.	Mineral parageneses
A. Fine-grained gneisses	
436	Bi. Pl. Kf. Qt.
173	Mus. Pl. Kf. Qt.
252	Bi. Graph. Pl. Kf. Qt.
440	Gar. Bi. Pl. Kf. Qt.
440	Cord. Bi. Pl. Kf. Qt.
362	Cord. Bi. Pl. Qt.
350–1	Hb. Bi. Pl. Kf. Qt.
47–3	Bi. Ep. Pl. Kf. Qt.
85–2	Gar. Bi. Mus. Pl. Qt.
39	Sill. Bi. Pl. Kf. Qt.
2	Sill. Gar. Bi. Mus. Pl. Kf. Qt.
153	Bi. Mus. Graph. Gar. Pl. Kf. Qt.
219–1	Gar. Cord. (tourm.) Bi. Pl. Kf. Qt.
B. Layered gneisses	
386–1	Bi. Pl. Qt.
8	Bi. Pl. Kf. Qt.
101	Gar. Bi. Pl. Kf. Qt.
148	Gar. Bi. Pl. Qt.
2	Gar. Bi. Mus. Pl. Kf. Qt.
209–2	Hb. Bi. Pl. Qt.
41	Cord. Gar. Bi. Pl. Qt.
264	Cord. Bi. Pl. Kf. Qt.
118	Cord. Gar. Bi. Pl. Kf. Qt.

Table 1 contd.

139	Cord.	Bi.	Mus.	Graph.	Pl.	Kf.	Qt.
121	Clino-pyr.	Gar.	Bi.	Pl.	Kf.	Qt.	
92–2	Sill.	Bi.	Pl.	Kf.	Qt.		
118	Sill.	Gar.	Bi.	Pl.	Qt.		
133–1	Sill.	Gar.	Bi.	Pl.	Kf.	Qt.	
264	Sill.	Cord.	Bi.	Pl.	Kf.	Qt.	
119–1	Sill.	Cord.	Gar.	Bi.	Pl.	Qt.	
403	Co.	Sp.	Gar.	Bi.	Mus.	Pl.	Qt.
440	Co.	Sp.	Cord.	Bi.	Pl.	Qt.	
403	Co.	Sp.	Cord.	Gar.	Hb.	Bi.	
C. Skarns							
Fine-grained gneiss area							
187	Ol.	Calc.					
187	Ol.	Diop.	Calc.				
47	Ep.	Hb.	Bi.	Pl.	Qt.		
Layered gneiss area							
33–1	Ol.	Diop.	Hb.	Act.	Calc.	Pl.	Qt.
14	Diop.	Gross.	Scap.	Calc.	Hb.	Pl.	Qt.
32–3	Diop.	Hb.	Calc.	Pl.	Qt.		
33–1	Diop.	Hb.	Pl.	Kf.	Qt.		
14	Diop.	Zoi.	Hb.	Calc.	Pl.	Qt.	
218	Gross.	Hb.	Bi.	Pl.	Qt.		
32–3	Hb.	Pl. (anti-meso-perth.)	Kf.	Qt.			
Granitic migmatite area							
25	Sp.	Ol.	Diop.	Clino-humite	Phlog.	Calc.	
25	Ol.	Gross.	Phlog.	Calc.			
389	Diop.	Woll.	Zoi.	Hb.	Pl.		
25	Diop.	Hb.	Phlog.	Calc.			
25	Diop.	Orth-pyr.	Ep.	Calc.	Hb.	Bi.	Mus.
103–4	Diop.	Zoi.	Hb.	Bi.	Pl.	Kf.	Qt.

1. *Quartz*

Quartz grains occur commonly as a polygonal mosaic in most rocks and their grain size is less than 0.2 mm in the fine-grained gneisses and up to several mm in the layered gneisses. Coarsening of grain size is observed from the fine-grained gneisses to the migmatites. Two characteristic fabrics of quartz: 1. the dimensional fabric during the development of S_2 layering, and 2. intense mylonitic texture in the F_3 disturbance, will be described below.

1. Where the recrystallized thin alternation of impure quartzite and argillite is folded into tight, isoclinal F_1 folds, the quartz grains in the quartzitic layers have strongly elongated shape with sutured contacts and intense wavy extinction. The elongation direction of grains is about 45–55° to the borders of compositional layers and is parallel to one of the conjugate shear planes shown by biotite arrangement in the neighbouring mica-rich layers (Pl. 1–2). This fabric of quartz is believed to have been formed simultaneously with the F_1

folding. Most quartz grains in the fine-grained gneisses show no wavy extinction, but have more or less sutured grain contacts. However, in the rocks with well developed S_2 layering, quartz grains form a mostly polygonal unstrained mosaic of medium to coarse grain size. This evidence indicates that the fine-grained gneisses with the S_1 and F_1 folds have been preserved only where the development of S_2 and post-F_1 annealing grain growth are incomplete.

2. Intensely strained, elongated quartz grains with typical sutured grain contacts are characteristic in the matrix of diaphtolitic rocks formed by the F_3 disturbance (Pl. 2–2). These quartz grains form thin layers abutting against ovoidal plagioclase porphyroclasts. The mylonitic quartz grains occur as the matrix of some granitic gneisses where they are several times larger than those in the diaphtolitic rocks, but still show typical sutured contacts and weak wavy extinction. It is believed that the fine mylonitic quartz grains were coalesced into medium to coarse grains after the F_3 disturbance.

2. *Feldspars*

Plagioclase forms a sub-angular polygonal mosaic in all metamorphic rocks, and is more dominant than potash feldspar except in the granitic gneisses and migmatites.

In the fine-grained gneisses which still preserve S_1, plagioclase grains are of small size (less than 0.5 mm) and are always very "dusty" owing to included minute sericite flakes and opaque pigments. Some relatively larger grains show clear polysynthetic twin lamellae and are free of the "dust", having only a few round inclusions of quartz. The plagioclase An-content ranges from 25 to 35.

In the rocks with well developed S_2 compositional layering, the plagioclase grains are of medium size, 0.5 to a few mm across, showing granoblastic texture with quartz. In the layered gneisses folded by the F_2 deformation, plagioclase is distinctly porphyroblastic, up to 5 to 10 mm size, with composition of An 20–25. The shape is ovoidal to idiomorphic with a few inclusions of quartz, garnet and biotite. Antiperthitic texture is common. Most idioblastic plagioclase grains are evidently earlier than the F_2 folding, because they have no linear arrangement on the gneissosity plane, but are folded into the F_2 folds (OHTA 1969, Pl. I–e). A few orthoclase perthite grains ($2Vx=70$ to 75) occur in the coarse-grained layered gneisses with the plagioclase porphyroblasts and biotite-cordierite-garnet-sillimanite paragenesis.

The plagioclase grains have been mechanically crushed into porphyroclasts during the F_3 disturbance.

Large sub-angular plagioclase crystals in the granitic gneisses are associated with large microcline perthite grains of $2Vx=83$ to 90, and both are superimposed on the mylonitic sutured quartz. These plagioclase crystals are identical with those in the grey granite and have weak normal compositional zoning from An 20 to albite. Saussuritization of the An-rich core of these plagioclase crystals is often seen in the granitic gneisses and the grey granite in which microcline perthite occurs as a major constituent.

3. *Biotite and muscovite*

Biotite occurs in almost all rocks, while muscovite is of restricted occurrence. The biotite in the folded S_1 layers is as very small flakes (Table 2). About half of the biotite flakes are concentrated along S_1 argillaceous layers and are folded with S_1, while the rest tend to be parallel to the planes of S_2, especially around the fold closures (Pl. 1–1).

Biotite occurs as large flakes in the well developed, thick S_2 mafic layers which are not affected by the F_3 disturbance. The large biotite flakes form elongated clots on the folded S_2 cleavage, being parallel to the F_2 fold axes. When sillimanite occurs, the biotite often shows symplectite texture with vermicular quartz and the colour of the biotite is very faint (Table 2). Faint pleochroism is also seen when sillimanite is superimposed on the biotite. A few muscovite flakes are found in the sillimanite-bearing rocks, interlocking with biotite.

Large flakes of biotite in folded S_2 are disrupted into fine flakes where the S_2 layering is intersected by S_4. Where the granitic metatects are dominant along S_4, randomly oriented hornfelsic flakes of biotite of medium size are superimposed on the disrupted fine flakes. These indicate mechanical crushing during the F_3 disturbance and successive annealing coarsening of biotite by the thermal effect of the grey granite when it was emplaced.

Decomposition of biotite into chlorite is only seen locally in the granitic gneisses and grey granite. Chloritization is always seen in the sheared zone associated with the intrusion of post-tectonic Hornemantoppen granite.

4. *Cordierite*

Cordierite is not found in rocks which have well preserved S_1 structure. This mineral occurs as small- to medium-grained, equidimensional round grains in the rocks having distinct compositional layering of S_2, and is located between micaceous and quartzo-feldspathic layers. Clear mosaics of plagioclase, poikiloblastic garnets, and large flakes of biotite occur in the same rock. This

Table 2.

Nature of biotites

Host rock		Fine-grained biotite gneiss	Micaceous layered gneiss	Sill.-gar.-biotite gneiss	Sp.-co. clot bg. gneiss	Mylonitic mica gneiss	Granitic gneiss (hornfelsic)	Grey granite
Tectonic phase		S_1	S_2	S_2	F_2–F_3	S_4	post F_3	F_4
Grain size (mm)		max=0.5 av=0.2	max=a few tens av=0.5	several tens –a few tens	several tens –a few tens	less than 0.2	a few tens –0.5	several tens
Preochloism	X	pale brown	pale brown	colourless	pale brown	pale brown	pale brown	pale brown
	Y=Z	foxy red brown	dark foxy brown	pale brown	dark brown	pale foxy red-brown	dark brown	deep brown
Ref. indeses	N_Z	1.655	1.665	——	1.665	1.644	1.652	1.654
	N_X	1.653	1.660	——	1.660	1.644	1.650	1.652

occurrence suggests that the cordierite was first formed after F_1. Some cordierite grains enclose large flakes of biotite and are large porphyroblasts up to a few mm across.

Cordierite is cracked and pinitized in the rocks folded by F_2, and in the granitic layers of sillimanite-bearing rock the cordierite grains are almost entirely transformed to sericite pseudomorphs superimposed by fibrolitic sillimanite. Large pale green clots of cordierite often occur in the quartzo-feldspathic metatects sub-concordantly folded by F_2; they are also pinitized intensely.

In the spinel-corundum-bearing rocks, cordierites occur as thin envelopes around the spinel-corundum clots as a kind of reaction rim (Pl. 3–1), and in the extremely micaceous layers as large xenomorphic grains.

No cordierite is found in the rocks with the S_4 diaphtolitic cleavages, but many granitic metatects in the agmatitic and nebulitic migmatites contain pinitized cordierite clots.

5. *Garnet*

Garnet is not found in S_1 because in most of the compositionally suitable rocks S_1 has been entirely transformed into S_2 by F_1 folding. However, most garnet grains in S_2 are poikiloblastic, including elongated small grains of quartz as straight inclusion trails which have not been rotated from the surrounding cleavages. These inclusions suggest that the garnet began to grow from the S_1 recrystallization phase.

The poikiloblastic garnets have inclusion free mantles, sometimes with sub-idiomorphic outlines in S_2. Some of them are disrupted into fragments without decomposition and have S- or Z-formed crystal shape, indicating their syntectonic growth during F_2.

Thus, the garnets grew through all stages from the S_1 to post-F_2 episode. This is supported by the observation that a large garnet half encloses a spinel-corundum clot (Pl. 3–2) and another includes green spinel and sillimanite around the margins of a large grain (Fig. 2–2). In a coarse-grained (sillimanite)-cordierite-garnet-biotite gneiss, a garnet glomeroblast evidently overgrows cordierite (Fig. 2–3), indicating that the almandine⇌cordierite + almanadine reaction (HIRSCHBERG and WINKLER, 1968) has taken place.

Large biotite flakes of S_2 abutt against garnets in most of the layered gneisses, but a narrow symplectite zone of pale coloured biotite and potash feldspar intergrowth occurs along the contacts in the sillimanite-bearingrocks.

In the S_4 diaphtolitic rocks with mylonitic sutured quartz, small fragments of garnet occasionally occur in the chlorite aggregates. Red sub-idiomorphic garnets occur very often in the cross cut quartzo-feldspathic veins in less migmatized gneisses.

6. *Sillimanite*

This mineral occurs only in the biotite clots parallel to the F_2 fold axes and itself forms elongated seams on folded S_2. Most sillimanite is fibrolite in radial and sub-parallel bundles, superimposed on biotite flakes and is often

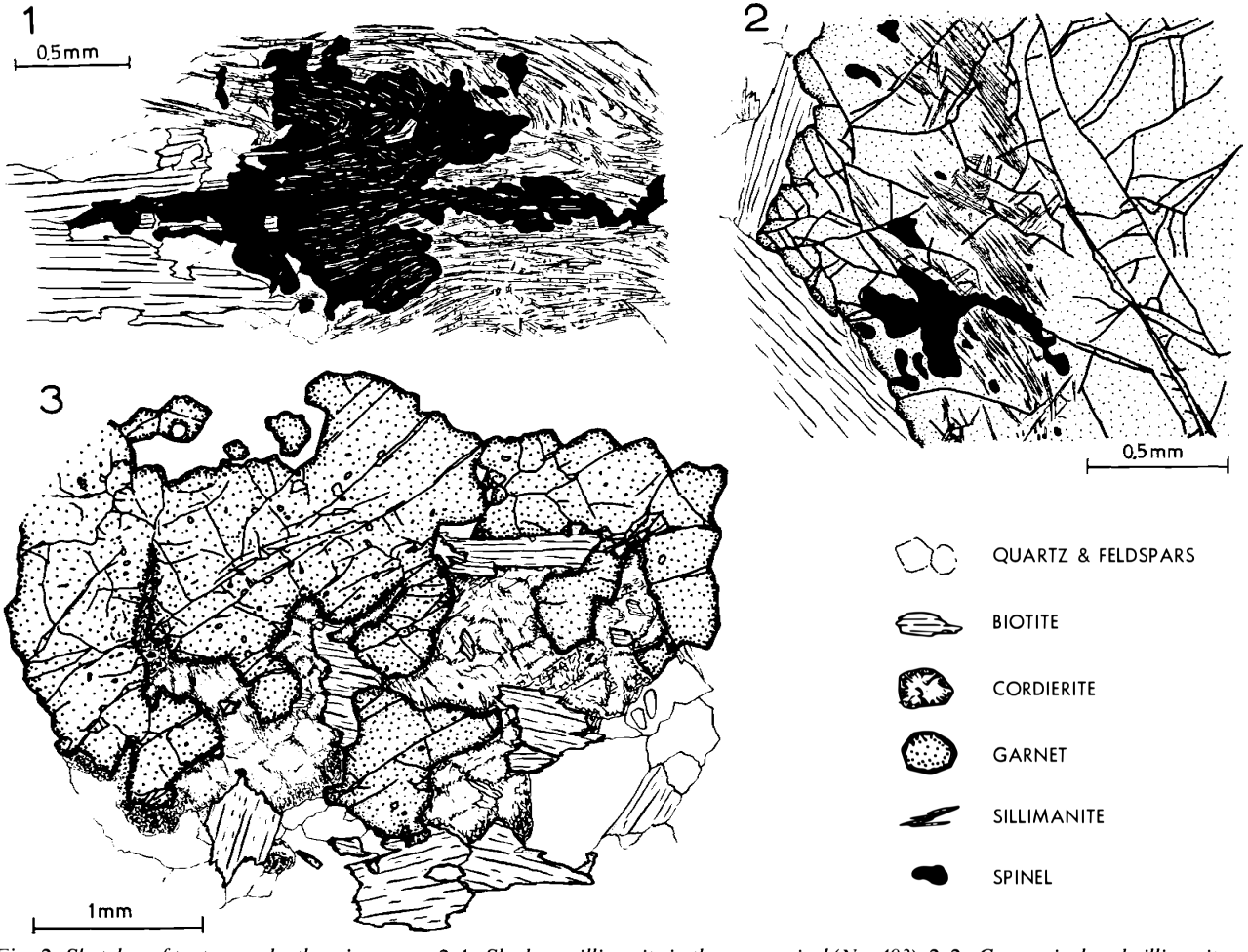

Fig. 2. *Sketches of texture under the microscope.* 2–1. *Shadowy sillimanite in the green spinel (No. 403).* 2–2. *Greenzpinel and sillimanite included in the margin of a large garnet idioblast (No. 456).* 2–3. *A garnet glomeroblast superimposed on the cordierite-biotite-quartz-feldspar matrix (No. 119).*

included in the coarse-grained mosaic of quartz and plagioclase. Sometimes, sillimanite occurs as radial fibers on completely pinitized cordierite. Thin fibrolite sillimanite bundles occur on the pinitic fine aggregate of muscovite in the spinel-corundum-bearing rocks, showing roughly parallel growth. It is difficult to judge whether these sillimanite needles were formed from muscovite or decomposed into muscovite. Prismatic, idiomorphic sillimanites occur in some garnet-biotite gneisses but there is no muscovite in them. Thus, the identification of a second sillimanite isograd is uncertain.

No sillimanite has been found in the rocks formed earlier than F_2 or in those later than S_4. Therefore, the sillimanite of this area was formed during the metamorphic culmination of the F_2 to the F_2–F_3 interval.

7. *Spinel and corundum*

These two minerals make small elongated clots with circular or irregular profile (Pl. 3–1) parallel to the F_2 fold axis. Some clots show obliquely crossing longitudinal profile (Pl. 4). Corundum, as very small polygonal grains less than 0.05 mm across, does not occur in all clots but is always associated with spinel. They have blue colour in part. The spinel is green hercynite, equally as small as corundum (from 0.05—0.1 mm) and of round or vermicular shape. The spinel shows symplectite-like texture in the most dense and finest parts of the clots, mostly in the core. The coarsest grains are situated in the middle part and relatively widely-spaced medium sized grains occur around the margin of the clots, thus forming a zonal distribution of grain size. The coarse spinel rarely has faint shadows of included fibrous sillimanites which appear almost to have disappeared (Fig. 2–1). The matrix of these clots is a felt of fine muscovite. Most clots are enveloped by thin cordierite rims in the biotite-rich layers and by plagioclase rims when they occur adjacent to the quartzo-feldspathic layers. A clear mosaic of plagioclase (An 60) makes up some parts of the matrix of the clots. Coarse biotite flakes of pale coloured pleochroism occasionally occur in the clots and are superimposed by spinel and corundum. The modal composition of clots is given in Table 3. According to the optic data, biotite, cordierite and spinel are all iron-rich varieties.

The rocks including these clots occur as a narrow discontinuous zone about 6 km long, a few km west of the grey granite border. They may extend further to the south east of Magdalenefjorden where the same type of clots with corundum a few cm long occur in the micaceous gneiss.

The mineralogy, elongated shape, and the arrangement of the clots parallel to the F_2 fold axis suggest strongly that they are pseudomorphs after a long prismatic, Fe and Al rich mineral. The absence of anhydrous Al-silicates in the rocks of earlier than F_2 episode origin in this area suggests that the dehydration reactions consuming hydrous minerals masked the P–T field of andalusite and kyanite. Therefore, the most probable pre-existing minerals are Fe, Al-rich hydrous minerals, such as chloritoid and staurolite. Cordierite, although it is anhydrous, is also a possibility, but it co-exists stably with the clots. Comparing the regional distribution of this special rock to that of chloritoid-bearing rocks in Prins Karls Forland (ATKINSON 1960) and Mitrahalvøya

Table 3.

Modal composition of the spinel-corundum clots

Bulk rock

Sample No.	Bi	Cord	Hb	Gar	Op	Sp-Co clot
403	63.7	15.7	8.5	0.8	0.8	10.8

Spinel-corundum clots

Sample No.	Bi	Cord	Seri	Sp	Co	Op	Remarks
403–1	1.7	4.6	46.2	43.9	1.3	2.2	with pl rim
403–2	–	44.9	29.5	10.9	10.9	3.8	with cord rim
403–3	–	34.5	45.1	–	15.4	5.0	with cord rim
403–4	–	40.5	19.9	27.8	7.3	4.5	with cord rim
440	5.9	–	80.9	11.0	–	2.2	with pl rim

Refractive index of the constituent minerals, sample No. 403

	Biotite	Garnet	Cordierite	Spinel
Refractive Index	N_z=1.665, 1.655 N_x=1.660, 1.653	1.795	N_x=1.555 N_y=1.568 N_z=1.573	1.810

(TVETEN, pers. comm.), where chloritoid occurs in a narrow zone of intense shearing, chloritoid seems to be the most probable mineral. An obliquely crossing outline of elongated clots (Pl. 4) also supports this opinion despite the zonal distribution of staurolite and andalusite around the migmatitic granite in the SW Innvika, north central Nordaustlandet (FLOOD et al. 1969). Sillimanite inclusions in the coarse-grained spinel (Fig. 2–1) indicate that the latter formed later than the formation of sillimanite fibrolite, and this supports the proposal of decomposition of staurolite at a higher temperature than the first appearance of sillimanite (HOSCHEK 1969).

The possible reactions are as follows:

$$\overset{4Chd}{4FeAl_2SiO_5(OH)_2} + \overset{Bi}{(OH)_2KFe_3AlSi_3O_{10}} + 5O = \overset{Hercy}{FeAl_2O_4} + \overset{Mus}{(OH)_2KAl_3Si_3O_{10}} + \overset{3Co}{3Al_2O_3} + \overset{2Mt}{2Fe_3O_4} + \overset{4Qz}{4SiO_2} + 8H_2O$$

and

$$\overset{2St}{2(OH)_2Fe_2Al_9Si_4O_{22}} + \overset{Bi}{(OH)_2KFe_3AlSi_3O_{10}} + O_2 = \overset{4Hercy}{4FeAl_2O_4} + \overset{Mt}{Fe_3O_4} + \overset{Mus}{(OH)_2KAl_3Si_3O_{10}} + \overset{4Co}{4Al_2O_3} + \overset{8Qz}{8SiO_2} + 2H_2O$$

The cordierite rim around the clots might be formed by the following reaction:

$$\overset{Hercy}{FeAl_2O_4} + \overset{Mt}{Fe_3O_4} + \overset{Co}{Al_2O_3} + \overset{10Qz}{10SiO_2} \rightleftharpoons \overset{2Cord}{2Fe_2Al_4Si_5O_{18}} + \tfrac{1}{2}O_2$$

8. *Quartzo-feldspathic metatects*

A very few quartz veins and lenses with or withour albitic plagioclase cut sharply across the rocks with the S_1 and F_1 folds. When the S_2 layering is folded by F_2, numerous quartzo-plagioclase veins and layers occur with sharp contact against the surrounding rocks and are tightly folded, mostly less complexly than the folded S_2, but some are further intensely ptygmatically folded (OHTA 1969, Pl. II–a). Plagioclase porphyroblasts sometimes occur beyond the contact with the surrounding rocks to make the contact unclear. Clusters of plagioclase porphyroblasts are often situated around the F_2 fold crests, having crescent and lensoid shape.

These quartz-plagioclase rocks have a polygonal matrix of quartz, with weakly wavy extinction, and large sub-idiomorphic plagioclase (An 20 to 25) including small grains of quartz and biotite, and sometimes garnet. Interstitial microcline perthite (2Vx=80 to 90) is very rare. There are scattered large flakes of biotite. Sillimanite, garnet and cordierite occur at the contacts between these veins and the surrounding rock, without alteration. Thus, these quartzo-feldspathic rocks are granodioritic metatect formed in the early part of the F_2 deformation in the period of maximum metamorphism and independent of any hydration or retrogressive reactions.

The S_4 diaphtolitic cleavages are followed only by quartz. The granitic gneisses are concordant with S_4 and have almost granitoid texture with large plagioclase and microcline and gneissic matrix in which biotite is partly converted into chlorite. The granitic metatects of similar composition in the agmatite also develop along S_4 and irregular fractures.

This evidence shows that the granitic parts of migmatites and granitic gneisses developed in close relation to the emplacement of grey granite in the F_3 episode and was associated with retrogressive metamorphism.

Pegmatitic and aplitic veins cut across all structures mentioned above. They have cordierite clusters in the migmatitic rocks, while garnet, quartz, feldspars

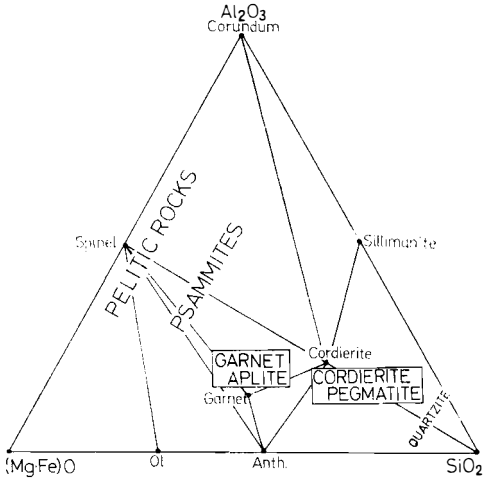

Fig. 3. *Al_2O_3–(Mg · Fe) O–SiO_2 diagram showing the mixing of psammitic and quartzitic rocks with resultant products of garnet aplite and cordierite pegmatite under the condition of upper amphibolite facies.*

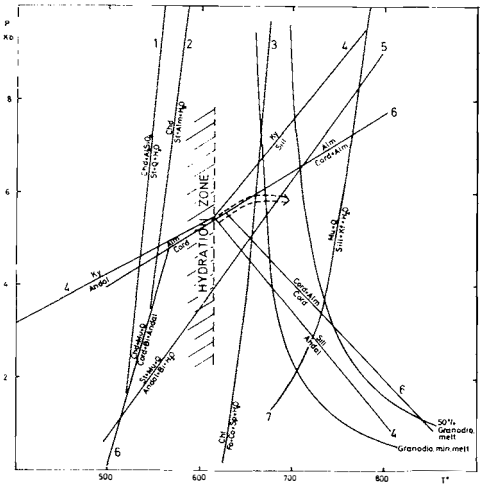

Fig. 4. *The P–T condition of metamorphism. 1 and 2:* GANGULY *(1969); 3:* YODER *in* EITEL *(1965); 4:* RICHARDSON *et al. (1969); 5:* HOSCHAK *(1969); 6:* HIRSCHBERG *and* WINKLER *(1968); 7.* MIYASHIRO *(1960); melting curves of granodiorite;* PIWINSKII *(1968).*

and a little of biotite occur in those cutting less migmatitic ones. The difference of constituent minerals is believed to represent different degrees of assimilation between the metatects and the surrounding rocks (Fig. 3).

C. SUMMARY AND DISCUSSION

The metamorphism of Hecla Hoek rocks in relation to the deformation phases in the Smeerenburgfjorden area is summarized in Figs. 4 and 5. The type of metamorphic facies series dependent on the P/T gradient is masked by dehydration reactions lower than the stability field of sillimanite, judging from the absence of kyanite and andalusite. This suggests that P_{H_2O} was very high and possibly equal to the P_{total}. For this reason, the abundance of migmatitic granite in this part of Spitsbergen is reasonable. In the hydrous zone, cordierite is always associated with almandine, and this suggests that the P/T gradient, according to HIRSCHBERG and WINKLER (1968), was intermediate and very near to the kyanite-andalusite inversion line (Fig. 4). An intermediate P/T gradient is also indicated by the growth of almandine porphyroblasts over cordierite in the sillimanite-bearing rocks (Fig. 2–3). This happened during the F_2 deformation phase, but in the F_2–F_3 interval the almandine-cordierite paragenesis was again stable. Thus, the P/T gradient of metamorphism during the F_2 to F_2–F_3 interval roughly coincides with the almandine/almandine+cordierite line of Fig. 4. The P/T gradient of this reaction line is 1.25 Kb/100 °C as given by HIRSCHBERG and WINKLER (1968). This P/T gradient is intermediate between the Barrovian type and the Buchan type of NE Scotland. Definite Buchan type series (low P – high T series), thus, could not be distinguished in the present area.

Formation of granodioritic metatects in the F_2 episode, associated with sillimanite and spinel-corundum-bearing gneisses, probably took place around the 5.5 Kb pressure with high P_{H_2O} and in the temperature range of 650–700°C.

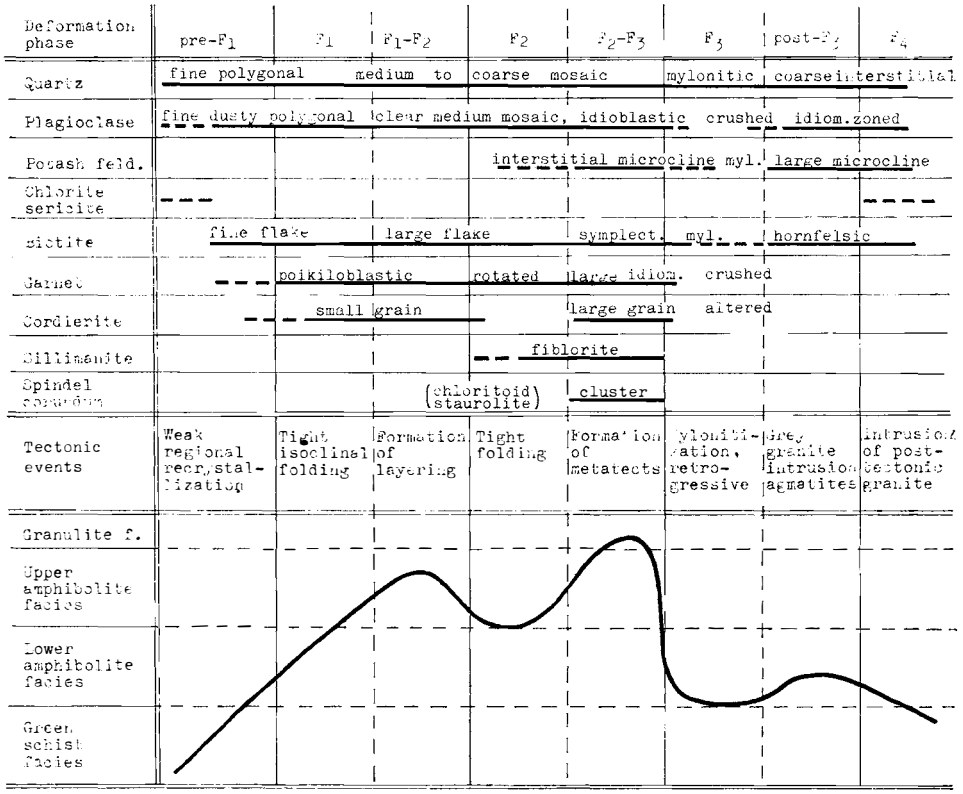

Fig. 5. *Metamorphism and deformation phases.*

GEE and HJELLE (1966) made a reconnaissance survey of the Northwest Anticlinorium from Kongsfjorden to the NW corner and found that the regional fold axes generally plunge gently to the south. Therefore, the rocks of the present area represent the lower structural succession of Lower Hecla Hoek, and the Kongsfjorden area in the south represents a shallower tectonic level. The metamorphic grade increases gradually from south to north in the Northwest Anticlinorium. In this Anticlinorium (on Danskøya where cordierite and sillimanite-bearing rocks are dominant), HJELLE (pers. comm.) found a few rocks with kyanite showing inversion to sillimanite from the grain margins. The present author studied the rocks of the Magdalenefjorden area where sillimanite, garnet and cordierite are common but no kyanite has been found in preliminary microscopic examination. TVETEN (pers. comm.) found biotite and almandine zones on Mitrahalvøya in the southern part of the Anticlinorium with occasional andalusite and sillimanite. All this information indicates that the main part of the Northwest Anticlinorium is characterized by the "intermediate" metamorphic facies series between the Barrovian and Buchan type facies series, and the southern part was metamorphosed under conditions of the Buchan type metamorphic facies series.

In contrast, the Ny Friesland anticlinorium and Biskayerhuken areas in the eastern and central part of norh Spitsbergen, are characterized by kyanite-

staurolite-bearing rocks which indicate typical Barrovian type metamorphic facies series. ZWART (1967) classified the Norwegian Caledonides into the Barrovian type based on the occurrences of these index minerals. On the other hand, the occurrences of andalusite, cordierite, and staurolite in Nordaustlandet indicate that the metamorphic conditions of this area are similar to the Northwest Anticlinorium. Recently, HORSFIELD (1972) reported the occurrence of glaucophane schist from the St. Jonsfjorden area. Thus, the Caledonian metamorphic rocks of Svalbard constitute a very complicated problem with respect to the regional distribution of different metamorphic facies series.

II. Modal and chemical composition

A. MODAL COMPOSITION OF THE ROCKS

Modal analyses of 32 rocks, all of which were also analysed chemically, have been carried out to clarify the change of mineralogical composition from the fine-grained gneisses to granitic rocks. A point-counter was used with thin sections; 1500 points for fine-grained rocks and 2000 points for coarse-grained rocks were counted for each specimen.

The data are given in Table 4 and are compared with the mesonorm calculated from chemical analyses. The thin sections studied in some cases, do not cover the whole lithologic variety of the analysed part of a specimen because some rocks are quite heterogeneous. Therefore, the modal analyses and the mesonorms do not coincide well. Especially the amount of calculated biotite differs in many samples owing to the procedure of the mesonorm calculation. The modal data are summarized on the Qt–Feld–Mf diagram and the Qt–Kf–Pl diagram (Figs. 6–A and 6–B).

The modal differences between the quartzo-feldspathic and micaceous layers are larger in the fine-grained gneisses than in the layered gneisses, and both quartzo-feldspathic and micaceous layers of the fine-grained gneisses have larger modal variation than the layered gneisses. The most quartzo-feldspathic bands of the fine-grained gneisses are impure quartzite which are not plotted on the diagrams.

The difference in modal composition between the quartzo-feldspathic and the micaceous layers is small or almost non-existent in the layered gneiss, although megascopically the layering structure is very distinct. This is mainly due to the porphyroblastic introduction of feldspar in the micaceous layers, and on the whole the amount of plagioclase increases slightly in these rocks compared with the fine-grained gneisses (Fig. 6–B). This indicates that the large modal difference within the fine-grained gneisses gradually disappears during the formation of layered gneisses. However, the grain size increases in the layered gneisses, and small domains of extreme composition occur, such as plagioclase porphyroblastic masses, biotite seams, and spinel-corundum clots. Biotite enriched patches accompany cordierite and garnet, sometimes sillimanite.

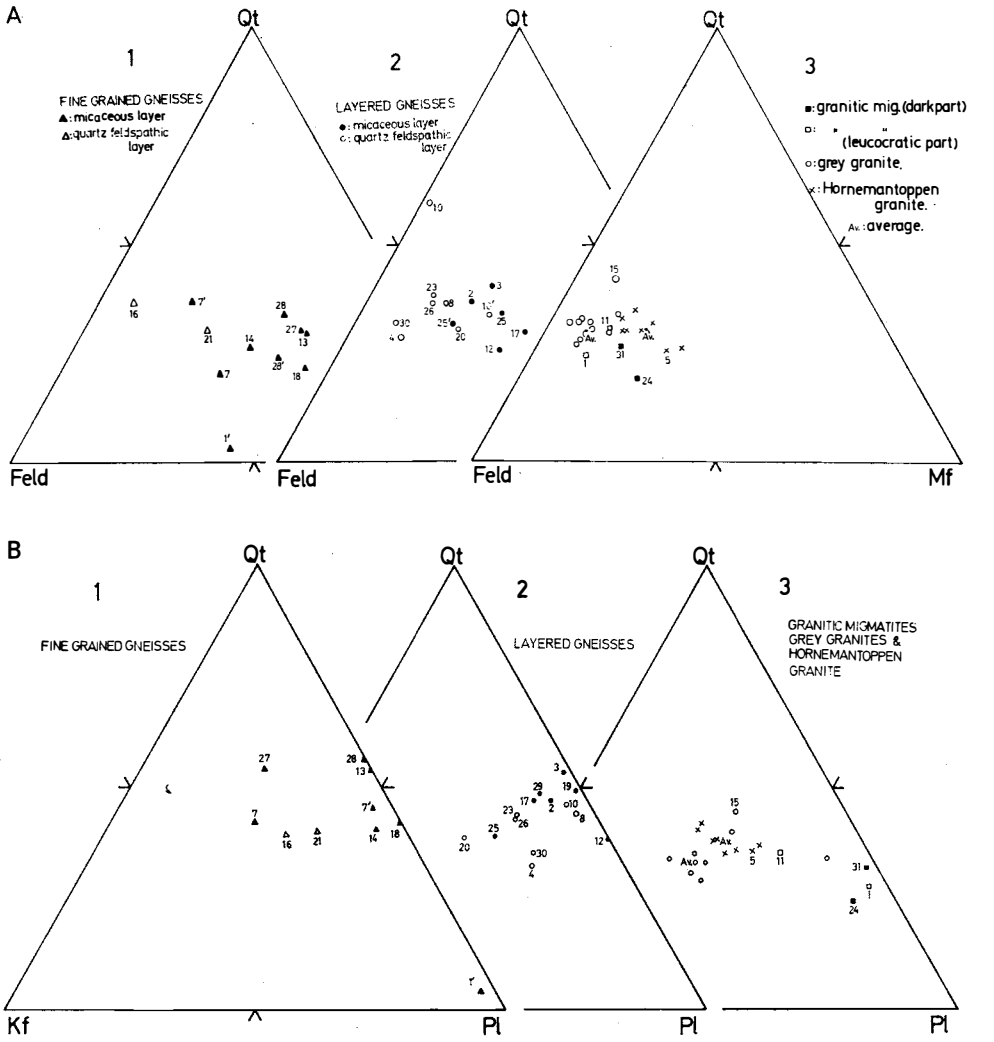

Fig. 6. ***Modal composition of the rocks.*** **6–a.** ***Modal Qt-Feld-Mf diagram.*** **6–b.** ***Modal Qt-Kf-Pl diagram.*** ***(Symbols are the same as Fig. 6–a.) The open circles and crosses without number in the 3 figure are from*** HJELLE ***(1966), calculated from the mode. The suffixed numbers in all figures are correlated to Tables 4 and 5.***

The modal composition of the granitic migmatite and grey granites is characterized by the decrease of mafic minerals and increase of potash feldspar. Some relatively basic schlieren in the heterogeneous granitic migmatites are characterized by a large amount of plagioclase. The grey granites have nearly eutectoidal Qz–Kf–Pl ratios.

The Hornemantoppen granite is an igneous-looking rock in the field and this genetic inference is supported by the projection of the modal composition on the Qz–Kf–Pl diagram, which roughly coincides with the experimental and statistical minimum of the diagram (HJELLE 1966). This granite is more mafic in composition than the granitic migmatites and the grey granites.

Table 4.

Modal composition and Mesonorm of the rocks

Sample No.	1 (16–4)	1 (16)	1 (16)	2 (24–2)	2 (24–2)	3 (49–1)	3 (49–1)	4 (52–3)	4 (52–3)	5 (58)	5 (58)	6 (74)
Miner.	Mode	Mode	Meson.	Mode	Meson.	Mode	Meson.	Mode	Meson.	Mode	Meson.	Meson.
Qt	2.36	24.60	28.98	37.25	28.99	40.38	19.47	28.67	27.29	25.65	25.81	16.21
C			3.58		5.15		3.46		4.15		3.42	
Or	1.99	3.80	15.64	5.61		1.34	4.59	16.39	23.63	16.84	18.74	17.12
Ab	51.99	61.90	30.56	35.97	32.24	34.15	34.46	43.90	29.98	30.21	35.65	28.35
An			9.22		14.90		7.74		5.61		6.32	20.28
Bi	42.21	9.27	8.98	19.56	13.42	23.19	23.97	10.63	6.81	11.57	6.88	
Act												
Di												13.26
Pyx					1.05							
Wo												0.89
Chl										2.52		
Seri												
Gar	0.99			1.62								
Cord												
Sill	0.18											
Sph		0.16	1.28		1.98		3.10		0.99	0.87	1.25	1.50
Mt	0.27	0.29	1.50		1.76	0.16	2.66	0.27	1.28	0.63	1.68	2.11
Ap			0.28		0.52		0.55		0.25		0.25	0.28
Ep						0.65						
Orth						0.16		0.14				
Zir												
Hb												
Tour												
Scap												
Sum Salic	56.34	90.30	87.96	78.83	81.27	75.87	69.72	88.96	90.67	72.70	89.94	81.96
Sum mafic	43.66	9.70	12.04	21.17	18.73	24.13	30.28	11.04	9.33	27.30	10.06	18.04

The sample numbers in parentheses are correlated to the locality in Fig. 1.

Table 4 (cont.)

Sample No.	7 (92–1a)	7 (92–1a)	8 (92–1b)	8 (92–1b)	8 (92–1b)	9 (92–2)	9 (92–2)	10 (93–1)	10 (93–2)	10 (93–2)	11 (109)	11 (109)
Miner	Mode	Meson.	Mode	Mode	Meson.	Mode	Meson.	Mode	Mode	Meson.	Mode	Meson.
Qt	19.98	20.70	36.57	36.74	24.54	39.63	26.33	34.33	59.72	37.77	30.14	29.84
C		3.68			3.13		4.20			9.52		2.99
Or		2.85	3.14	3.06	33.64	27.09	28.16	3.33	18.93	23.35	15.10	19.13
Ab	47.01	37.29	43.57	40.82	29.38	26.27	33.76	36.04	19.84	24.24	41.17	29.86
An		12.65			4.76		4.36			3.13		9.09
Bi	32.75	15.26	16.72	19.13	2.96	6.64	2.30	25.19	1.32	1.67	12.62	6.48
Act												
Di												
Pyx												
Wo												
Chl												
Seri												
Gar												
Cord												
Sill												
Sph		2.89			0.36		0.21			0.06		1.06
Mt	0.18	2.99		0.26	0.93	0.37	0.37	0.68	0.20	0.17	0.62	1.33
Ap	0.09	0.68			0.30		0.30			0.08		0.22
Ep												
Orth								0.43			0.35	
Zir												
Hb												
Tour												
Scap												
Sum Salic	66.99	78.17	83.28	88.00	95.45	88.99	96.82	73.70	98.49	98.01	76.41	90.91
Sum mafic	33.01	21.83	16.72	12.00	4.55	11.01	3.18	26.30	1.51	1.99	23.59	9.09

Table 4 (cont.).

Sample No.	12 (110)	12 (110)	13 (151)	13 (151)	14 (178–2)	14 (178–2)	15 (198)	15 (198)	16 (217)	16 (217)	17 (219–1)	17 (219–1)
Miner	Mode	Meson.	Mode	Meson.	Mode	Meson.	Mode	Meson.	Mode	Meson.	Mode	Meson.
Qt	26.01	32.11	29.58	31.79	26.00	34.34	42.54	32.01	36.69	29.66	30.19	31.97
C		4.99		4.85		2.22		3.16		4.87		6.70
Or				2.54	4.01	5.08	20.27	23.66	22.37	23.35	6.80	11.2 7
Ab	41.67	17.27	24.66	25.67	33.77	26.72	29.44	29.32	33.36	31.41	27.03	25.32
An		21.13		12.23		15.44		5.77		6.59		5.20
Bi	30.42	19.35	43.17	16.91	35.98	11.83		3.91	6.66	2.90	26.56	15.04
Act												
Di												
Pyx		0.30										
Wo												
Chl							3.84		0.39			
Seri											5.95	
Gar	1.89		0.42								0.39	
Cord											2.16	
Sill												
Sph		2.32		2.65		1.57		0.65		0.47		2.19
Mt		2.12	0.17	3.03	0.25	2.57	1.25	1.29	0.54	0.65	0.15	2.07
Ap		0.41		0.32		0.24		0.22		0.11		0.24
Ep							2.67					
Orth												
Zir											0.77	
Hb												
Tour												
Scap												
Sum Salic	67.68	75.51	54.24	77.08	63.78	83.79	92.20	93.93	92.42	95.88	64.02	80.46
Sum mafic	32.32	24.49	45.76	22.92	36.22	16.21	7.80	6.07	7.58	4.12	35.98	19.54

Table 4 (cont.)

Sample No.	18 (252)	18 (252)	19 (264)	19 (264)	20 (276)	20 (276)	32 (284–1)	32 (284–2)	32 (284–2)	21 (297)	21 (297)	22 (310)
Miner.	Mode	Meson.	Mode	Meson.	Mode	Meson.	Mode	Mode	Meson.	Mode	Meson.	Meson.
Qt	21.19	36.93	30.27	32.27	30.37	26.07	29.92	0.92	13.32	29.89	27.46	28.77
C		4.62		7.54		4.66					3.80	3.80
Or		3.02	0.63	7.54	22.32	28.65	11.89		9.90	13.35	24.46	19.05
Ab	28.76	31.91	30.51	27.75	25.34	27.77	33.33	28.50	19.75	31.26	28.76	36.93
An		7.80		6.20		4.57			19.11		6.48	6.52
Bi	49.60	10.88	31.06	13.51	21.56	5.79	24.55			24.59	6.12	3.78
Act									25.16			
Di									2.03			
Pyx												
Wo												
Chl								2.42				
Seri			5.63									
Gar												
Cord			0.95									
Sill												
Sph		1.89		2.30		1.06		3.08	5.43		0.97	0.42
Mt	0.45	2.49	0.95	2.68	0.25	1.13	0.31	4.17	4.64	0.55	1.78	0.63
Ap												0.11
Ep		0.46		0.22		0.30		0.25	0.66		0.17	
Orth										0.37		
Zir					0.16							
Hb								60.67				
Tour												
Scap												
Sum Salic	49.95	84.29	65.91	81.29	78.03	91.72	75.14	29.42	62.08	74.50	90.96	95.06
Sum mafic	50.05	15.71	34.09	18.71	21.97	8.28	24.86	70.58	37.92	25.50	9.04	4.94

Table 4 (contd.)

Sample No.	23 (353)	23 (353)	24 (386–1)	24 (386–1)	33 (389)	33 (389)	33 (389)	31 (394)	31 (394)	34 (425)	34 (425)	25 (429)	25 (429)
Miner.	Mode	Meson.	Mode	Meson.	Mode	Mode	Meson.	Mode	Meson.	Mode	Meson.	Mode	Meson.
Qt	37.76	27.96	19.14	24.06			24.66	26.52	26.53	26.70	29.57	31.59	24.42
C		3.03		4.11			5.36		5.59		3.37		4.65
Or	13.84	26.58	6.67	6.22				2.07	9.39	0.55	0.92	17.60	13.84
Ab	34.99	28.47	52.00	30.99		7.31	33.37	54.28	30.81	59.39	34.07	30.41	26.53
An		6.59		11.76			6.17		8.91		20.50		7.10
Bi	12.42	4.95	21.26	17.18			5.35	14.43	14.01	12.73	8.32	20.03	16.46
Act													
Di					30.03	60.00							
Pyx							20.94						
Wo						14.40							
Chl								2.42					
Seri													
Gar													
Cord													
Sill													
Sph	0.07	0.08		2.60	0.57	1.71	2.43		2.46		1.24		3.05
Mt	0.43	1.25	0.78	2.38	1.14	0.23	1.39	0.28	2.04	0.14	1.70	0.22	3.64
Ap		0.28	0.16	0.70			0.32		0.17	0.07	0.30	0.15	0.32
Ep													
Orth	0.50												
Zir										0.07			
Hb										0.34			
Tour													
Scap					46.35	13.94							
Sum Salic	86.59	92.64	77.81	77.14	0.00	7.31	69.57	82.87	81.31	86.64	88.44	84.60	76.54
Sum mafic	13.41	7.36	22.19	22.86	100.0	92.69	30.43	17.13	18.69	13.36	11.56	15.30	23.46

Table 4 (cont.)

Sample No.	26 (432)	27 (436)	27 (436)	28 (440)	28 (440–5)	28 (440–5)	29 (449a)	29 (449b)	29 (449)	30 (456)	30 (456)
Miner.	Meson.	Mode	Meson.	Mode	Mode	Meson.	Mode	Mode	Meson.	Mode	Meson.
Qt	26.11	30.01	22.19	24.09	34.44	38.54	32.96	34.59	32.70	32.24	30.03
C	4.30		6.43			5.24			6.38		4.19
Or	29.83	11.71	28.07	0.84	0.46	7.26	1.30	6.19	6.15	15.45	14.63
Ab	27.60	13.54	17.77	32.60	26.45	25.50	37.92	30.31	29.89	44.18	34.34
An	5.01		1.81			6.85			4.86		9.02
Bi	5.55	43.37	18.40	42.04	37.93	11.82	26.98	28.54	14.47	7.93	5.58
Act											
Di											
Pyx											
Wo											
Chl											
Seri		0.91					0.44				
Gar											
Cord											
Sill											
Sph	0.64		2.82			2.31			2.60		0.83
Mt	0.61	0.46	2.34	0.42	0.55	2.27	0.37	0.37	2.79	0.21	1.24
Ap	0.34		0.17			0.22			0.15		0.13
Ep											
Orth											
Zir					0.18						
Hb											
Tour											
Scap											
Sum Salic	92.85	55.26	76.27	57.53	61.35	83.39	72.18	71.09	79.99	91.87	92.21
Sum mafic	7.15	44.74	23.73	42.46	38.66	16.61	27.79	28.91	20.01	8.14	7.79

Analysed samples (both modal and chemical analysis).

1 (16) Plagioclase porphyroblastic granodioritic gneiss, micaceous layer of the layered gneiss. (□).
2 (24–2) Fine grained garnet-biotite gneiss in the layered gneiss. (●)
3 (49–1) Coarse-grained granitic gneiss. (●)
4 (52–3) Granodioritic gneiss. (○)
5 (58) Granodiorite, Hornemantoppen quartz monzonite. (+)
6 (74) Potash feldspar porphyritic granodiorite. (+)
7 (92–1a) Fine-grained banded gneiss. (▲)
8 (92–1b) Plagioclase porphyroblastic leucocratic gneiss. (○)
9 (92–2) Garnet bearing aplitic granite in the fine-grained gneiss. (△)
10 (93–2) Plagioclase porphyroblastic gneiss. (○)
11 (109) Gneissose granodiorite. (□)
12 (110) Poikiroblastic garnet-biotite gneiss. (●)
13 (151) Fine-grained biotite gneiss. (▲)
14 (178–2) Fine-grained biotite gneiss. (▲)
15 (198) Biotite gneiss in the granitic gneiss. (+)
16 (217) Fine-grained felsic gneiss. (△)
17 (219–1) Garnet-cordierite-biotite gneiss in the nebulitic migmatite. (●)
18 (252) Fine-grained hornfelsic biotite gneiss. (▲)
19 (264) Plagioclase porphyroblastic cordierite-biotite gneiss. (●)
20 (276) Potash feldspar porphyroblastic mylonitic biotite gneiss. (○)
32 (284–2) Biotite amphibolite. (×)
21 (297) Augen gneiss, catacalstic blastoporphyritic biotite gneiss. (○)
22 (310) Veined granitic migmatite. (□)
23 (353) Cataclastic plagioclase porphyroblastic biotite gneiss. (○)
24 (386–1) Heterogeneous granodiorite. (■)
33 (389) Skarn origin amphibolite. (×)
31 (394) Granodiorite. (■)
25 (425) Meta-hornblende gabbro. (×)
34 (429) Potash feldspar porphyroblastic biotite gneiss. (●)
26 (432) Mylonitic feldspar blastoporphyritic leucocratic gneiss. (○)
27 (436) Fine-grained schistose biotite gneiss. (▲)
28 (440–5) Fine-grained biotite gneiss. (▲)
29 (449) Plagioclase porphyroblastic biotite gneiss. (●)
30 (456) Plagioclase porphyroblastic biotite gneiss. (○)

26–B Grey granite. (○)
26–C Grey granite. (+)
64–C Grey granite. (+)
} HJELLE's samples.

The sample numbers correspond to those of all figures and the numbers in parentheses are the localities in Fig. 1. Symbols are the same for all figures.

B. BULK CHEMICAL COMPOSITION OF THE ROCKS

In all, 37 chemical analyses, including 3 samples from HJELLE, have been carried out, using X-ray fluorescence spectrography, titration, and flame photometry techniques (Table 5). The data are calculated to cation proportions, Niggli values, the katanorm, and the mesonorm and are summarized in diagrams. The chemical compositions of the grey granite and the Hornemantoppen granite, calculated from modal analyses by HJELLE (1966), are added for comparison in some of the diagrams.

Table 5.

Chemical composition of the rocks

No.	1	2	3	4	5	6	7	8	9	10	11	12	13
Locality No.	16	24–2	49–1	53–3	58	74	92–1 a	92–1b	92–2	93–2	109	110	151
SiO_2	67.80	63.50	59.90	69.15	68.20	66.60	60.10	69.80	70.30	73.15	68.65	62.05	63.65
TiO_2	0.60	0.92	1.47	0.47	0.59	0.75	1.35	0.17	0.10	0.03	0.49	1.08	1.23
Al_2O_3	15.80	17.12	15.75	16.32	15.99	16.42	17.08	16.28	16.78	18.64	15.28	17.20	15.53
Fe_2O_3	1.40	1.64	2.52	1.21	1.59	2.10	2.80	0.88	0.35	0.16	1.23	1.97	2.81
FeO	2.87	4.24	7.19	2.52	2.23	2.66	5.32	1.29	0.93	0.50	2.23	5.37	5.10
MnO	0.14	0.08	0.12	0.06	0.06	0.07	0.13	0.04	0.02	0.02	0.06	0.10	0.12
MgO	1.05	1.90	2.98	0.69	0.96	1.50	1.70	0.27	0.17	0.20	0.73	2.64	2.23
CaO	2.41	3.88	2.92	1.61	1.83	2.92	4.06	1.25	1.12	0.70	2.25	5.15	3.45
K_2O	3.52	1.38	3.28	4.68	3.85	3.02	2.05	5.93	4.93	4.10	3.80	1.99	2.15
Na_2O	3.33	3.49	3.80	3.31	3.92	3.29	4.06	3.23	3.70	2.68	3.22	1.87	2.77
P_2O_5	0.13	0.24	0.26	0.12	0.12	0.14	0.32	0.14	0.14	0.04	0.10	0.19	0.15
$H_2O(\pm)$	1.20	1.25	0.65	0.75	1.17	1.04	1.75	1.30	1.37	0.67	1.45	1.10	1.15
Total	100.25	99.64	100.84	100.89	100.51	100.51	100.72	100.58	99.91	100.89	99.49	100.71	100.34

No.	14	15	16	17	18	19	20	32	21	22	23	24	33
Locality No.	178–2	198	217	219–1	252	264	276	284–2	297	310	353	386–1	389
SiO_2	67.70	70.40	70.70	65.45	68.30	64.30	68.55	56.70	67.75	70.75	69.00	61.95	63.40
TiO_2	0.73	0.30	0.22	1.02	0.87	1.06	0.50	2.48	0.45	0.20	0.41	1.22	1.13
Al_2O_3	14.44	14.58	17.00	16.00	14.18	16.57	16.65	11.87	15.83	16.30	15.39	16.56	13.50
Fe_2O_3	2.39	1.19	0.61	1.92	2.29	2.47	1.06	4.24	1.65	0.59	1.16	2.24	1.29
FeO	3.23	1.37	1.29	4.85	3.66	4.60	2.23	2.31	2.80	1.58	2.08	4.96	7.83
MnO	0.09	0.04	0.03	0.11	0.10	0.09	0.04	0.27	0.07	0.06	0.04	0.17	0.21
MgO	1.86	0.53	0.19	1.67	1.31	1.53	0.54	5.77	0.42	0.24	0.41	2.27	4.59

CaO	3.68	1.46	1.53	1.88	2.40	2.08	1.44	9.53	1.69	1.50	1.75	3.62	2.20
K_2O	2.05	4.25	4.20	3.40	1.60	2.61	5.37	1.60	4.65	3.57	4.88	2.82	0.55
Na_2O	2.89	3.14	3.45	2.74	3.42	2.98	3.04	2.10	3.11	4.05	3.08	3.39	3.61
P_2O_5	0.11	0.10	0.05	0.11	0.21	0.10	0.14	0.30	0.08	0.05	0.13	0.33	0.15
H_2O (±)	0.80	1.37	0.36	1.44	2.53	1.42	1.07	2.21	1.20	0.70	1.20	1.23	1.52
Total	99.97	98.73	99.63	100.59	100.87	99.81	100.63	99.38	99.70	99.59	99.53	100.76	99.98

No.	31	25	34	26	27	28	29	30	HJELLE's samples		
Locality No.	394	425	429	432	436	440–5	449	456	26–b	26–c	64–c
SiO_2	63.60	64.89	61.75	68.60	61.05	69.15	65.15	69.05	70.80	68.45	69.40
TiO_2	1.15	0.57	1.42	0.30	1.31	1.07	1.20	0.39	0.18	0.35	0.27
Al_2O_3	16.97	17.32	15.73	16.58	16.55	14.20	15.32	16.38	16.24	16.40	16.37
Fe_2O_3	1.91	1.57	3.39	0.57	2.17	2.10	2.57	1.16	0.29	1.05	0.81
FeO	4.31	2.44	5.46	1.94	5.03	3.38	4.74	2.08	1.22	2.73	1.87
MnO	0.07	0.03	0.12	0.04	0.08	0.16	0.07	0.05	0.02	0.06	0.03
MgO	1.74	1.19	2.08	0.51	2.53	1.65	1.74	0.58	0.34	0.51	0.31
CaO	2.68	4.57	2.59	1.41	1.38	2.22	1.88	2.13	1.31	1.80	1.28
K_2O	3.00	1.00	3.98	5.52	6.50	2.40	2.48	3.00	4.03	4.08	5.57
Na_2O	3.35	3.66	2.88	3.01	1.92	2.75	3.21	3.74	3.50	3.74	2.77
P_2O_5	0.08	0.14	0.15	0.16	0.08	0.10	0.07	0.06	0.06	0.11	0.10
H_2O (±)	1.64	2.49	1.73	1.06	1.80	1.63	1.58	0.87	2.25	1.22	1.11
Total	100.50	99.87	101.28	99.70	100.40	100.81	100.01	99.49	100.24	100.50	99.89

Analyst: Y. OHTA

1. *Alkali compositions*

A distinct increase of K_2O with nearly constant amount of Na_2O is represented in the K_2O–Na_2O diagram (Fig. 7). The original psammitic sedimentary rocks, which might have had a composition very close to the present fine-grained gneisses, are assumed to have had a relatively low K_2O content with small variation of Na_2O. The quartzo-feldspathic layers of all metamorphic rocks have generally higher K_2O than the micaceous ones and roughly the same alkali composition range as that of the grey granite, which has somewhat high Na_2O, reflecting a large amount of plagioclase porphyroblasts. Two samples, Nos. 12 and 27, are extremely low in Na_2O. Both are paleozomes in the granitic migmatite.

The mesonorm calculation and modal analyses show that the K_2O mainly occurs in biotite in the micaceous layers and in potash feldspar in the quartzo-feldspathic layers in all metamorphic rocks (Table 4).

When the katanorm quartz and feldspars are plotted on the Q–Ab–Or diagram (Fig. 8–a), the majority of the quartzo-feldspathic layers of the layered gneisses are not on the minimum line but in the potash feldspar field of the diagram, while the end products of migmatization, such as the granitic migmatites and grey granites, coincide with the minimum line of the diagram. These end products are located in the intermediate field between the micaceous rocks of different kinds of gneisses and the quartzo-feldspathic parts of the layered gneisses. This relationship supports inferences based upon macroscopic observations that the granitic end products are a homogenized mixture of the micaceous and quartzo-feldspathic layers (Fig. 3). Flow structures are also common in these homogenized rocks, indicating a mobilization. Such rocks project around the minimum trough of the diagram.

In the Or–Ab–An diagram (Fig. 8–b), the quartzo-feldspathic layers of the layered gneisses are roughly in the minimum trough of the diagram. This

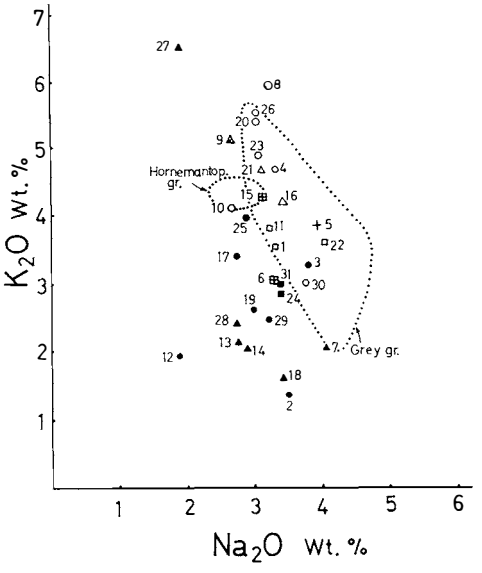

Fig. 7. *K_2O–Na_2O diagram. Dotted areas: grey granites and Hornemantoppen granites, including* HJELLE's *data (Symbols are the same as in Fig. 8).*

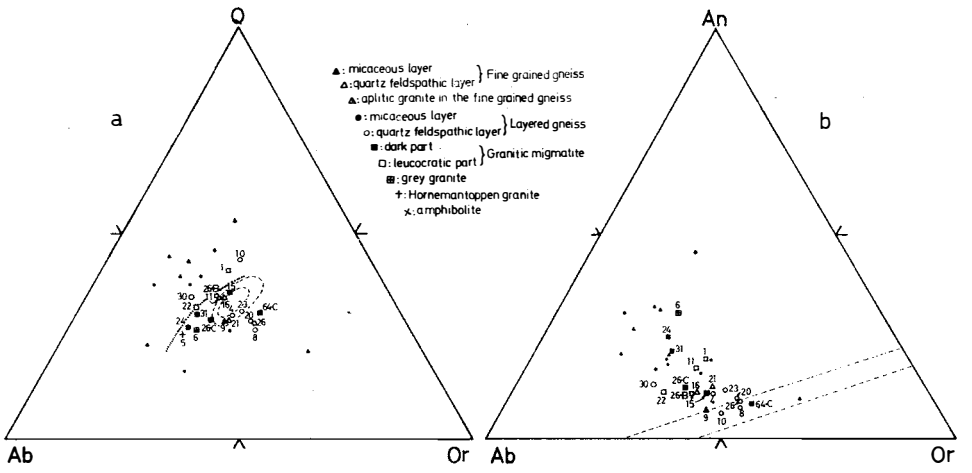

Fig. 8. *Katanorm diagrams.* 8–a. *Qt-Ab-Or diagram.* 8–b. *An-Ab-Or diagram. The micaceous layers of the gneisses are not numbered. Broken lines and dotted curve are the experimental and empirical minimum trough of each diagram.*

indicates that the feldspathic material introduced into these rocks from the outside might be derived from the lowest melting product of the country rocks under rising temperature in the lower level. The granitic end products are situated around the intermediate field between the micaceous layers and the quartzo-feldspathic layers of the layered gneisses on both diagrams of Fig. 8. This indicates that these end products were not eutectic crystallization products but a mixture of two different compositions, one of which is of eutectoidal material which is enough to mobilize the whole rock to form flow structure.

2. *Niggli value-variation diagrams*

Different terms of Niggli values are plotted against the si value (Figs. 9–A and 9–B). The most distinct feature throughout these diagrams is a good separation of the micaceous layers and quartzo-feldspathic rocks of all metamorphic rocks, owing to the difference of the si value.

The major Niggli values, such as al, fm, c, and alk, show roughly smooth curves (Fig. 9-A) with some amount of scattering of the micaceous layers in the c and alk diagrams. In general the curvatures of each curve change between micaceous and quartzo-feldspathic layers. The increase of feldspars in quartzo-feldspathic rocks is supported by the al and alk diagrams where the quartzo-feldspathic rocks have higher values than the micaceous ones. This increase of al and alk is roughly compensated for by the decrease of fm. The c values do not differ much between these two different compositional layers. The calculated An contents based on the mesonorm have nearly the same pattern as the c variation diagram.

The grey granites, the compositions of which have been calculated from modal analyses by HJELLE (1966), have nearly the same position as the present metamorphic rocks in the fm and alk diagrams. They have slightly lower al and higher c than the quartzo-feldspathic layers of the metamorphic rocks.

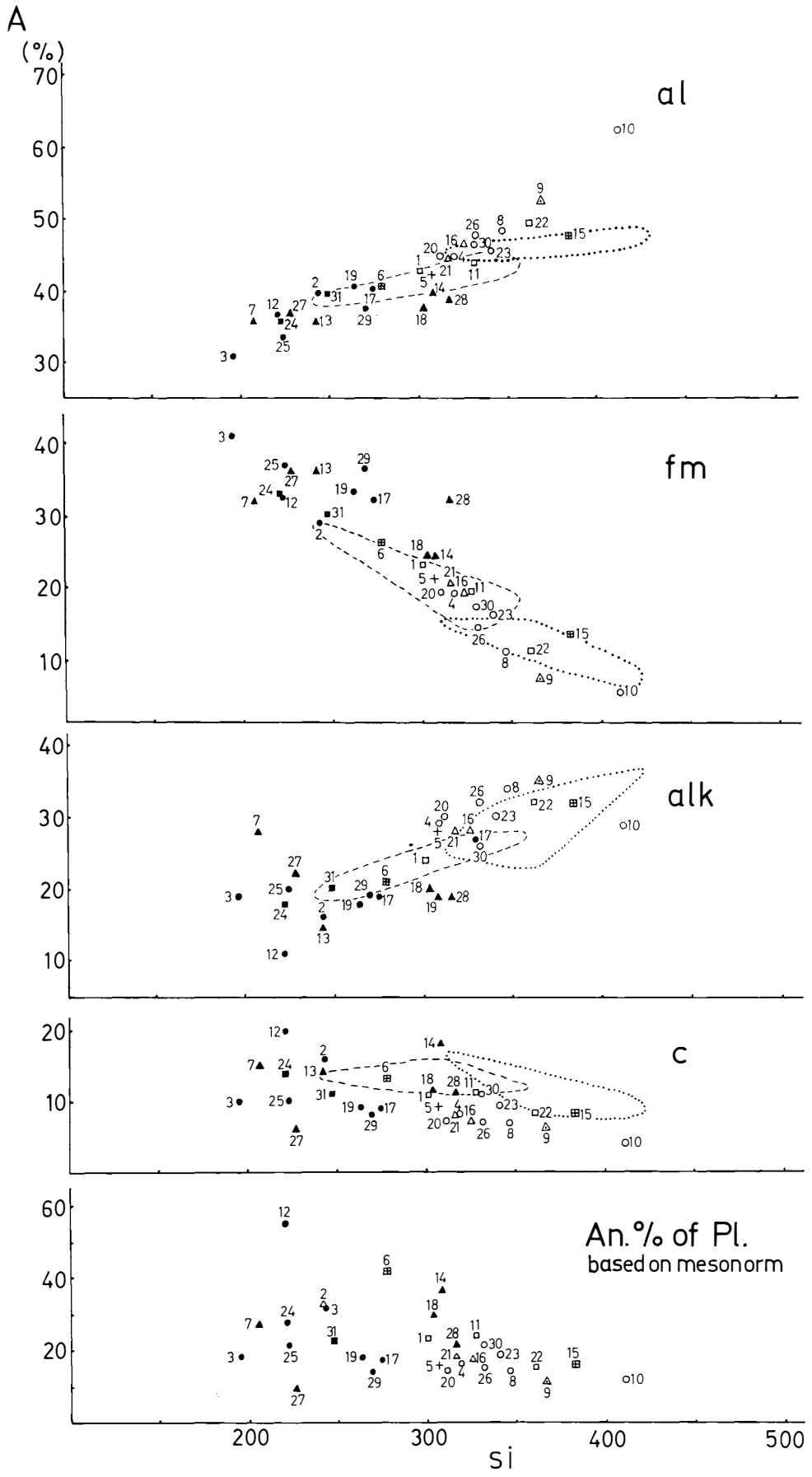

Fig. 9. *Niggli value variation diagram (Symbols are the same hereafter as Fig. 8). 9–A. The diagrams for al, fm, alk, c, and An content of plagioclase calculated from mesonorm. Dotted line areas: grey granites.*

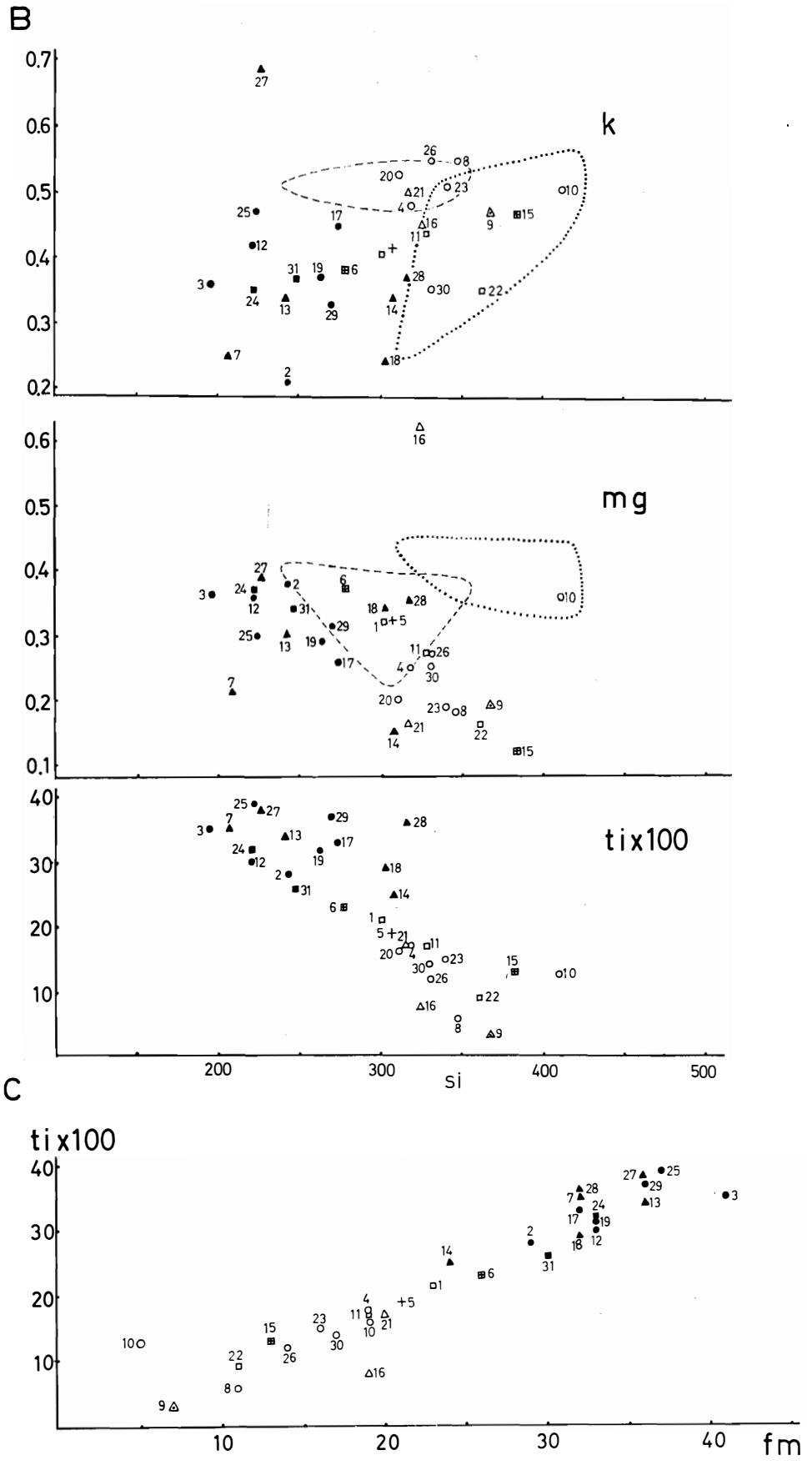

Broken line areas: Hornemantoppen granites. Both include HJELLE*'s data.* 9–B. *The diagrams of k, mg, and ti. Dotted line areas and broken line areas are the same as in* 9-A. 9–C. *Niggli value fm-ti diagram, showing a positive relation between iron and titanium.*

The al position of the grey granites shows a very small increase with the si increase compared with the quartzo-feldspathic layers.

The Hornemantoppen granites, the compositions of which are also from HJELLE (1966), project in the middle field between the micaceous and quartzo-feldspathic rocks in all variation diagrams.

The k, mg, and ti values are also plotted against si (Fig. 9-B). The micaceous rocks are all well separated from the quartzo-feldspathic rocks in these diagrams. The largest scattering of points occurs in the si–k diagram. The k values increase with si, while the mg values have a weak negative correlation with si.

The values for the grey granite are somewhat different from those of the quartzo-feldspathic layers; the k values are slightly lower and the mg values are distinctly higher.

The ti values show distinctly linear and negative correlation with si, but they show no strict regular relation to the mg values. As ti shows a systematic positive correlation with iron in these rocks (Fig. 9-C) whose main mafic constituent is biotite, the titanium and iron correlation roughly reflects the constant ratios of ti/total Fe in the biotites. However, judging from Fig. 10, the Fe/Fe+Mg ratios in the biotite may have a distinct range. The Mg^{2+} is higher in the layered gneisses and granitic migmatites than the fine-grained gneisses.

3. *Cation ratios*

All analyses, except those of the amphibolites, are shown on the $Mg^{2+}-(Fe^{2+}+Fe^{3+})-(Na^{+}+K^{+})$ diagram and $K^{+}-Na^{+}-Ca^{2+}$ diagram (Figs. 11–1 and 12–1). These elements show a systematic variation and the micaceous layers are distinctly separated from the quartzo-feldspathic ones.

Unfortunately there are no comparable geochemical data from other metamorphic rocks from Spitsbergen. Therefore, the data of Scottish Caledonian metamorphic rocks, summarized by MERCY (1963), were used for comparison with the present data (Figs. 11–2 and 12–2) and also with the modal data of granitic rocks of NW Spitsbergen by HJELLE (1966).

Concerning the relative ratios among Mg^{2+}, $Fe^{2+}+Fe^{3+}$ and $Na^{+}+K^{+}$, the quartzo-feldspathic rocks have nearly constant $Fe^{2+}+Fe^{3+}/Mg^{2+}=3.35:1$, with a small variation from 5.25: 1 to 2.2: 1, when the relative $Na^{+}+K^{+}$ varies from 70% to 95%. The micaceous rocks are projected as a cluster

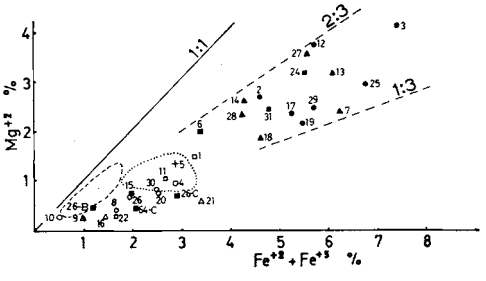

Fig. 10. *Mg^{2+}—$Fe^{2+}+Fe^{3+}$ diagram. Dotted and broken lines are the same hereafter as in Fig. 9.*

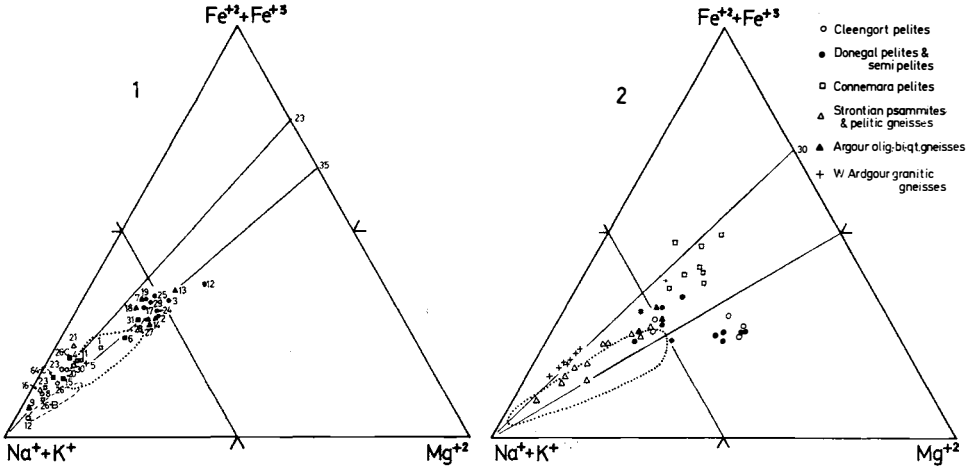

Fig. 11. *Total iron-alkali-magnesium diagram in comparison with the Scottish Caledonian metamorphic rocks. 1: rocks from the present area, including* HJELLE's *data. 2: Scottish Caledonian rocks. Dotted line area: Caledonian granites.*

around the relative $Fe^{2+}+Fe^{3+}=30\%$, $Na^{+}+K^{+}=53\%$, and $Mg^{2+}=17\%$; however, they are also scattered along a rough trend at $Fe^{2+}+Fe^{3+}$: $Mg^{2+}=$ 1.86: 1. Thus the quartzo-feldspathic rocks are characterized by higher relative $Na^{+}+K^{+}$ and also higher relative $Fe^{2+}+Fe^{3+}$ than the micaceous rocks. However, as a whole, the plots of both rocks show a smooth curve on the diagram. Compared with the Moine and Dalradian metamorphic rocks, which have slightly higher relative $Fe^{2+}+Fe^{3+}$ than the Caledonian granites in Scotland (Fig. 11–2), the present data projected much higher relative $Fe^{2+}+Fe^{3+}$. Only granitic gneisses of the Western Ardgour area, Scotland, have a trend similar to the present Spitsbergen rocks. There are no extremely pelitic rocks, as some Donegal pelites and Cleengort pelites which have high relative $Fe^{2+}+Fe^{3+}$ and Mg^{2+} proportions. The causes of the differences between the present rocks and Scottish rocks are mainly intense assimilation of micaceous rocks by quartz-rich metatects during migmatization and probably initial lack of typical argillaceous rocks as suggested by low content of Mg^{2+} of the micaceous rocks in the present area.

The grey granites in the northwestern part of Spitsbergen have an evidently higher relative Mg^{2+} ratio than the quartzo-feldspathic parts of metamorphic rocks, as seen in the mg variation diagram (Fig. 9–B). The general position of these grey granites is roughly the same as of the Scottish Caledonian metamorphic rocks, but the relative Mg^{2+} is lower than that of the Scottish Caledonian granites.

The Hornemantoppen granite occupies a middle position between the micaceous and quartzo-feldspathic rocks.

In the $K^{+}-Na^{+}-Ca^{2+}$ diagram (Fig. 12–1), the trend of the quartzo-feldspathic rocks is different from that of the micaceous ones; the former have a constant Na^{+}: Ca^{2+} ratio about 4: 1 while the latter have constant relative Na^{+}, roughly 50% with large scattering. The position of the quartzo-feldspathic

rocks on the diagram roughly coincides with that of the Scottish Moine and Dalradian metamorphic rocks, while that of the micaceous rocks shows the same trend as the Scottish Caledonian granites (Fig. 12–2). There is no rock in the present area having high relative K^+ like the pelites from Connemara and other localities. Such high relative K^+ is common among originally pelitic sedimentary rocks and a roughly constant $Na^+ : Ca^{2+}$ ratio is frequently met with in pelitic and semipelitic sediments. However, the micaceous metamorphic rocks in the present area, which of course have been modified by metamorphic differentiation, are completely different from the above mentioned attitudes of pelitic sedimentary rocks and are consistent with some kinds of graywacke sediments. On the other hand, the quartzo-feldspathic rocks, the trend of which roughly coincides with that of the meta-sedimentary rocks, are actually metablastic rocks occurring along the secondary axial plane cleavages and are an introduced end product of the granitization and mobilization process.

The absolute Na^+ and K^+ in the grey granites are roughly the same as in the quartzo-feldspathic rocks, however, they project between the micaceous and quartzo-feldspathic parts of metamorphic rocks in the $Na^+ - K^+ - Ca^{2+}$ diagram. This is because of the high Ca^{2+} in these granites and indicates that these rocks are a mixture and a homogenized product of the two lithologically different parts.

The Hornemantoppen granite has a significantly different position from the rocks mentioned above.

MERCY (1963) concluded that the granitic gneisses of the Western Ardgour are a different series from the Caledonian granites and might be a partial melting product of the meta-sedimentary rocks developed at a relatively lower temperature than the latter. The quartzo-feldspathic rocks in the present metamorphic rocks have much higher relative K^+ and $Fe^{2+}+Fe^{3+}$ than the

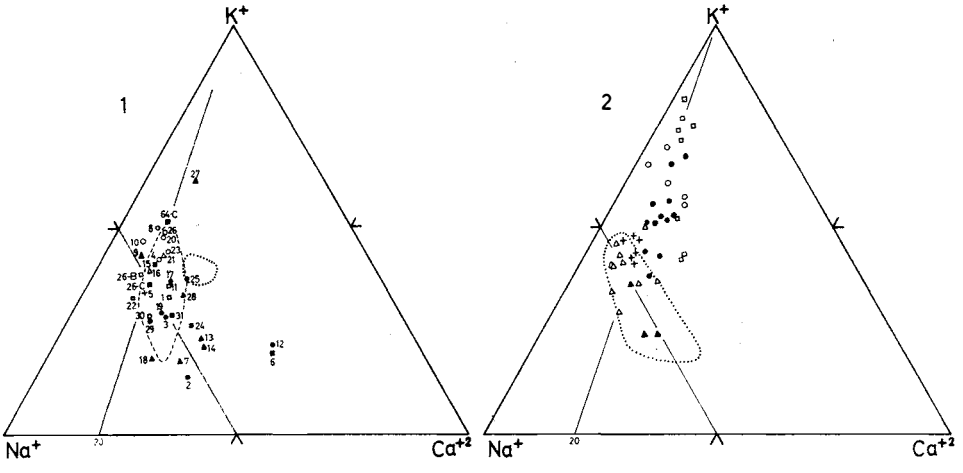

Fig. 12. *K^+—Na^+—Ca^{2+} diagram in comparison with the Scottish Caledonian metamorphic rocks. 1: Rocks of the present area, including* HJELLE's *data. 2: Scottish Caledonian rocks. Symbols are the same as in Fig. 11–2.*

Table 6.
Oxidation ratios of the rocks

	Sample No.	Fe^{3+}/Fe^{2+} ratio		Sample No.	Fe^{3+}/Fe^{2+} ratio
Fine grained banded gneisses.					
Qz-feld. layer	7 (92–1a)	0.47	Micaceous layer	9 (92–1b)	0.34
	13 (151)	0.50			
	14 (178–2)	0.66		16 (217)	0.43
	18 (252)	0.56			
	27 (436)	0.39		21 (297)	0.53
	28 (440–5)	0.56			
	Average	0.52		Average	0.43
Layered gneisses.					
Qz-feld. layer	2 (24–2)	0.35	Micaceous layer	4 (52–3)	0.43
	3 (49–1)	0.32		8 (91–1b)	0.61
	12 (110)	0.33		10 (93)	0.28
	17 (219–1)	0.36		20 (276)	0.43
	19 (264)	0.48		23 (353)	0.50
	25 (429)	0.56		26 (432)	0.27
	29 (449)	0.49		30 (456)	0.50
				26–B	0.22
	Average	0.41		Average	0.41
Granitic migmatites.					
Qz-feld. Part.	24 (386–1)	0.41	Dark part	1 (16)	0.44
	31 (394)	0.40		11 (109)	0.50
				22 (310)	0.34
	Average	0.41		Average	0.43
	Grey granites.			Amphibolites.	
	6 (74)	0.71		32 (284–2)	1.65
	15 (198)	0.78		33 (389)	0.15
	26–C	0.34		34 (425)	0.58
	64–C	0.39			
	Average	0.74—0.36		Average	0.86

Scottish Caledonian granites and suggest that they might also be a partial melting product developed under nearly the same conditions as the Western Ardgour granitic gneisses. The higher oxidation ratios, Fe^{3+}/Fe^{2+}, of the present rocks, viz. from 0.41 to 0.55 in averages of each kind of gneisses (Table 6), indicate that the volatile contents of these rocks are larger in amount than the Western Ardgour granitic gneisses.

Experimental works by WYLLIE & TUTTLE (1961) and WINKLER & VON PLATEN (1961) support the idea that the granite-granodiorite melt could have been formed through partial melting under rising temperature in a regional

metamorphism. The product of the lowest partial melting is an aplitic granite composed of quartz and alkali feldspar. Thus the partial melting products, the leucocratic rocks of aplitic granite composition, permeated along the axial plane cleavages of the fine-grained gneisses and formed the layered gneisses. When these mobilized products were added in large amounts, the rocks became agmatite and nebulite where a movement of the molten materials took place. However, the extreme heterogeneity of these migmatitic rocks indicates that the migration of major constituent elements was not sufficient to form a large homogeneous granitic body and the small amounts of grey granites are the end product of homogenization.

C. SUMMARY OF BULK CHEMISTRY

(a) The major element distributions of the micaceous parts of metamorphic rocks indicate that the original rocks may be graywacke sediments, having high relative Ca^{2+} proportion and intermediate relative Na^{+}, while the quartzo-feldspathic parts of the rocks of weakly recrystallized gneisses are evidently impure quartzite.

(b) The quartzo-feldspathic rocks in the layered gneisses have the most potassic composition, indicating that they are partial melting products of psammitic sediments under rising temperature during metamorphism. The layered gneisses were formed by introduction of such granitic material along the axial surface cleavages of the F_1 folding.

(c) In all Niggli variation diagrams both micaceous and quartzo-feldspathic rocks exhibit a smooth curve, suggesting a geochemical series. This series is a mixing process of the partial melting products and regional metamorphic rocks of psammitic composition.

(d) The granitic migmatites in the present area represent a homogenization process between the two lithologic types mentioned above. A bodily movement of material was dominant in these rocks.

(e) The grey granites are the end products of the homogenization. They have a higher relative Ca^{2+} and Mg^{2+} than the quartzo-feldspathic layers of the layered gneisses, suggesting they have been formed under a higher temperature than that of the partial melting products.

(f) Compared with the Scottish Caledonian metamorphics, the present rocks have lower relative $K^{+}+Na^{+}$ and lower relative Na^{+}. This difference is mainly owing to the lack of extremely pelitic rocks in the present area.

The grey granites, in comparison with the Scottish Caledonian granites, have lower relative Mg^{2+}, higher relative $Fe^{2+}+Fe^{3+}$, lower relative Ca^{2+}, and higher relative K^{+}, indicating that they were formed under lower temperature than the Scottish Caledonian granites. Some granitic gneisses from the Scottish territory have the same chemical trend as the grey granites.

(g) Judging from the $Mg^{2+}/Fe^{2+}+Fe^{3+}$ ratios of bulk rocks, the biotites in these metamorphic rocks have a wide range of $Mg^{2+}/Fe^{2+}+Fe^{3+}$ ratios, and the $Ti/Fe^{2+}+Fe^{3+}$ ratio may be constant.

III. Summary

Megascopic petrographic characteristics of the metamorphic and granitic rocks were given in a previous paper (OHTA 1969).

1. DEFORMATION PHASES

Three tectonic phases of regional metamorphism and a post-tectonic intrusion phase were established, based on the nature of the mesoscopic tectonic elements (Fig. 5):

F1. Formation of schistosity and recrystallization, resulting in the fine-grained gneisses.
F2. Development of layered structure along the axial plane cleavages of the folded fine-grained gneisses to form the layered gneisses.
F3. Formation of granitic migmatite and emplacement of grey granites.
F4. Intrusion of the post-tectonic Hornemantoppen granite.

2. METAMORPHIC GRADE AND FACIES SERIES

The highest metamorphic grade achieved in the F_2 deformation is upper amphibolite facies to lower granulite facies. Sillimanite-cordierite-garnet-biotite and corundum-hercynite-cordierite parageneses in the micaceous layered gneisses and spinel-forsterite-clinohumite-phlogopite paragenesis in the dolomitic marble (Table 1–C) are characteristic. The reaction between cordierite and almandine with co-existence of sillimanite indicates that the metamorphic facies series is intermediate between the Barrovian (intermediate P and T) and the Buchan (low P and high T) types of metamorphism. Masking of the P–T field of kyanite and andalusite suggests a high P_{H_2O} condition during metamorphism. Abundance of syntectonic granite and migmatite in this area can be explained by this condition. The condition in which the granitic metatects formed is estimated at about 5.5 Kb pressure with high P_{H_2O} and in the temperature range of 650–700°C.

3. GEOCHEMICAL CHARACTERISTICS OF THE ROCKS

The fine-grained gneisses have a wider modal variation than the layered gneisses which were homogenized by plagioclase porphyroblastesis. However, the latter have local extreme composition domains as quartz- and feldspar-masses and mafic mineral clusters.

The micaceous layers of all metamorphic rocks are thought to have been derived from greywacke sediments, while the quartzo-feldspathic layers of the layered gneisses are considered to be partial melting products under rising temperatures. The grey granites occupy the intermediate position between the micaceous and quartzo-feldspathic layers on the cation triangle diagrams and it is concluded that they are a mixing product between the two compositional layers. The plots of all these rocks show a smooth curve on the Niggli-value variation diagrams and indicate that they belong to one series of mixing

processes. The high oxidation ratios of these rocks suggest a high P_{H_2O} condition during metamorphism. This is also evaluated from the studies of metamorphism and makes the abundance of syntectonic granites and migmatites in this area reasonable.

Acknowledgements

The author wishes to thank the director of Norsk Polarinstitutt, Dr. T. GJELSVIK, and the leader of 1966 expedition, Mr. K. Z. LUNDQUIST, for giving him the opportunity to study in the north-western part of Spitsbergen and for financial help. He is also very much indebted to Mr. A. HJELLE and Mr. E. TVETEN for their discussions and to Mr. A. FOUGNER and Mr. T. JOHNSRUD for their helpful assistance during the whole period of the expedition. He is deeply indebted to the late Prof. T. F. W. BARTH for many critical discussions on chemical problems related to granite, and to Prof. P. REITAN for his critical reading of the manuscript and improvement of the language. Thanks are also expressed to Mr. I WATANABE for photographing thin sections and Mr. W. INGEBRETSEN for making thin sections.

References

ATKINSON, D. G., 1956: The occurrence of chloritoid in the Hecla Hoek formation of Prince Charles Foreland, Spitsbergen. *Geol. Mag.* **93**. 63–71.

CHINNER, G. A., 1966: The distribution of pressure and temperature during Dalradian metamorphism. *Geol. Soc. London Quart. Jour.* **122**. 159–186.

EITEL, W., 1965: *Silicate science*, IV. New York.

FLOOD, B., D. G. GEE, A. HJELLE, T. SIGGERUD, and T. S. WINSNES, 1969: The geology of Nordaustlandet, northern and central part. *Norsk Polarinstitutt Skr.* Nr. 146.

FRIEDMAN, M. G., 1953: The spinel-silica reaction succession; a study of incompatible mineral phases. *Journ. Geol.* **62**. 366–374.

GANGULY, J., 1969: Chloritoid stability and related parageneses; theory, experiments and applications. *Am. Jour. Sci.* **267**. 910–944.

GAYER, R. A., D. G. GEE, W. B. HARLAND, J. A. MILLER, H. R. SPALL, R. H. WALLIS, and T. S. WINSNES, 1966: Radiometric age determination on rocks from Spitsbergen. *Norsk Polarinstitutt Skr.* Nr. 137. 1–39. Oslo.

GEE, D. G. and A. HJELLE, 1966: On the crystalline rocks of north-west Spitsbergen. *Norsk Polarinstitutt Årbok* 1964. 31–45. Oslo.

HARLAND, W., 1961: An outline structural history of Spitsbergen. *Geology of the Arctic*. **1**. 68–132. Toronto.

HARLAND, W. B., R. H. WALLIS, and R. A. GAYER, 1966: A revision of the lower Hecla Hoek succession in central north Spitsbergen and correlation elsewhere. *Geol. Mag.* **168** (1). 70–97.

HIRSCHBERG, A. and H. G. F. WINKLER, 1968: Stabilitätsbeziehungen zwischen Chlorit, Cordierit und Almandin bei der Metamorphose. *Contr. Miner. Petrol.* **18**. 17–42.

HJELLE, A., 1966: The composition of some granitic rocks from Svalbard. *Norsk Polarinstitutt Årbok* 1965. 7–30. Oslo.

— 1974: The geology of Danskøya and Amsterdamøya north-west Spitsbergen. *Norsk Polarinstitutt Skr.* Nr. 158 (this volume).

HORSFIELD, W. T., 1972: Glaucophane schists of Caledonian age from Spitsbergen. *Geol. Mag.* **109** (1). 29–36.

HOSCHEK, G., 1969: The stability of staurolite and chloritoid and their significance in metamorphism of pelitic rocks. *Contr. Miner. Petrol.* **22.** 208–232.

JOHNSON, M. R. and F. H. STEWART, 1960: On Dalradian structures in north-east Scotland. *Trans. Edinb. geol. Soc.* **18.** 94–103.

KRASIL'ŠČIKOV, A. A., 1965: Some aspect of the geological history of north Spitsbergen. *Geology of Spitsbergen.* **1.** 32–48. English edition, 1970.

MERCY, E. L. P., 1963: The geochemistry of some caledonian granitic and metasedimentary rocks. *The British Caledonides.* (Ed.: JOHNSON, M. R. W. and F. H. STEWART). 189–216. London.

MIYASHIRO, A., 1960: Thermodynamics of reactions of rock-forming minerals with silica. I–IV, *Jap. Jour. Geol. Georg.* **31.** 71–78, 79–84, 107–111, 113–120, 241–246, and 247–252.

NOCKOLDS, S. R. and R. ALLEN, 1953: The geochemistry of some igneous rock series. *Geochim. et Cosmochim. Acta.* **4.** 105–142.

OHTA, Y., 1969: The geology and structure of metamorphic rocks in the Smeerenburgfjorden area, north-west Vestspitsbergen. *Norsk Polarinstitutt Årbok* 1967. 52–72.

— 1974: Geology and structure of the Magdalenefjorden area, Spitsbergen. *Norsk Polarinstitutt Skr.* Nr. 158 (this volume).

PIWINSKII, A. J., 1968: Experimental studies of igneous series, Central Sierra Nevada Batholith, California. *Journ. Geol.* **76.** 548–570.

RICHARDSON, S. W., M. C. GILBERT, and P. M. BELL, 1969: Experimental determination of kyanite-andalusite and andalusite-sillimanite equilibria; The Aluminum silicate triple point. *Am. Jour. Sci.* **267.** 259–272.

WINKLER, H. G. F. and H. VON PLATEN, 1961: Experimentelle Gesteinsmetamorphose, IV–V. *Geochem. et Cosmochem. Acta.* **24.** 48–69 and 250–259.

WYLLIE, P. J. and O. F. TUTTLE, 1961: Hydrothermal melting of shales. *Geol. Mag.* **98.** 56–66.

ZWART, H. J., 1967: The duality of orogenic belts. *Geologie en Mijnbouw.* 46e Jaargang. 283–309.

PLATES

PLATE 1.

A. – Northern Amsterdamøya, with Hakluytodden and Ytterholmane. View towards the south-west.
B. – Northern Danskøya, with Virgohamna. View towards the west.

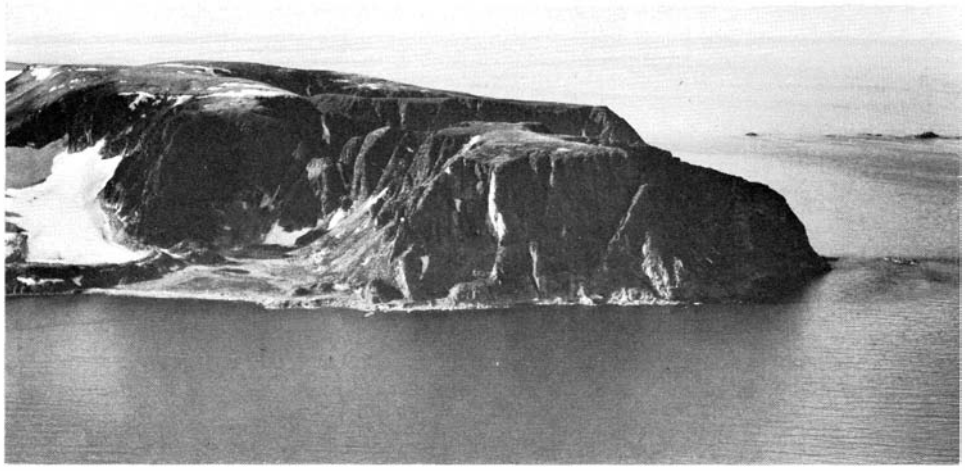

A

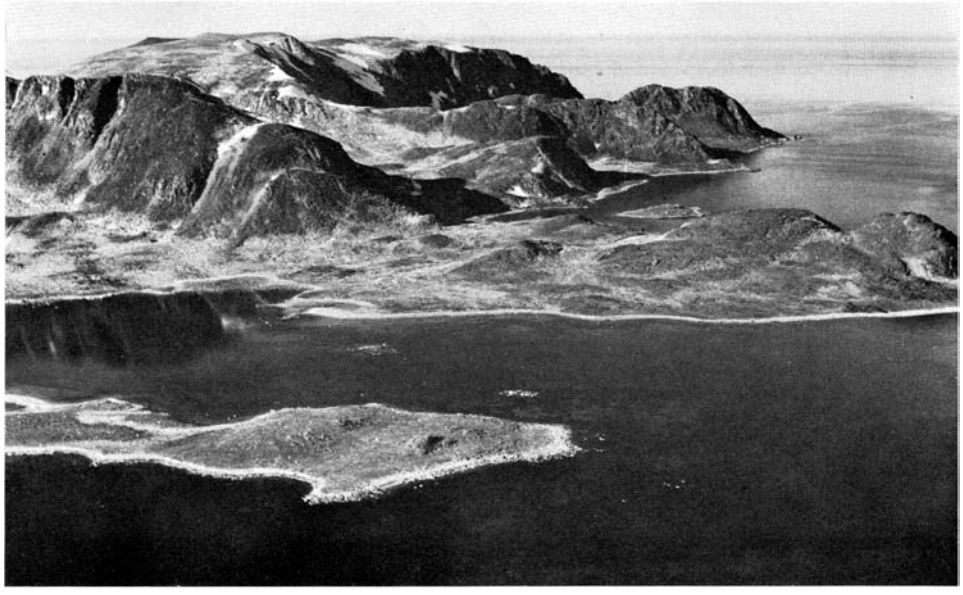

B

PLATE 2.

A. – Agmatitic migmatite, c. 2 km south-west of Hakluytodden, Amsterdamøya.
B. – Agmatitic migmatite with dyke of post-tectonic granite, westernmost part of Amsterdamøya. Height of section c. 20 m. In the lower left arrow points towards a man as a scale.
C. – Marble inclusion with skarn rim, in biotite gneiss, north-eastern Moseøya.
D. – F2 fold in biotite gneiss, with aplite core. Northern side of Kobbefjorden, Danskøya.

A

B

C

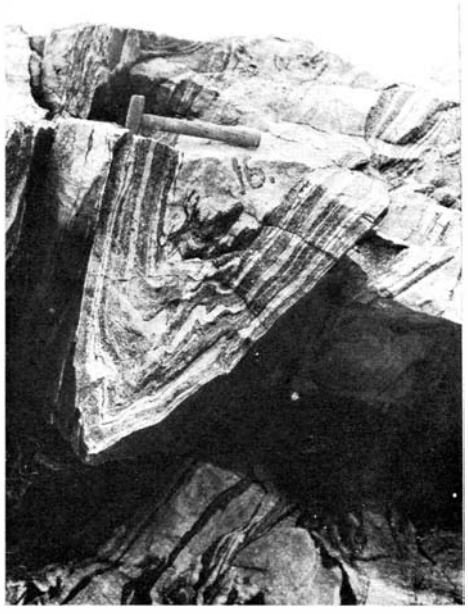

D

PLATE 1

1. Biotite schist with many quartz lenses along the cleavages (west side of Hoelfjellet).
2. Sillimanite-garnet-biotite gneiss with characteristic chevron folds (southern side of Evatindane).
3. Layered gneiss (northern side of Miethebreen).
4. Small isoclinal folds in the layered gneiss (southern side of Ytstekollen).

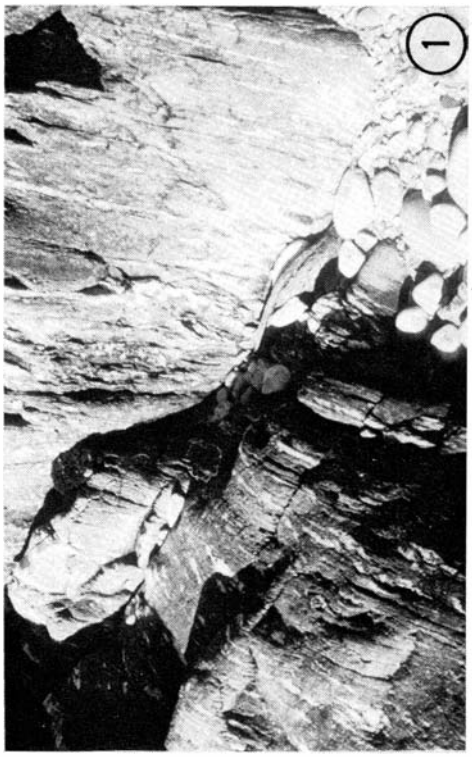
1

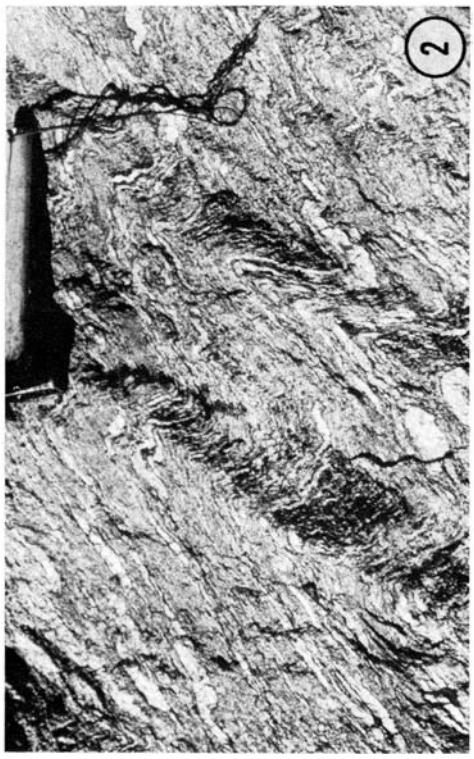
2


3

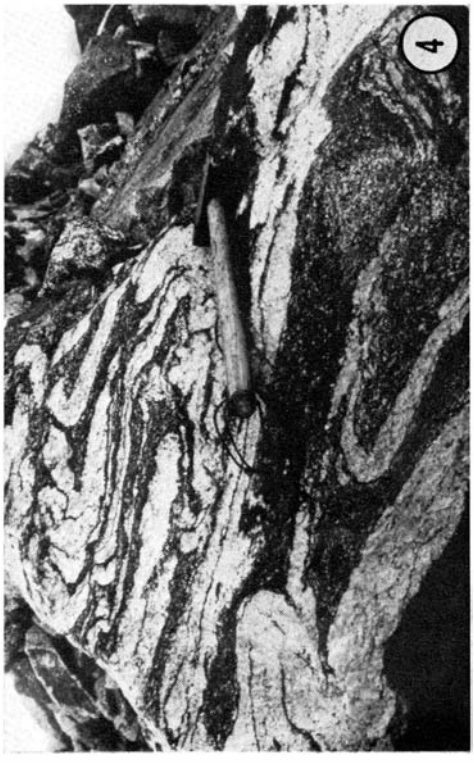
4

PLATE 2

1. Diktyonitic migmatite with plagioclase porphyroblasts (Gravnesodden).
2. Plagioclase porphyroblastic gneiss (west side of Walterfjellet).
3. Nebulitic gneiss with shadows of small-folded structures and quartz lenses (Gravneset).
4. Nebulitic gneiss with the shadow structure of an agmatitic migmatite (Gravneset).

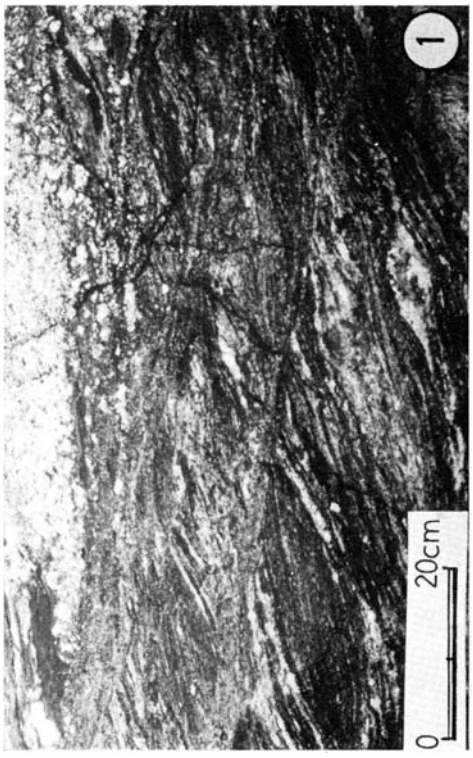
1
0
20cm

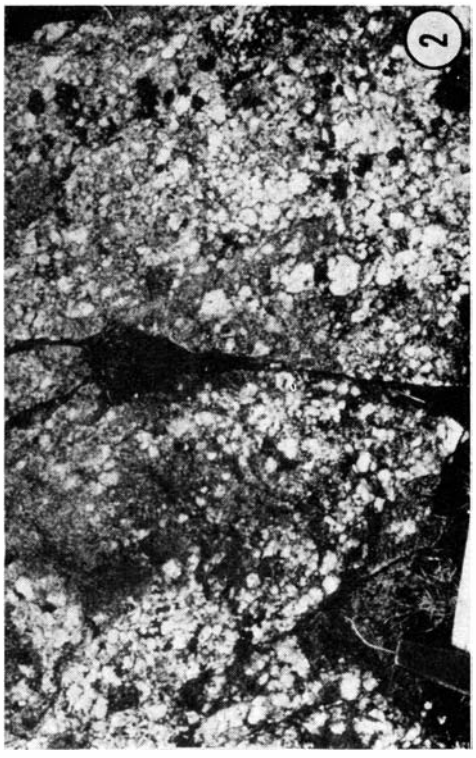
2

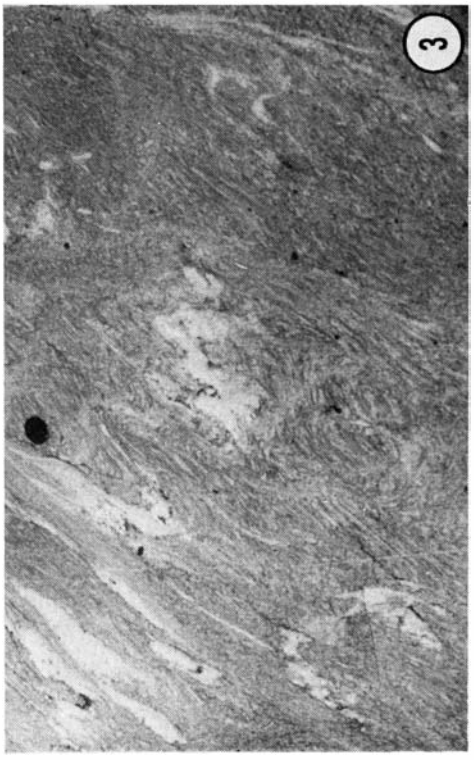
3

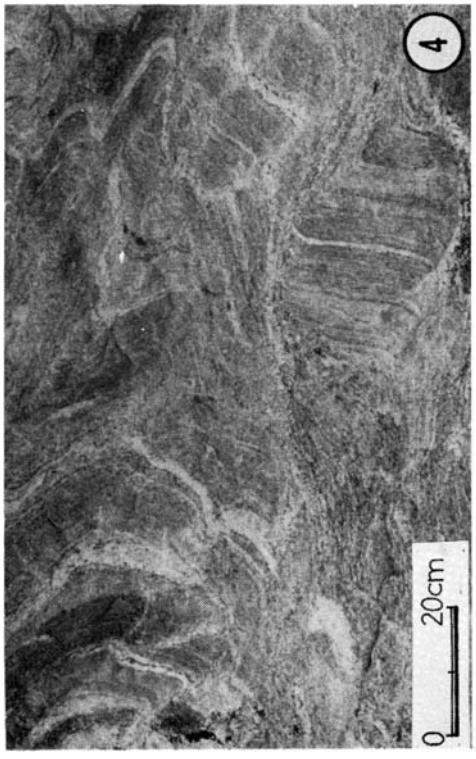
4
0
20cm

PLATE 3

1. Open synform structure on the northern side of Knatten. The white layers are crystalline limestone.
2. Refolded quartz layer (rf. Fig. 7 western shore of Walterfjellet).
3. Two phases of deformation in the quartzitic gneiss. The small-fold axes are folded by the open later undulation whose axis is parallel to the hammer shaft (northern side of Buchanbreen).

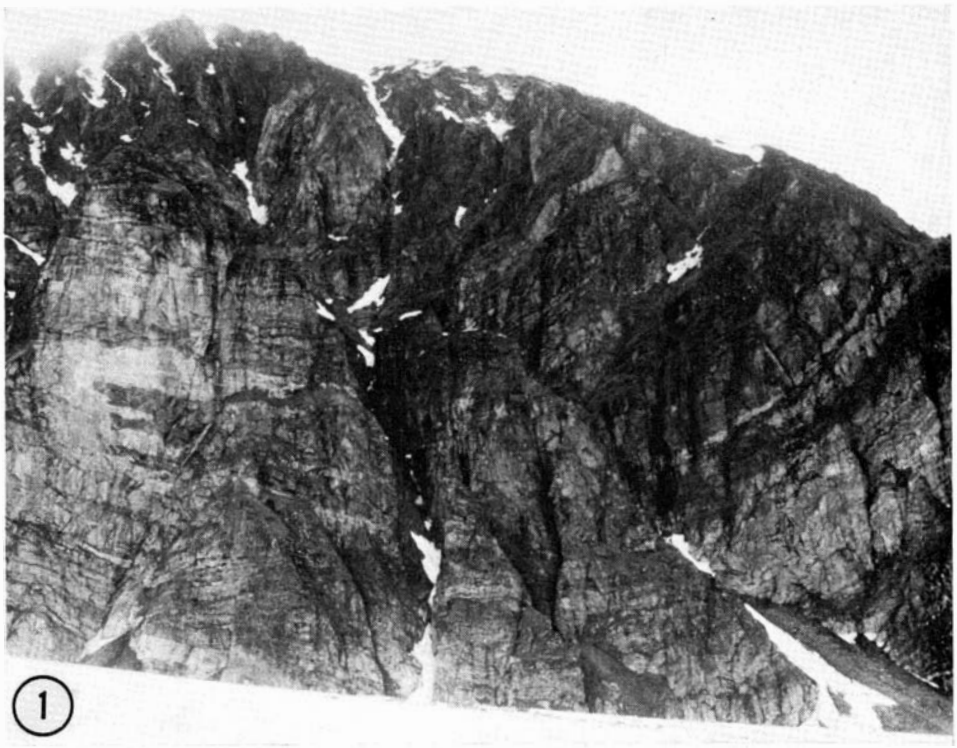
1


2


3

PLATE 4

1. Heterogeneous grey granite with gneiss paleozomes near the border of the granite (west side of Høystakken).
2. The boundary of grey granite and the quartzitic layered gneiss (east side of Skarpeggen).
3. Agmatitic migmatite (eastern part of Ytstekollen).
4. Agmatitic migmatite (northern side of Walterfjellet).


1


2


3


4

PLATE 1

1. Small folded part of the fine-grained biotite gneiss. The biotite layer marks original compositional banding while some biotites arrange parallel to the axial plane of the F_1 fold (Sample No. 440).
2. Dimensional preferred orientation of quartz in the quartzitic layer of the fine-grained gneiss (No. 52). Right half: quartzite, left half: meta-sandstone.

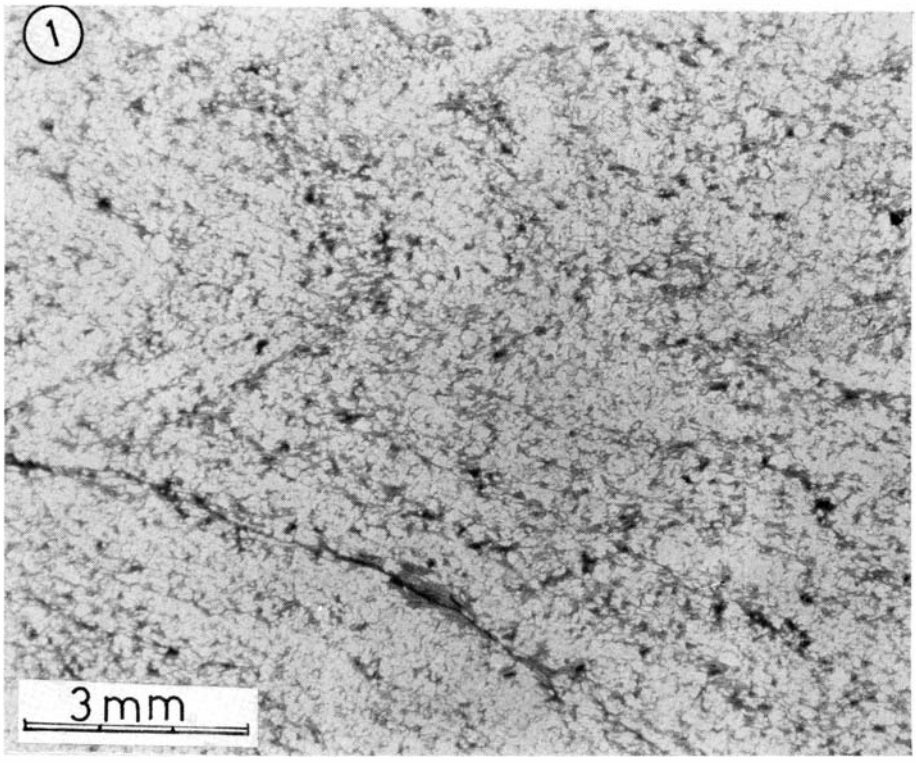
1
3mm

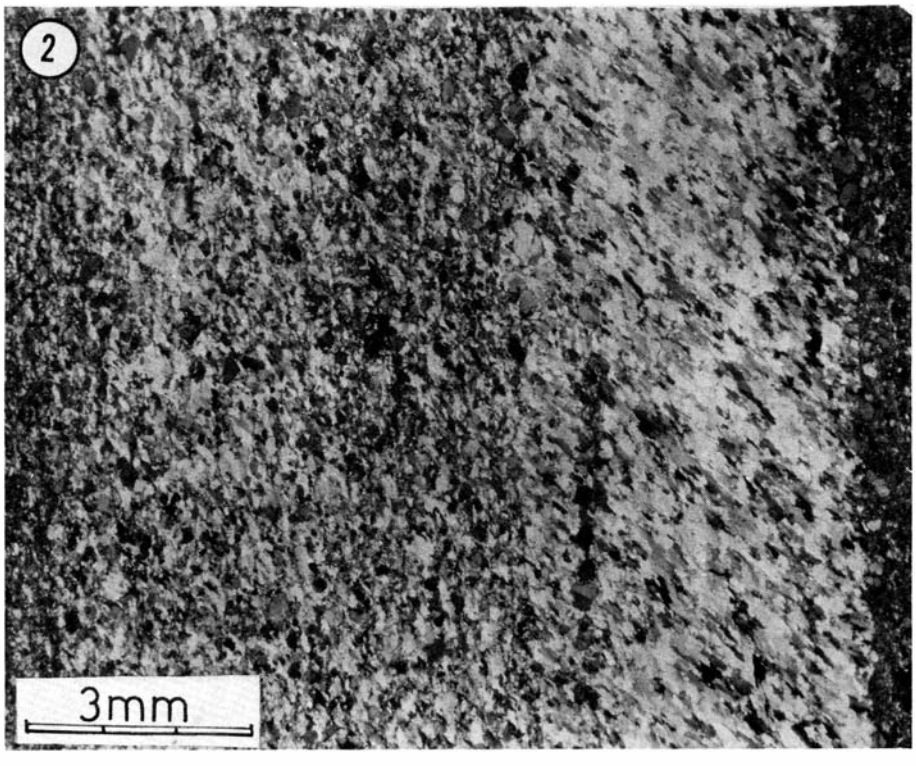
2
3mm

PLATE 2

1. Strongly compressed folds of the layered gneiss (northern side of Frambreen).
2. The leucocratic layer of the layered gneiss. The feldspar grains are crushed into fragments and become ovoidal in shape as in an augen gneiss (No. 456).

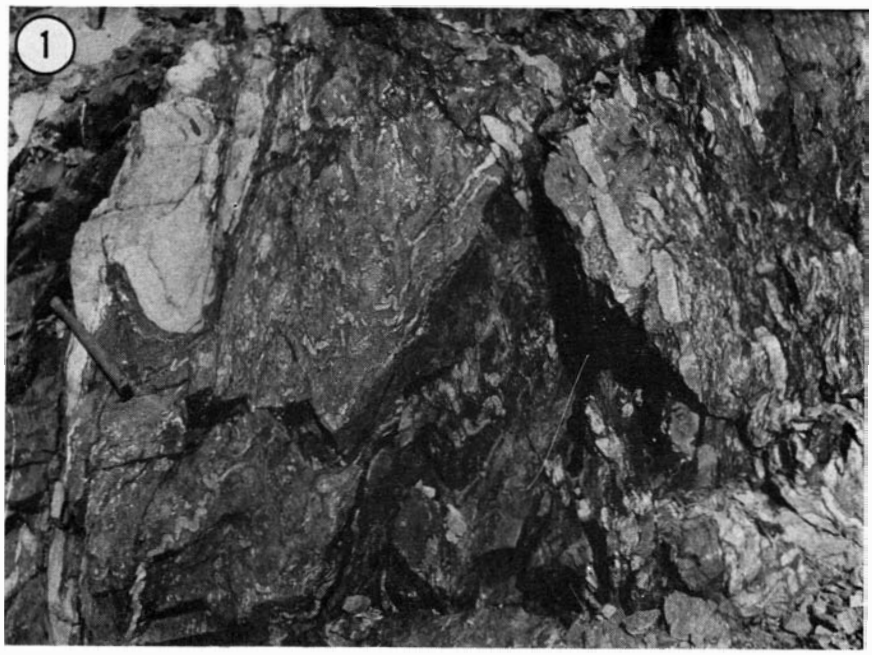
1

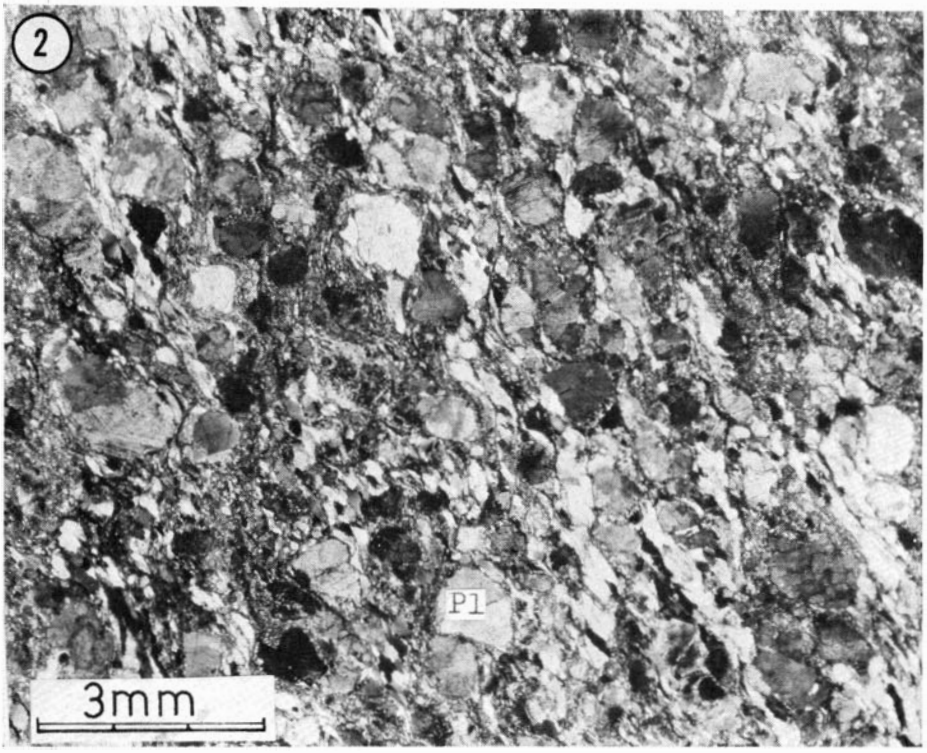
2
Pl
3mm

PLATE 3

1. Spinel-corundum clots in the biotite layered gneiss (No. 403).
2. Spinel-cordierite clot enclosed at the margin of a large garnet (No. 403).

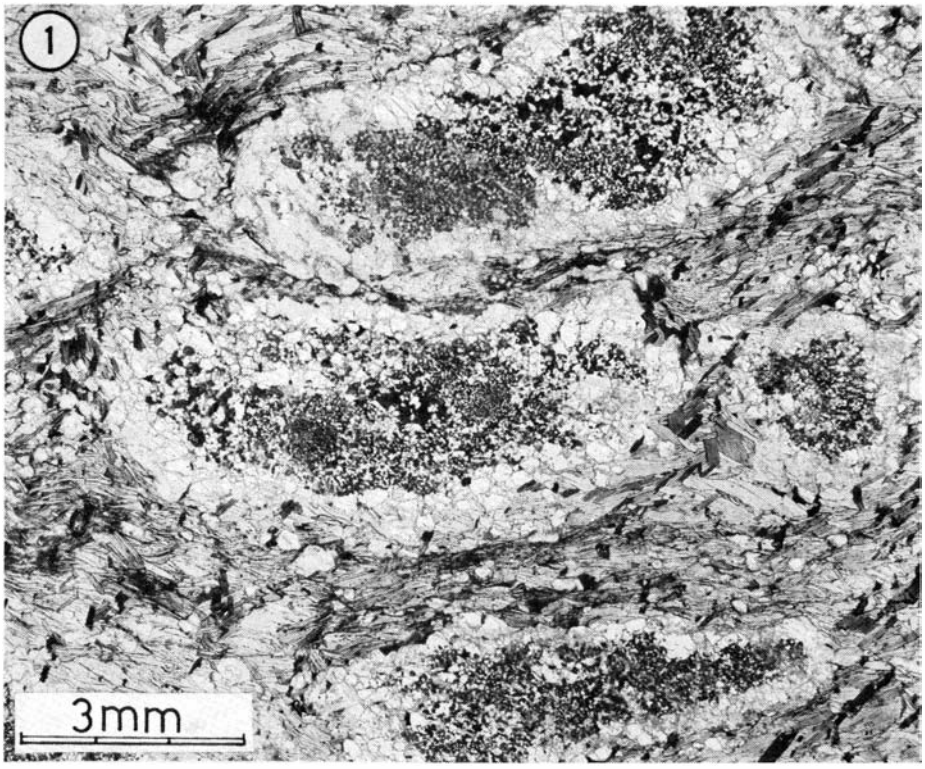
1
3mm

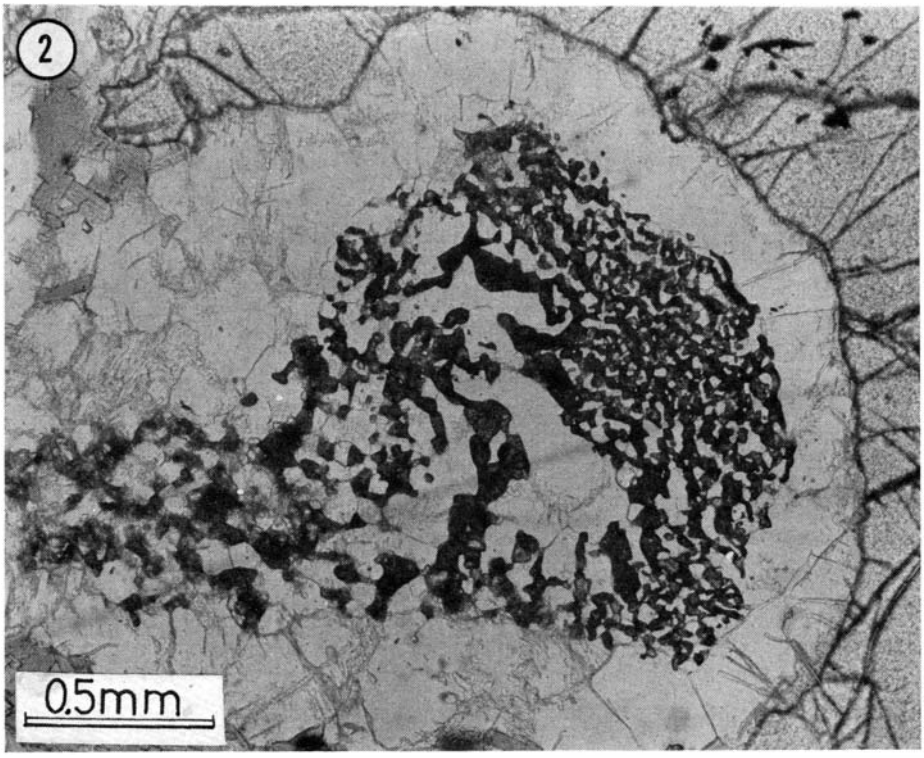
2
0.5mm

PLATE 4

A large spinel-corundum clot with oblique cross outline (No. 403).

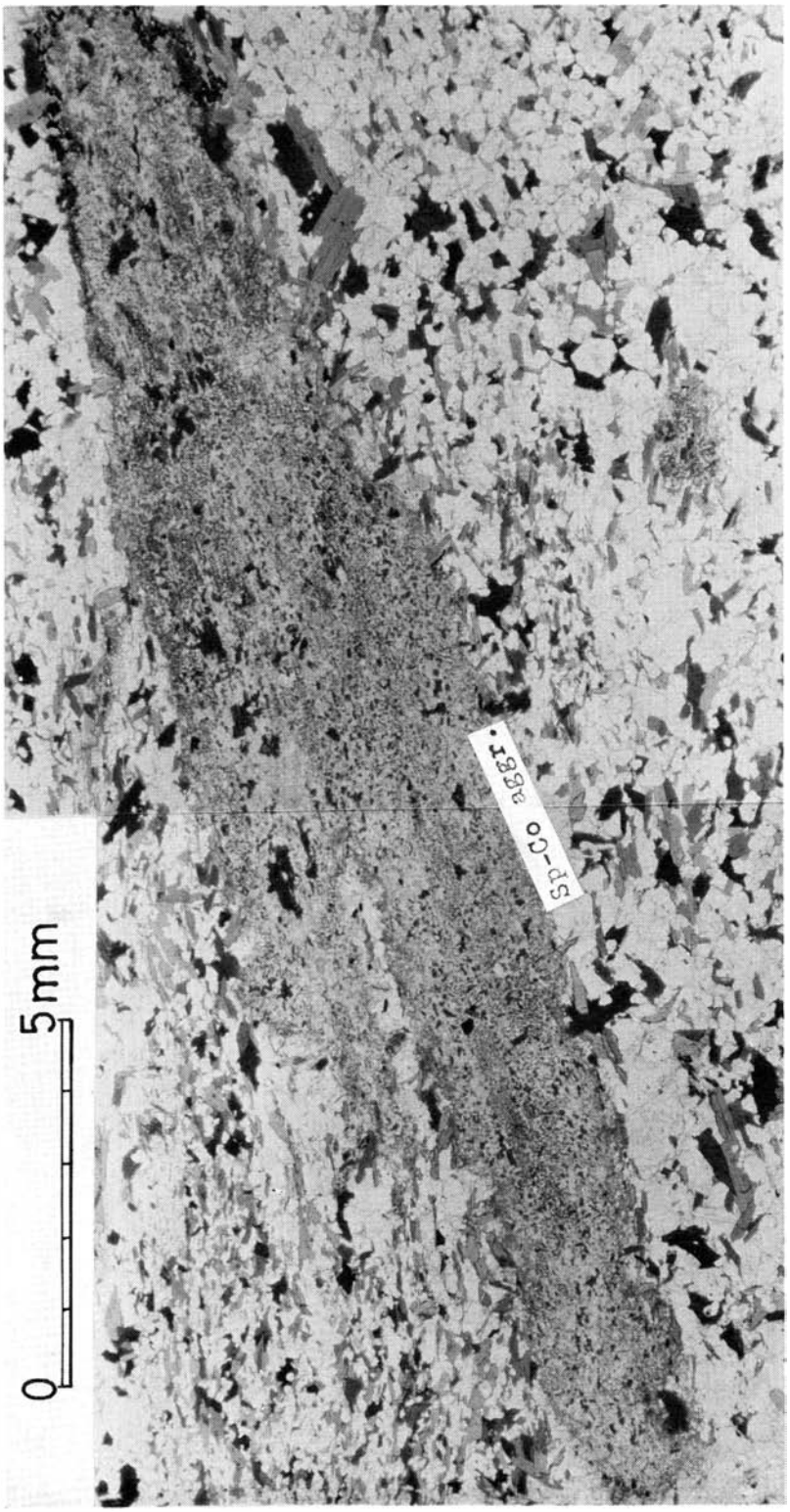
Sp-Co aggr.
0
5mm